LKB1, CCL2, AND MACROPHAGES: A NEW AXIS OF ENDOMETRIAL CANCER PROGRESSION

APPROVED BY SUPERVISORY COMMITTEE

_____

Diego H. Castrillon, M.D/Ph.D.

_____

Rolf Brekken, Ph.D.

_____

James Amatruda, M.D/Ph.D.

_____

Lawrence Lum, Ph.D.

DEDICATION

Dedicated to my grandmother, Genevieve A. Peña and my aunt, Evangelina Zertuche

I hope I shined a light on this subject worthy of the light you shined on others.

LKB1, CCL2, AND MACROPHAGES: A NEW AXIS OF ENDOMETRIAL CANCER PROGRESSION

by

CHRISTOPHER GEORGE PEÑA

DISSERTATION

Presented to the Faculty of the Graduate School of Biomedical Sciences

The University of Texas Southwestern Medical Center at Dallas

In Partial Fulfillment of the Requirements

For the Degree of

DOCTOR OF PHILOSOPHY

The University of Texas Southwestern Medical Center

Dallas, Texas

May, 2015

ACKNOWLEDGMENTS

I offer my utmost gratitude, respect, and love to my fiancé Lilly Flores, who *literally* followed me on my journey to graduate school in a city she had never lived in, a profession she had never worked, and a lifestyle she had never experienced. Moving to Dallas was a bold move for the both of us, and it was wonderful getting to know you in this city. We did this together, and I'm so excited for what the future holds for us.

I could get a million PhDs, and this effort would never equal the amount of support and dedication my amazing family has given me since I was a child. My mom, dad, sister, and nephew Isaac are the source of my inspiration and happiness. Every-day conversations with you on the phone made even the toughest days easier to handle. I truly could not have done this without you.

To Duygu Saatcioglu, Gina Aloisio, Ileana Cuevas, Mohammad Ezzati, and former members of the Castrillon Lab: This dissertation is the result of your input, advice, and overall efforts. I am so blessed to have been able to work with people as unique and brilliant as you. More importantly, thank you all for being my friends.

I'd like to thank members of my thesis committee: Drs. Rolf Brekken, James Amatruda, and Lawrence Lum. I appreciate all of your advice and input for this project. Importantly, thank you for sitting through an hour of WIPS before our committee meetings. Your time and patience was greatly appreciated.

Lastly, my deepest thanks to my mentor Diego Castrillon. Your unwavering support throughout the highs and lows of this project has molded me into the best scientist I could ever become. Your confidence in my ability allowed me to pursue different avenues of science and for this, I am truly grateful. It was a privilege learning from you.

LKB1, CCL2, AND MACROPHAGES: A NEW AXIS OF ENDOMETRIAL CANCER PROGRESSION

CHRISTOPHER GEORGE PEÑA

The University of Texas Southwestern Medical Center at Dallas, 2015

DIEGO CASTRILLON, M.D/Ph.D.

Cancer of the uterus is a common malignancy in women with no adequate treatments for tumors that have progressed beyond the uterus. The serine-threonine kinase LKB1 has been identified as a potent suppressor of uterine cancer. Combined genetic, proteomic, and *in vivo* studies in genetically engineered mouse models show that loss of LKB1 protein is associated with high grade, high stage tumors with unfavorable clinical outcomes. However, the mechanism(s) by which LKB1 drives malignant transformation of uterine cancers remains unclear.

Here I show that LKB1 unexpectedly suppresses tumor progression via pAMPK dependent secretion of the inflammatory cytokine CCL2. *Lkb1* inactivation *in vivo* resulted in abnormal production of CCL2, which led to recruitment of pro-tumorigenic macrophages (aka immunosuppressive macrophages) responsible for tumor invasion. Conditional inactivation of *Ccl2* in an *Lkb1*-driven mouse model of endometrial cancer slowed tumor progression, increased survival, and significantly reduced infiltration of macrophages in the tumor microenvironment. In human primary endometrial cancers (EMCAs), loss of LKB1 protein was strongly associated with increased CCL2 and macrophage density. Additionally, high stage and high grade EMCAs were characterized by loss of LKB1 protein, elevated production of CCL2, and increased macrophage density. These data demonstrate that CCL2 is a potent effector of LKB1 loss in endometrial cancer, creating new therapeutic opportunities for targeting CCL2 and the tumor microenvironment.

TABLE OF CONTENTS

PRIOR PUBLICATIONS

Peña CG, Nakada Y, Saatcioglu HD, Aloisio GM, Cuevas I, Zhang S, Miller D, Wong KK, DeBerardinis RJ, Amelio AL, Brekken RA, and Diego Castrillon (2015). LKB1 loss promotes endometrial tumor progression via the CCL2-dependent recruitment of macrophages. *(submitted, under review).*

Peña CG and Diego Castrillon (2015). Mouse models of LKB1 driven endometrial cancer. Springer: Molecular Genetics of Human Endometrial Carcinoma. *(editing).*

Peña CG, Camacho K, Silva P, and Luis Torres (2014). STEM Education: A Bridge for Latinos to Opportunity and Success. League of Latin American Citizens. <http://lulac.org/advocacy/issues/education/stem-white-paper/>.

Aloisio GM, Nakada Y, Saatcioglu HD., **Peña CG**, Baker MD, Tarnawa ED, Mukherjee J, Manjunath H, Bugde A, Sengupta A, Amatruda JF, Cuevas I, Hamra K, and Diego H. Castrillon (2014). PAX7 expression defines germline stem cells in the adult testis. The Journal of Clinical Investigation, 124(9):3929–3944.

Nakada Y, Stewart TG, **Peña CG**, Zhang S, Zhao N, Bardeesy N, Sharpless N, Wong KK, Hayes DN, and Diego H. Castrillon (2013). The LKB1 Tumor

Suppressor as a Biomarker in Mouse and Human Tissues. PLoS ONE 8(9): e73449.

Akbay EA, **Peña CG**, Ruder D, Michel JA, Nakada Y, Pathak S, Multani AS, Chang S, and Diego Castrillon (2012). Cooperation between p53 and the telomere-protecting shelterin component Pot1a in endometrial carcinogenesis. Oncogene. 32(17):2211-9.

Chen Z, Cheng K, Walton Z, Wang Y, Ebi H, Shimamura T, Liu Y, Tupper T, Ouyang J, Li J, Gao P, Woo MS, Xu C, Yanagita M, Altabef A, Wang S, Lee C, Nakada Y, **Peña CG**, Sun Y, Franchetti Y, Yao C, Saur A, Cameron MD, Nishino M, Hayes DN, Wilkerson MD, Roberts PJ, Lee CB, Bardeesy N, Butaney M, Chirieac LR, Costa DB, Jackman D, Sharpless NE, Castrillon DH, Demetri GD, Jänne PA, Pandolfi PP, Cantley LC, Kung AL, Engelman JA, and Wong KK (2012). A murine lung cancer co-clinical trial identifies genetic modifiers of therapeutic response. Nature, 483(7391):613-7.

Sharma J, Li Q, Mishra BB, **Pena C**, Teale JM (2009). Lethal pulmonary infection with Francisella novicida is associated with severe sepsis. Journal of Leukocyte Biology, 86(3):491-504.

LIST OF FIGURES

LIST OF TABLES

LIST OF ABBREVIATIONS

4EBP1: eukaryotic translation initiation factor 4E-binding protein 1

AB: antibody

AKT: protein kinase B

AMPK: AMP-activated protein kinase

ARID1A: AT-rich interactive domain-containing protein 1A

CCL2: C-C motif ligand 2

CLO: clodronate

CREB: cAMP response element-binding protein

CRTC: CREB transcriptional coactivator

CTNNB1: catenin (cadherin-associated protein), beta 1

DNA: deoxyribose nucleic acid

EGFR: epidermal growth factor receptor

ELISA: enzyme-linked immunosorbent assay

EM: immortalized endometrial cells

EMCA: endometrial cancer

FBXW7: f-box/WD repeat-containing protein 7

IHC: immunohistochemistry

IF: immunofluorescence

KRAS: Kirsten rat sarcoma viral oncogene homolog

LKB1: liver kinase B1

M1: classically activated macrophage

M2: alternatively activated macrophage

MO25: mouse protein 25

MTOR: mammalian target of rapamycin

PBS: phosphate buffered saline

PIK3CA: catalytic subunit of PI3K

PJS: peutz-jeghers syndrome

PPP2R1A: serine/threonine-protein phosphatase 2A

PTEN: phosphatase and tensin homolog

RNA: ribonucleic acid

S6: ribosomal protein S6 kinase

SIK: salt inducible kinase

SPRR2F: small proline-rich protein 2F

STRAD: sterile-20-related adaptor

TAM: tumor associated macrophage

TMA: tissue microarray

TME: tumor microenvironment

TP53: tumor protein p53

TSC1: tuberous sclerosis complex gene 1

CHAPTER ONE

Introduction

ENDOMETRIAL CANCER

Structure and function of the endometrium

The human endometrial layer is composed of columnar epithelial cells arranged adjacently and bound to a basement membrane, ultimately forming enclosed glands. These glands secrete and transport substances necessary for the survival and development of the embryo [1]. Connective-tissue stromal cells surrounding glandular epithelia provide them with growth and differentiation signals, which are responsible for their epithelial like appearance and behavior [2]. The endometrium lines the uterine cavity and is adjacent to the smooth muscle myometrium that promotes contractions throughout pregnancy [3]. The majority of uterine cancers arise from the endometrium of the uterus. Though cancers known as uterine sarcomas develop in the myometrium, they do so infrequently [4].

The endometrium is regulated by a network involving hormonal signals relayed from maturing ovarian follicles to the epithelium and stroma during the menstrual cycle in humans [5]. In the earlier phase of the cycle, thickening of the uterine lining occurs when estrogen is released by granulosa cells in the ovarian

follicle to endometrial epithelial cells and their surrounding stroma, inducing their growth and proliferation.

As the next phase begins, progesterone is released by the remainder of the mature follicle called the corpus luteum. Progesterone causes differentiation of the endometrial glands and the secretion of mucous and other factors. At this point in time, if fertilization and embryo implantation do not take place, the corpus luteum collapses on itself. This reduces the levels of both estrogen and progesterone. Apoptosis in the glands and stroma begins, and the subsequent dead cells are sloughed off during menstrual flow as new follicles begin their activation. This cycle continues throughout a woman's lifetime until follicular activity is completely exhausted, at which point menopause begins and the endometrium atrophies over time [5].

Histologic and genetic classification of endometrial cancer

Endometrial cancer (EMCA) arises when genetic mutations or molecular alterations compromise any one of these highly regulated processes; the end result being the hyper-proliferation of cells that invade from uterine stroma to neighboring myometrium and beyond. EMCA is the most common gynecologic malignancy and the fourth most common malignancy in women [6]. Most patients with disease confined to the uterus are treated successfully. For advanced stages of endometrial cancer, however, median survival is less than a year [7].

EMCAs can be classified into two-general categories based off clinical and histological features. These categories are referred to as type I and type II [8]. Type I EMCAs are generally well differentiated or low grade, resemble normal columnar epithelium, and are often of the endometrioid adenocarcinoma subtype. Though these cancers appear normal, there is reduced stromal connective tissue between proliferating glands. Furthermore, these glands are no longer confined to stroma and have started invading into neighboring myometrium, thus compromising the structure of the uterus. Due to their well-differentiated and epithelial-like features, most type I EMCAs do not display aberrant loss of estrogen and progesterone receptors, and are thus classified as ER/PR positive [8]. Development of type I EMCAs is linked to estrogen signaling unopposed by progesterone. This is often due to obesity, hormone-receptor positivity [9], and anovulatory cycles before and throughout menopause [10].

Non-serous-like, type I endometroid tumors have frequent mutations in *PIK3CA*, *KRAS*, *EGFR*, *CTNNB1*, and *PTEN* [9]. The former three are oncogenes that possess significantly elevated copies when examined in endometrial cancer cell lines [11]. Of the latter three, mutations in *CTNNB1* are common among lower grade adenocarcinomas with non-defective DNA mismatch repair mechanisms, suggesting other mutational mechanisms for this gene. *PTEN* non-sense and missense mutations are common across low-grade and high-grade endometrioid subtypes from clinical specimens, with defective DNA mismatch repair mainly common to high grade mutations [9].

Type II EMCAs develop from atrophic endometrium in older women and are not hormonally driven. These cancers carry a worse prognosis for patients than those with type I EMCAs. Type II cancers resemble high grade, non-endometrioid histology with either serous or clear cell features. This includes the presence of papillae, nuclear atypia, and in some cases cilia [12]. Genetically, type II serous tumors have frequent non-sense mutations in the tumor suppressor *TP53*, often compromising its function [9]. Other mutations common to type II EMCAs are found in *PIK3CA*, *FBXW7*, *PPP2R1A* and *ARID1A*. Compared to type I EMCAs, type II EMCAs are rich in gene duplication and gene deletion events. Further, abnormal karyotypes are common to type II EMCAs.

According to the Cancer Genome Atlas, mutations in the PI(3)K/AKT pathway occur in endometrial cancer more than cancers of any other tissues [9]. Regardless of classification, many of the genes mentioned among type I and II EMCAs converge on downstream components of this pathway, including mTOR. Of note, the tumor suppressor gene *LKB1* negatively regulates mTOR activity via the metabolic sensor AMPK. Evidence from the Cancer Genome Atlas and studies in human patients show that *LKB1* loss plays an important role in the development and progression of endometrial carcinomas, a phenomenon described extensively in the following chapter.

CHAPTER TWO

Introduction

LKB1 BIOLOGY AND ITS ROLE IN ENDOMETRIAL CANCER

Introduction

In humans, the *LKB1* gene on chromosome 19p13.3 encodes the protein Liver kinase B1 (LKB1), also called Serine/threonine kinase 11 (STK11) [13]. The nascent mRNA transcript of *LKB1* is composed of ten exons [14], resulting in a 433 amino acid (48 kDa) protein [15] responsible for regulating cellular metabolism, growth, and polarity. Ubiquitous expression of LKB1 in adult tissues [16] and its conservation throughout evolution [17] demonstrates its overall importance to these cellular functions, and suggests that LKB1 loss via mutations in the locus or other mechanisms can be an important driver for disease. In support of this, *LKB1* loss-of-functional mutations transmitted through the germline result in Peutz-Jeghers syndrome (PJS), an autosomal dominant condition characterized by benign polyps in the gastrointestinal tract, mucotaneous pigmentation, and an increased risk for different kinds of cancers [18]. Downregulation of LKB1 by somatic mutations facilitates malignant transformation of the lung, skin, and cervix [19, 20].

LKB1 loss, through somatic mutations and other mechanisms in the endometrium, promotes the same effect as loss of LKB1 expression characterizes

21% of primary endometrial tumors [21]. Evidence from clinical studies and mouse models highlights an important role for LKB1 in suppression of endometrial cancer (EMCA) [9, 22, 23]. Studies of high grade, high stage EMCAs show significant loss of LKB1 expression [22]. Importantly, loss of LKB1 across EMCA mouse models is associated with rapid disease progression and spread, leading to unfavorable clinical outcomes [22-25]. To better understand these results, basic LKB1 biology (including epigenetic and protein regulation, as well as its control over different cellular functions) will be discussed, highlighting diverse mechanisms of LKB1 loss, potentially malignant pathways associated with it, and the role these pathways have in endometrial cancer. Genetically engineered mouse models based on conditional inactivation of LKB1 in the uterus will be reviewed in chapter 3, as well as their use in discovering novel pathways as potential therapeutic targets.

LKB1 cancer genetics

LKB1 exists as a single homolog in the human genome and as several orthologs belonging to *M. musculus, C. elegans*, *Drosophila*, and *Xenopus.* In humans, *LKB1* is located on chromosome 19p13.3 and spans 23 kilobases. It is transcribed in the telomeric to centromeric direction, which results in a mature transcript of 9 coding exons and 1 non-coding exon [26]. Location and extent of LKB1 mRNA expression in adult human and fetal tissues has been characterized by *in situ* hybridization, revealing widespread LKB1 expression in all tissues

(including endometrium) with high accumulation in epithelia and seminiferous tubules of the testis. In general, fetal tissues express more LKB1 than adult [27].

Genetic *Lkb1* loss in uterine tissue (ie the cervix and endometrium) has been well documented. In one study, sequencing and multiplex ligation probe amplication (MLPA) of human cervical cancers showed nonsense mutations via both deletions and insertions in the *LKB1* locus. This occurred in 12% of the cohort examined among all cervical cancer subtypes [28]. Although MLPA further indicated that exonic *LKB1* deletions occurred in both one and two alleles, this had no bearing on progression free survival of patients. *LKB1* deletions, whether homo- or heterozygous, had significantly accelerated disease progression.

Loss of LKB1 expression is known to exist in endometrial cancers [21, 22]. However, important data obtained by deep sequencing efforts has been scarce until the recent efforts of the Cancer Genome Atlas (CGA) Project. Through copy number analysis of nearly 400 EMCA cases, the CGA has shown that chromosomal region 19p13.3, the *LKB1* locus, was the most frequently deleted chromosomal region among all surveyed cases and histological subtypes ($q=2.75x10^{-43}$) [9]. In contrast, only one missense and one truncating *LKB1* mutation were discovered in separate patients (0.5% of total patients). Taken together, these results demonstrate that chromosomal deletions and mutations in endometrial cancer can propagate the loss of LKB1 expression in tissues, though there may be other mechanisms.

The question remains whether one or two functional copies of *LKB1* are necessary to suppress oncogenesis. *LKB1* loss of heterozygosity and haploinsufficiency has been rigorously explored with mouse models, and appears greatly influenced by the organ system studied and experimental conditions. For example, loss of a single functional *Lkb1* allele via conditional inactivation in cooperation with oncogenic *Kras* propagated pancreatic ductal adenocarcinoma [29] and lung tumors across histological subtypes [30]. Transgenic $Lkb1^{+/-}$ mice succumbed to polyposis and eventual death, though this effect was accelerated in $Lkb1^{+/-}$; $p53^{+/-}$ mice [31]. Though these results favor *Lkb1* as a haploinsufficient tumor suppressor, the deletion of both *Lkb1* floxed alleles in the lung cancer model further accelerated disease progression.

Results from EMCA mouse models show more variability. Conditional deletion of both *Lkb1* floxed alleles with epithelial specific *Cre* in endometrium was necessary to drive lethal, fully penetrant tumors in mice, whereas deletion of one allele had no effect [23]. When uterine injection of adeno-*Cre* was used to delete two *Lkb1* alleles, endometrial tumors developed but with far less penetrance [22]. In another study using adeno-*Cre* delivery to delete two copies of *Lkb1*, additional deletion of *Pten* was necessary to drive tumorigenesis [25]. Lastly, transgenic mice harboring a null *Lkb1* allele developed uterine tumors, but with less penetrance and in a significantly longer period of time [22]. Variability between tissue expressed *Cre* and adeno-*Cre* suggests efficient deletion of *Lkb1* can influence tumor progression in these models. However, consistent with other

tumor models, deletion of both *Lkb1* copies does seem necessary to accelerate tumor progression and mortality.

Transcriptional regulation of LKB1

Small percentages of LKB1 deletion and mutation [9] suggest that other mechanisms (both epigenetic and protein regulatory) are involved in reduced LKB1 expression. Computational analyses of the LKB1 promoter region have shown the presence of multiple estrogen responsive elements (EREs) [32], STAT binding/interferon gamma-activated sequence (GAS) motifs [33], P53 binding sites, activator protein-1 (AP-1) binding sites, and CCAAT/enhancer binding protein (C/EBP) sites [34]. Of these, the former three have been tested for their effect on *LKB1* transcription *in vitro*.

Estrogen Receptor-α (ER-α) is capable of binding EREs. In MCF-7 breast cancer cells, binding of ER-α to the *LKB1* promoter region downregulates *LKB1* mRNA and protein, and subsequent knockdown of ER-α increases promoter activity and transcriptional LKB1 levels. The treatment of cells with 17β-estradiol induced the same effects as ER-α [32, 35], demonstrating a repressive role of estrogen signaling on LKB1 status. Lowered LKB1 expression observed in subsets of human EMCAs [22] may in part be attributed to aberrant estrogen signaling [36], though this has not yet been tested.

The *LKB1* promoter also contains a STAT binding/interferon gamma-activated sequence (GAS), found active in MCF-7 and MDA-MB-231 cells.

Pharmacological activation of STAT with prolactin increased LKB1 transcripts and protein. Mutation in the binding of the GAS motif inhibited these effects concurrently with prolactin treatment, implicating a role for JAK-STAT signaling in *LKB1* transcriptional regulation [33]. Inflammation during menses is common to the uterus, yet a link between menses, JAK-STAT signaling, LKB1 expression and endometrial cancer has not been clearly defined.

The discovery of P53 binding sites in the *LKB1* promoter may be of clinical significance in endometrial cancer. In one study, laser-capture micro-dissection (LCMD) on high grade EMCA cases revealed a significant positive correlation between *LKB1* and *P53* mRNA. When an *LKB1* luciferase reporter was cloned into an endometrial cancer cell line (ECC-1), modulation of P53 levels with siRNA dramatically reduced *LKB1* transcription, whereas P53 overexpression had the reverse effect. Binding of P53 to these sites was validated by chromatin immunoprecipitation. High grade EMCA cases evaluated in this study showed a strong correlation between P53 and LKB1 protein expression levels [34]. Notably, mutations in P53 occur frequently (>70%) in subsets of EMCAs characterized by chromosomal instability [37] and 25% in high grade tumors [9]. Given this information, it is imperative to investigate LKB1 expression in cases of absent P53 expression, and whether or not targeting cancerous pathways associated with LKB1 loss would be of therapeutic benefit in these subsets.

Other mechanisms of LKB1 transcriptional regulation include methylation at CpG islands in the promoter region. Primary papillary breast, testicular, and

colorectal carcinoma cases showed *LKB1* promoter hypermethylation at CpG islands. In colorectal cell lines featuring promoter hypermethylation, *LKB1* transcripts were undetectable [38, 39]. Pancreatic carcinoma cell lines show similar qualities; interestingly, *LKB1* expression in these cell lines can be restored by treatment with demethylating agent 5-aza-2'-deoxycytidine [40]. Although these studies suggest that LKB1 promoter hypermethylation can account for LKB1 loss in various cancers, this seems to be context dependent. Evaluation of low and high grade endometrioid endometrial cancer cases, for example, showed reduced *LKB1* transcripts but no evidence of promoter hypermethylation [34]. Further, deep sequencing of uterine cancers collectively shows few DNA methylation changes in the *LKB1* promoter [9]. Therefore, the change in *LKB1* expression at the epigenetic level possibly stems more from aberrant transcription factor activity and less from hypermethylation.

Structure, regulation, and binding proteins in mammalian cells

LKB1 is composed of 433 amino acids that form a central catalytic protein kinase domain surrounded by N- and C- terminal regulatory domains [41]. Phosphorylation of LKB1 in the regulatory domains can occur at 8 total sites; half of these are direct targets of LKB1 itself that include Thr185, Thr189, Thr336, and Ser404. Phosphorylation of these sites does not affect kinase activity or localization in vitro, whereas sites phosphorylated by upstream kinases (Ser31,

Ser325, Try366, and Ser431) can influence LKB1 cellular localization and enzymatic activity [26, 41-44].

Whereas phosphorylation can affect LKB1 activity and localization, ubiquitination has been implicated in the stabilization of LKB1. Pull down experiments have shown as association of the molecular chaperones HSP90 and CDC37 with the kinase domain of LKB1. Pharmacological inhibition of these molecular chaperones resulted in ubiquitination and degradation of LKB1 into the proteasome [45], suggesting their function is to stabilize LKB1 during times of cellular stress. Paradoxically, this interaction was also shown to reduce LKB1 kinase activity [46]. As LKB1 plays a central role in regulating cell behavior during metabolic stress (described below in more detail), it can be expected that heat-shock proteins and chaperones upregulated during cellular stress maintain LKB1 stability during a critical time when it is needed.

Aside from post-translation modifications, LKB1 kinase activity is governed by the heterotrimeric complex formed between the association of LKB1 with two proteins called sterile-20-related adaptor (STRAD) and mouse protein 25 (MO25). MO25 serves as a scaffolding protein that binds to the c-terminus of STRAD, enhancing its binding to LKB1. STRAD subsequently promotes the active confirmation of LKB1 [47, 48]. In vitro models have shown the interaction of these two proteins with LKB1 is critical for constitutive kinase activity [49, 50]. The STRAD/MO25 complex is equally essential for translocating LKB1 from the nucleus to the cytoplasm and cell membrane, where it performs the majority of its functions [50].

The regulation of LKB1 stability and activity by association with different proteins (STRAD/MO25, chaperones) leaves open the possibility that LKB1 expression levels in cancer are not solely the result of genetic and epigenetic alterations, but also the presence and/or absence of other functional proteins. Evidence for this depends on the protein(s) analyzed. Although loss of heterozygosity in *STRAD* has been observed in subsets of sporadic adenocarcinomas and Peutz-Jeghers patients, no somatic mutations that would weaken the interaction between STRAD and LKB1 were found [51]. Similar results were seen in a European cohort of PJS patients for STRAD and MO25 [52]. In contrast, point mutations in *LKB1* weakening the interaction between LKB1 and chaperones was discovered in a case of testicular cancer, making LKB1 in these cells more vulnerable to degradation [45]. Mechanisms such as this have yet to be explored in cancers of the uterus.

Identification of AMPK and related substrates

The discovery of AMPK as a substrate for LKB1 phosphorylation began in the yeast *Saccharomyces cerevisiae*. Protein kinases Elm1 (elongated morphology-1), Sak1 (snf-1 activating kinase-1), and Tos3 (target of Sbf-3) were identified by co-purification with the *AMPK* homologue *Snf-1* (sucrose non-fermenting-1) [53, 54]. Genetic knockout of these proteins resulted in absent phosphorylation at SNF-1's threonine activation loop, significantly reducing its activity [55]. Expression of Tos3 in vitro demonstrated phosphorylation of

human AMPK on threonine 172. Furthermore, Tos3 shared sequence similarity to LKB1. This led to testing and validation of LKB1-mediated AMPK phosphorylation in various models [55-57].

The threonine activation loop and surrounding residues of AMPK were shown to be evolutionarily conserved with an orthologue of AMPK (AMPKα2) as well as 12 other AMPK family members [58] in humans, suggesting their involvement as substrates for LKB1 phosphorylation. Decisively, phosphorylation of AMPK family members at the threonine activation loop by LKB1 greatly enhanced their activity in kinase assays, thus confirming them as true LKB1 substrates. In LKB1 deficient HeLa cells, the activity of AMPK family members was restored by expressing wildtype *LKB1*, thus showing *in vivo* regulation of AMPK by LKB1.

Regulation of energetics by LKB1-AMPK

AMPK is a heterotrimer consisting of a catalytic subunit (AMPKα) and two regulatory subunits (AMPKβ and AMPKγ). The β subunit is a scaffolding protein on which the AMPK complex assembles, whereas the γ subunit facilitates binding to adenosine monophosphate [59]. AMPK is fully active when AMP binds the AMPK complex at the cystathioninebeta-synthase (CBS) domain located on the AMPK gamma subunit, which in turn stimulates the phosphorylation of Thr172 in the T loop of the catalytic subunits AMPKα1 and 2 [60]. AMP binding to the γ subunit induces a conformational change that can

inhibit dephosphorylation of Thr172, thus keeping pAMPK in its active conformation.

In times of metabolic stress or when cellular nutrients are low, the ratio of ATP/AMP in cells decreases. Elevated AMP binds AMPK, and upon LKB1 phosphorylation, activated pAMPK phosphorylates a number of proteins responsible for energy restoration and conservation. The activation of catabolic pathways involving the cellular uptake of glucose and beta oxidation of fatty acids restores energy [61]. Activated AMPK inhibits anabolic pathways such as fatty acid and cholesterol synthesis through phosphorylation of the metabolic enzymes Acetyl-CoA carboxylase (ACC) and HMG-CoA reductase (HMGR) [62].

To conserve energy, pAMPK decreases ATP- consuming processes such as protein synthesis and cell growth [63] by regulation of the mTOR pathway. Activated pAMPK phosphorylates the tuberous sclerosis tumor suppressor complex (TSC1) [64] and the protein raptor [65]; the former inhibits mTOR signaling through the GTPAse rheb [66] and the latter, when phosphorylated, inhibits mTOR by the recruitment the 14-3-3 adaptor protein to mTOR [65]. The net result of either process is the inability of mTOR to activate key proteins (ribosomal S6 [67] and 4EBP1) involved translation of mitogen stimulated mRNAs responsible for cell cycle initiation and proliferation [64].

Involvement of LKB1-AMPK-mTOR in cancer

Deregulation of the LKB1-AMPK-MTOR pathway has been well documented in a variety of cancer models, albeit with different outcomes based on tissue type. It is conceivable that *LKB1* loss could result in less restraint on cell growth and proliferation, and would therefore facilitate neoplastic growth by elevating mTOR signaling. In support of this, *Lkb1* null gastrointestinal polyps from *Lkb1* mutant mice show elevated signaling downstream of mTOR [68]. Deletion of LKB1 in the liver, in addition to metabolic defects, also reverses AMPK activity and increases mTOR signaling [69]. ErbB2-mediated mammary gland tumorigenesis, a mouse model of breast cancer, saw elevated mTOR signaling when genetic *Lkb1* deletion occurred [70]. Lastly, conditional deletion of *Lkb1* in endometrial epithelium produces invasive tumors characterized by elevated phosphorylated ribosomal S6 [23], an effect also observed in *Lkb1/Pten* double knockout animals [25] and in animals harboring Lkb1 deletion in uterine stroma [24]. Importantly, all three EMCA animal models display therapeutic sensitivity to mTOR inhibitors such as rapamycin and BEZ235 (described below in more detail).

In contrast, there are also instances when unchecked mTOR signaling via LKB1 loss is adverse for cells, especially when nutrient availability is low. *Lkb1* null murine embryonic fibroblasts (MEFs) display hypersensitivity to apoptosis induced by energy stress compared to Lkb1 wildtype cells [71], while $Lkb1^{+/-}$ MEFS are resistant to transformation in combination with oncogenes such as *H-Ras* [72]. Transient knockdown of AMPK via shRNA in pancreatic cancer cell lines significantly diminishes their tolerance to glucose deprivation. Additionally,

stable shRNA-AMPK pancreatic cell lines do not grow in orthotopic mouse models [73]. Although the mechanism as to why LKB1 loss stunted cell growth in these models was not explained, it was discovered that LKB1-AMPK phosphorylation is critical for stabilization of the cell cycle dependent kinase inhibitor (CDKI) P27, which is critical for cell survival through autophagy induction [74]. Therefore, it is not uncommon for endogenous LKB1 to activate substrates conducive to preserving cells during harsh conditions. To prevent cells from transformation, the effects of losing these "pro-survival" signals must outweigh the acquired effects of hyperactive mTOR signaling.

Closer examination of downstream mTOR targets further supports this argument, and reconciles this paradox of aberrant LKB1-AMPK-mTOR signaling being both helpful and obstructing for cancer cell growth. In one instance, a non-small cell lung carcinoma (NSCLC) cell line, A549, which displays no LKB1 expression and elevated mTOR signaling, was shown to produce hypoxia-inducible factor-1α (HIF-1α) under normal nutrient conditions. Upon treatment with the mTOR inhibitor rapamycin, HIF-1α levels significantly dropped. Importantly, HIF-1α transformed the metabolic profile of these cells during nutrient depravation and enabled their survival during these conditions [75]. Another study implicating LKB1-AMPK in regulation of HIF-1α in MEFs [76] has been documented.

Downstream targets of MTOR-HIF-1α signaling have multiple protumorigenic effects. For example, a matrix remodeling protein called lysyl oxidase (LOX), normally downregulated by the LKB1-MTOR pathway, was

highly expressed in lung epithelium upon genetic *Lkb1* deletion. LOX expression negatively correlated with LKB1 status, and increased LOX expression facilitated the migration and anchorage independent growth of lung epithelial cells [77]. Additionally, mTOR induced activation of C-MYC and SREBP1, additional transcription factors that can facilitate tumor lipogenesis, cell growth, and angiogenesis in harsh conditions, has been observed [78, 79]. Taken together, these results suggest that cancer cells undergoing LKB1 loss and hyper mTOR activity can bypass cell death if they are able to upregulate (via mTOR or other mechanisms) survival or tumorigenic factors that allows them to adapt to their conditions. These factors must be able to outweigh the net effect of pro-survival signals that are diminished during LKB1 loss.

LKB1 regulation of CREB targeted genes by AMPK related family members

Phosphorylation of AMPK family members by LKB1 can regulate genes independent of mTOR activity. A subset of these genes is under control of the cyclic-AMP (cAMP) response element-binding protein (CREB). The CREB-transcriptional co-activator (CRTC) family, identified through high throughput screening of cDNAs that target cAMP responsive elements in luciferase vectors and the IL-8 promoter region [80, 81], aids in the transcription of CREB targeted genes; many of which regulate metabolic functions such as gluconeogenesis and lipid metabolism [82].

Several models have implicated LKB1 in the regulation of CRTC orthologues by phosphorylation of AMPK and another AMPK family member known as salt-inducible kinase (SIK). Initially, the CRTC2 orthologue was described as a phosphorylation target of AMPK. Under nutrient deprivation, activated AMPK phosphorylates CRTC2, which sequesters the transcriptional co-activator in the cytoplasm and prevents it from entering the nucleus and aiding CREB in transcription of target genes [83]. Phosphorylation of AMPK by LKB1 regulates this process in mouse hepatocytes [69].

LKB1 deficient HeLa cells illustrate the regulation of SIK on the CRTC1 orthologue. In the absence of LKB1, SIK was unable to phosphorylate CRTC1, leading to constitutive activation of CREB activity. Overexpression of LKB1 in HeLa cells restored SIK activity and minimized CREB transcriptional activation. Further, treatment of LKB1 expressing HEK293 cells with staurosporine, a CRTC1 inhibitor, elevated CREB activity [84]. CRTC3 has also been implicated as a SIK substate using macrophages as a model [85].

Aberrant CREB signaling in LKB1 deficient tumors

A chromosomal translocation in mucoepidermoid carcinoma (CRTC1-MAML2) [86] first uncovered elevated CRTC1 signaling as a potential oncogenic driver [87]**.** Future investigations began to show cancers characterized by LKB1 loss had enhanced CRTC1 activity. In lung tumors with endogenous LKB1, CRTC1 remained phosphorylated in the cytoplasm. Contrarily, *Lkb1* null tumors

showed enhanced nuclear staining for CRTC1, elevated CREB activity, and transcription of genes that facilitated cell growth [88, 89]. This same affect was seen in esophageal cancer cells, with the upregulation of CREB genes involved in invasion and metastatic behavior [90]. Lastly, a group of *Lkb1* null lung cancer cell lines displayed no phosphorylated CRTC1 staining and enhanced transcription of the inflammatory mediator COX2, which selectively responded to COX2 inhibitors when compared to LKB1 wildtype cells expressing phosphorylated CRTC1 [91].

A role for the LKB1-CRTC-CREB signaling axis has not been formally established in endometrial cancer. However, CREB does regulate endometrial cell proliferation under various conditions. For example, a well-established EMCA cell line, Ishikawa, utilizes CREB to transcribe cyclin D1 and promote cell cycle progression in the presence of bile acids [92] and leptin [93], an adipocyte derived hormone. As Ishikawa cells express LKB1, they may be an ideal cell line to investigate the effects of LKB1 loss on CRTC-CREB signaling. Most recently, knockdown of LKB1 via shRNA lentiviral transduction in immortalized endometrial epithelial cells resulted in the production of CCL2, as did conditional ablation of *Lkb1* in mouse endometrium (see chapter 6). This facilitated tumorigenesis by increased macrophage infiltration. Interestingly, CCL2 has been shown to be transcriptionally regulated by CREB [94-96], thus hinting at the possible involvement of LKB1 as a mediator of CREB genes both *in vitro* and *in vivo* with pro-tumorigenic effects, though this has yet to be tested.

LKB1 regulates cell polarity

Aside from energetics, LKB1 plays a major part in spatial organization of cellular components, or polarity. The discovery of a link between LKB1 and polarity was first discovered in *Par-4*, the *C. elegans LKB1* homologue. *Par-4*, when absent due to a missense mutation or RNA interference, failed to make asymmetric divisions necessary for the development of the anterior and posterior axis in embryos [97]. In higher organisms, a genetic screen uncovered *Lkb1* as a facilitator of anterior and posterior oocyte development. When phosphorylated by upstream kinases, LKB1 also mediated polarization of epithelial cells and the microtubule cytoskeleton in *Drosophila* [98]. In mammals, LKB1 was also implicated in polarization of mouse oocytes [99].

AMPK family members involved in LKB1 polarity regulation soon became clearer, albeit through studies in non-human organisms. For example, Madin-Darby canine kidney (MDCK) cells showed that LKB1 phosphorylation of AMPK was critical in the formation of epithelial tight junctions during energy stress. When AMPK dominant negative mutations were introduced in MDCK cells, tight junction assembly was inhibited and could only be rescued through mTOR inhibition [100, 101]. The LKB1-AMPK-mTOR pathway has also been documented to establish sertoli cell polarity and tight junctions in mice testes [102]. Further studies in mice discovered LKB1 phosphorylates the SAD kinases, which induced activation of microtubule-associated proteins that polarized dendritic/axonic polarization of neurons [103]. Studies in Drosophila showed LKB1-induced adherens junction formation in the eye possibly through SIK and

NUAK, another AMPK family member [104]. Examined closely, the results of these studies implicate Lkb1 in the regulation of cell polarity through diverse and tissue specific pathways, thus highlighting multiple points where polarity establishment can go awry and lead to cancerous phenotypes.

LKB1, polarity, and cancer

Loss of polarity facilitates cancer growth in a variety of ways. The disruption of mitotic spindle can lead to aneuploidy in epithelium [105] and accumulation of cytoskeletal components at the leading edge of cells [106], which triggers invasion into surrounding tissue. Misalignment of other critical cellular factors between stem and progenitor cells during division confers to the latter a more "stem-like," proliferative phenotype [107]. Lastly, disruption of epithelial and tight junctions precipitates a migratory, mesenchymal-like phenotype in cells, thus enhancing invasive and metastatic properties [108].

The involvement of LKB1 and polarity in humans was first demonstrated by intestinal epithelial cells *in vitro*. Ectopic STRAD expression in these cells activated LKB1, leading to the formation of an apical brush border by cytoskeletal rearrangement and the relocation of junctional proteins ZO-1 and P120 to their proper locations [109]. The link between STRAD, LKB1, and polarity was also seen in cultured cervical cancer cell lines, where loss of LKB1 resulted in reduced STRAD protein levels and misaligned lamellipodia and golgi

[110]. However, in spite of apparent polarity loss, these cells were unable to invade through a matrigel derived membrane.

Developmental abnormalities and more clinically malignant phenotypes in light of LKB1-driven cytoskeletal rearrangement were seen in studies involving hematopoetic stem cells (HSCs) and melanocytes [111, 112]**.** In the first study, a mouse line transgenic for *Mx-1-Cre*, a lymphocyte-specific promoter responsive to polyinosinic-polycytidylic acid (pI:pC), was crossed with $Lkb1^{f/f}$ mice. Following injection with pI:pC, HSCs were isolated and cultured from control and $Lkb1^{-/-}$ animals. HSCs with LKB1 loss were frequently apoptotic, displayed aberrant mitotic spindles, and contained abnormal numbers of chromosomes; features contributing to pancytopenia observed in *Lkb1-/-* mice [111].

The deletion of *Lkb1* in melanocytes affected mitotic spindle formation as well [112]. In this study, which employed a tamoxifen inducible *Cre* line, *Lkb1* loss in the background of oncogenic *Kras* produced melanocytes exhibiting metastatic behavior when assayed for migration in matrigel or by wound closure index. In comparison to isogenic *Kras* cells, *Lkb1* loss promoted phosphorylation of the SRC kinase YES, which when active, associates with actin filaments and regulates the cytoskeleton [113].

The aforementioned studies shared significance in that induction of polarity was observed through conventional tissue culturing assays. Recently, the advent of three-dimensional culturing models has enabled researchers to take a more accurate look at epithelial polarization while taking into account the role of

extracellular matrix, basement membrane, and other stromal-related proteins. A key study utilizing 3D cultures to investigate LKB1 took place in mouse mammary epithelial cells (MMECS). Adeno-*Cre* mediated *Lkb1* ablation showed abnormal morphology and delocalization of polarity markers in comparison to controls (ie apical markers like GM130 were located either laterally or basally). Importantly, *Lkb1* deletion led to basement membrane deterioration but did not facilitate tumorigenesis until coupled with *Myc* mutations. Tumor formation in *Lkb1* deficient, catalytically active *Myc* animals progressed more rapidly than *Myc* mutations alone [106].

Though the HSC, melanoma, and breast cancer models discussed suggest disruption of polarity is insufficient in promoting tumorous phenotypes and that additional oncogenic hits are required, a newly established 3D culture system of endometrial glands argues the contrary. Primary mouse endometrial epithelial cells grown in serum free media and matrigel developed glandular structures showing apical and basal polarity with correct positioning of tight and adherent junctions. shRNA mediated knockdown of E-cadherin in these cells resulted in a complete loss of cell polarity, which lead to β-catenin translocation and polymerization of stress fibers [114]. Though shRNA-E-cadherin cells were not assayed for invasiveness, the qualities described are common to cells with invasive properties. This further lends supports the idea that loss of cell polarity is common among adenocarcinomas of endometrial origin [115].

LKB1 polarity regulation has not been examined in 3D cultures of the endometrium. However, *in vivo* mouse models still can provide clues to its

function. Adeno-*Cre* deletion of *Lkb1* in endometrial epithelium resulted in invasive adenocarcinomas. Unexpectedly, *Lkb1*$^{-/-}$ epithelia strikingly resembled the appearance of normal cells when compared by H&E staining and electron microscopy. Markers of apical polarity, such as α-lectin, remained in the luminal portions of cells [22]. More efficient *Cre* delivery through the use of endometrial epithelial specific promoter *Sprr2f* still produced no changes in polarity, but did yield invasive tumors at shorter latency and higher penetrance [23]. In both studies, mitotic spindle effects were not observed.

Overall, these results imply that regulation of polarity by LKB1 is highly tissue specific and exhibits stronger regulation in cancers of the breast, skin, and cervix compared to the endometrium. LKB1 loss in these tissues may drive loss of polarity, but it seems that additional oncogenic hits (*K-ras*, *myc*) are necessary for aggressive tumor development. Though this may not be a requirement for endometrial epithelium in light of polarity loss, LKB1 does not seem to affect polarity via cyto-architecture in the studies highlighted. The well differentiated appearance of tumors from both the adeno-*Cre* or *Sprr2f-Cre* models suggests that mitotic defects and aneuploidy were not affected by *Lkb1* loss.

Cooperation between LKB1 and P53

The tumor suppressor P53 plays an important role in apoptosis and cell growth arrest. The mechanisms for this are not completely understood, but growing evidence supports LKB1 as a critical partner in P53-mediated apoptosis.

In HT1080 cells, expression of a dominant negative LKB1 mutant made cells resistant to the P53-mediated apoptosis agent paclitaxel. Expression of a dominant negative P53 mutant with wildtype LKB1 (known to induce apoptosis in this cell line) further inhibited cell death, with LKB1 physically associating with and stabilizing P53 [116]. As further support to this study, and the idea that LKB1 function plays an apoptotic role, homozygous deletion of *Lkb1* or *p53* with oncogenic *Kras* in mice significantly reduces tumor sensitivity to docetaxel, another anti-mitotic apoptosis inducing drug [117].

Mechanistic studies further link LKB1 as a stabilizer of P53 in the nucleus. Together, the binding of these two is necessary for the transcription of the CDKI P21 to induce G1-cell cycle arrest in MEFs [118, 119], an effect described previously in G361 melanoma cells [120]. Notably, LKB1 can also act through the downstream AMPK family member NUAK1 to phosphorylate and activate P53 to turn on P21 expression [121].

Cooperation between P53 and LKB1 has been observed in animal models of PJS. Loss of P53 increased the frequency of GI polyposis and significantly shortened the survival of $Lkb1^{+/-}$; $p53^{-/-}$ mice compared to $Lkb1^{+/-}$ mice [31]. Studies such as this have not been employed in EMCA mouse models, however. Though significant strides have been made in characterizing P53, chromosomal instability, and tumor progression in EMCAs [122], it has yet to be seen if concurrent *Lkb1* loss can enhance tumor progression in these models. This information is critical because 1) high grade tumors typically show loss of LKB1

expression [22] and chromosomal instability [123] and 2) p53 mutations are frequent in 10-20% of endometrial cancers [123].

Cooperation between LKB1 and PTEN

The PTEN phosphatase plays a substantial role in the suppression of mitogenic signaling by directly opposing the catalytic function of PI3K, which is to phosphorylate lipid messengers that transduce growth signals to downstream effectors such as AKT [124]. Interactions between LKB1 and PTEN have been well established. Yeast two hybrid screens revealed that LKB1 binds to and phosphorylates PTEN [125]. LKB1 can also induce *Pten* transcription [42].

Most importantly, LKB1 and PTEN converge on mTOR regulation. Whereas PI3K-AKT signaling can suppress TSC and thereby activate mTOR, PTEN and LKB1 both inhibit this effect [124]. This convergence is well illustrated in ovarian serous carcinoma, the most common subtype of ovarian cancer associated with poor prognosis and frequent mutations in LKB1, PTEN, and the mTOR regulator TSC1 [126]. In mice, deletion of *Lkb1* and *Pten* using an ovarian-specific *Cre*-promoter led to ovarian serous tumors with 100% penetrance, whereas deletion or *Lkb1* alone resulted in no tumor formation.

Additional models highlight the synergistic effects of losing both tumor suppressors in carcinogenesis. In the bladder, for example, conditional deletion of both *Lkb1* and *Pten* alleles ($Lkb1^{-/-}$; $Pten^{-/-}$) in epithelium resulted in fully penetrant urothelial tumor growth and animal mortality, whereas single $Lkb1^{-/-}$ or

Pten$^{-/-}$ animals displayed no tumor growth. Importantly, this was mediated through hyper-mTOR signaling as rapamycin treatment prevented tumor formation in double knockout mice [127]. Conditional deletion of *Lkb1* and *Pten* in the lung produced squamous cell carcinomas that displayed enrichment of upregulated mTOR target genes [128].

Mouse models of endometrial cancer have further illustrated the convergence of *Lkb1* and *Pten* on mTOR signaling. *Sprr2f-Cre* mediated deletion of *Lkb1* from endometrial epithelium resulted in tumors expressing high levels of PS6, a downstream mTOR marker. Further, these tumors were sensitive to mTOR inhibition by rapamycin [23]. A newer model of EMCA has been developed in which adeno-*Cre* delivery was used to conditionally delete both *Lkb1* and *Pten* from the endometrium, resulting in fully penetrant tumors, shortened survival, and markers of hyper PI3K and mTOR signaling (pAKT and PS6, respectively). Interestingly, the combination of *Lkb1* and *Pten* inactivation gave rise to higher grade, metastatic tumors found in the lung; an affect not typically seen in other EMCA models of Lkb1 loss. In spite of these malignant features, tumors were still therapeutically responsive to the dual PI3K/mTOR inhibitor BEZ235 [25], suggesting that these phenotypes were largely mTOR driven. Deletion of either *Lkb1* or *Pten* did not result in aggressive tumor formation, arguing that either gene can compensate for the other in suppressing mTOR activation.

Results from both studies correctly model human data, where loss of PTEN occurs in 77% of endometrial cancers and activating mutations of PI3K

occur 53% of the time (Cancer Genome Atlas) [9]. Interestingly, endometrial cancer cells in culture are more sensitive to rapamycin than other tissue [23], and ectopic expression of LKB1 in *Lkb1/Pten* deficient endometrial cells sensitizes them to PI3K inhibitors [25]. In summary, mouse models and human data suggest that *Lkb1* loss in a *Pten* deficient background is highly advantageous for tumor growth and progression, with downstream mTOR activity serving as one of the main culprits. In these tumors, especially those of the endometrium, mTOR inhibition could be therapeutically beneficial for patients.

Cooperation between LKB1 and KRAS

Oncogenic KRAS is an important messenger upstream of mitogenic pathways, including PI3K and MAPK signaling [129]. Given that LKB1 can inhibit many of the downstream effectors of these pathways, it is plausible that LKB1 and oncogenic KRAS can cooperate and accelerate tumorigenesis. Several mouse studies have demonstrated tremendous synergy between oncogenic *Kras* and *Lkb1* compared to the pairing of *Kras* with other tumor suppressors. In lung carcinoma, *Cre*-inducible oncogenic *Kras* and either germline *Lkb1* mutants ($Lkb1^{-/-}$) or conditional Lkb1 ($Lkb1^{f/f}$) alleles produced tumors resembling a variety of histological subtypes. Importantly, the *Kras;* $Lkb1^{-/-}$ pairing produced the shortest tumor latency, lowest median survival, and greatest number of metastases compared to *Kras;* $p53^{-/-}$ and *Kras;* $p16^{ink4a-/-}$ mice [30]. Aggressive, metastatic phenotypes were also seen in mouse melanoma models combining

oncogenic *Kras* and *Lkb1* loss. Compared to no distant metastases in either *Kras*; *p53*$^{-/-}$, *Kras*; *p16*$^{-/-}$, or combined *Kras*; *p53*$^{-/-}$;*p16*$^{-/-}$ mice, oncogenic *Kras* combined with homozygous *Lkb1* deletion produced tumor nodules in the lymph node, lung, liver, and spleen of animals [112].

Cultured cell lines from the melanoma model show that enhanced invasive/metastatic activity may be due to loss of LKB1 signaling to microtubule affinity-regulating kinase (MARK) family members, which were shown to be important for preventing invasion into collagen [130]. This appropriately ties in with LKB1 regulation of polarity, which may account for the enhanced metastatic potential of *Lkb1* mutants in an oncogenic *Kras* background compared to mutations in other tumor suppressor genes. Though an oncogenic *Kras; Lkb1* null model has not been generated for endometrial cancer, a study as such would prove significantly helpful. Oncogenic *Kras* signaling occurs in 24.6% of endometrial cancers [9], and has been shown to play a role in progression of primary to metastatic lesions [131]. As *Lkb1* mutations in an oncogenic *Kras* background promote metastasis formation in many tissues, sequencing *Kras* mets from the endometrium for *Lkb1* loss would go a long way in validating this hypothesis.

CHAPTER THREE

Introduction

MOUSE MODELS OF LKB1-DRIVEN ENDOMETRIAL CANCER

Originally a model to study polyposis in the GI tract [72], transgenic female *Lkb1*$^{+/-}$ mice not succumbing to disease spontaneously developed uterine neoplasms within a year's time [22]. Histologic examination of uterine growths revealed the presence of well-differentiated, endometrial adenocarcinomas that had infiltrated uterine myometrium and serosa. Abnormal growths in other tissues were not observed.

In spite of long latency and low penetrance (close to 50%) from *Lkb1*$^{+/-}$ mice, these results prompted further development of models that relied on *Lkb1* deletion specific to endometrial epithelium. The first of these was the use of adenoviral *Cre* vector injected into the uterine lumen of mice harboring conditional *Lkb1* alleles (*Lkb1*$^{f/f}$) at 6 weeks of age [22]. Histology of resultant tumors resembled those of *Lkb1*$^{+/-}$ mice, albeit with significantly shorter latency (9 weeks compared to 52 weeks) and higher penetrance (63%). Although survival analysis in this study was not performed, another paper demonstrated that deletion of both *Lkb1* alleles resulted in the same histological appearance as described and did not result in mortality of animals when assessed 300 days post *Cre*-injection [25].

The use of adeno-*Cre* for genetic deletion is beneficial for several reasons. First, the symmetry of the uterus allows contralateral injection of virus into a specific uterine horn, thus enabling investigators to examine results of *Lkb1* loss in a "normal" horn versus the tumor horn without any genetic variability. Secondly, as the uterus responds to various hormonal changes [132], the ability to examine the normal and tumor tissue simultaneously minimalizes any confounding effects due to estrous cycling that may occur while comparing two different animals. In light of this, successful characterization of uterine tumors by mitotic and apoptotic activity has been accomplished, showing that tumor cells within the same animal significantly differ in mitotic index and amount of apoptosis compared to normal cells [22]. Lastly, adeno-*Cre* can be delivered at any time throughout the animal's lifespan; thus, the effects of Lkb1 loss can be examined in an age specific context.

The drawback of adeno-*Cre* injections is the efficiency of *Cre* deletion (<1% in Contreras et. al), contributing to perhaps a longer tumor latency compared to other animal models of cancer. This makes it difficult to conduct drug studies in animals and time consuming to harvest tissue for downstream assays. Although the onset of tumors can occur more quickly in this model if additional genes are deleted (such as *Pten* [25]), this confounds the studying of the effects of single gene loss such as *Lkb1*.

The discovery of an endometrial epithelial tissue specific promoter called *Sprr2f* ameliorated the problem of low *Cre* efficiency, longer tumor onset, and variable penetrance. Fragments of the *Sprr2f* promoter were cloned into a

cassette of Cre recombinase, which was then utilized to create transgenic animals [23]. Tissue specific deletion of *Sprr2f-cre*; *Lkb1*$^{f/f}$ mice occurred at 50% efficiency by 6 weeks of age. Appearance of well differentiated, adenocarcinomas developed and invaded into the surrounding myometrium by 16 weeks of age and resulted in mortality by 30 weeks of age. Remarkably, this effect was 100% penetrant without the deletion of other tumor suppressor genes or constitutive activation of oncogenes, contrasting sharply to studies done using adeno-*Cre* deletion of *Lkb1* and many *Lkb1* mouse models in general.

The closest model to mirror the effect of tumorigenesis via solo *Lkb1* loss was done by conditional deletion in the stromal cells of the female reproductive tract. Using Cre recombinase under control of the stromal specific promoter Müllerian inhibiting substance receptor 2 (*Misr2-Cre*), biallelic inactivation of *Lkb1* in stroma facilitated growth of well-differentiated neoplasms in the myometrial compartment of the uterus at 9 weeks of age, eventually leading to endometrial cancer at 24 weeks [24]. Like the *Sprr2f-cre* lines, *Misr2-Cre* deletion of *Lkb1* produced this effect in every mutant animal studied.

Lessons from Lkb1 mouse models of endometrial cancer: Downstream effectors and potential therapeutic targets

Consistent across every murine model of *Lkb1* deletion in the epithelium or stroma was the invasion of highly-differentiated glands into myometrium and serosa. As *Lkb1* loss has been shown to affect polarity in other models, the

structural integrity of *Lkb1*$^{-/-}$ tumor cells in the endometrium was well maintained. Thus targeting any related pathways would have no effect. Interestingly, adeno-*Cre* deletion of both *Pten* and *Lkb1* resulted in high grade, metastatic tumors [25], suggesting that both these tumor suppressors converge on polarity regulation and that targeting downstream responses would be beneficial in this genetic background. In the aforementioned study, dual inhibition of mTOR and PI3K signaling with BEZ235 proved highly beneficial, and may serve as a key drug in metastatic LKB1 deficient endometrial cancers.

Early onset and full penetrance of *Sprr2f-Cre* and *Misr2-Cre* models allowed successful preclinical testing with the compound rapamycin, which was shown to significantly reduce tumor burden in both models. Most importantly, this illustrates that *Lkb1* loss in the uterine epithelium and stroma is largely driven by aberrant mTOR signaling, which is sufficient to induce tumorigenesis without cooperation from oncogenes or loss of other tumor suppressors. In light of this, both of these models allow the investigation of other downstream LKB1-AMPK-mTOR effectors and their contribution to endometrial cancer without interference from other genetic mutations. In my work described in later chapters, studying of the *Sprr2f-cre* model by has shown that hypo-AMPK phosphorylation by *Lkb1* deletion produced significant amounts of the chemokine CCL2, an affect also observed *in vitro* and in human tumor samples. Excess CCL2 resulted in the recruitment of tumor associated macrophages that significantly propagated epithelial invasion in to the myometrium. Importantly, these effects were

attenuated by genetic ablation of *Ccl2* or removal of macrophages by liposomal clodronate.

In Tanwar et. al, it was the hyperproliferation of stromal cells and growth of a myofibroblast cell population that influenced the transformation of adjacent $Lkb1^{+/+}$ epithelium. Additionally, these cells altered neighboring extracellular matrix by producing excess amounts of collagen, a feature shown to influence hyper- and neoplasticity in the endometrium [133]. Taken together, both studies illustrate that *Sprr2f-cre* and *Misr2-cre* are excellent platforms for uncovering the effects of neighboring cells and structures on endometrial cancer progression. A reasonable next step would be to elucidate additional signaling molecules from $Lkb1^{-/-}$ epithelium (like CCL2) or stroma through co-culturing of endometrial cells with different stromal populations (macrophages, myofibroblasts, etc.). If $Lkb1^{-/-}$ cells are selectively responsive to these signals, targeting them through antibodies or blocking their cognate receptors in conjunction with mTOR and/or PI3K inhibition could prove remarkably helpful.

CHAPTER FOUR

Results

INVESTIGATION OF POLARITY LOSS IN LKB1-DRIVEN ENDOMETRIAL CANCERS

Introduction

The *Sprr2f-Cre* model of *Lkb1*-driven endometrial adenocarcinoma is advantageous over other mouse models for the following reasons. First, the development of tumors with 100% penetrance [23] in the absence of other oncogene activation or tumor suppressor loss allows the opportunity to specifically explore LKB1 regulation of biological pathways without interference from other genes. Secondly, the invasiveness of *Lkb1*$^{-/-}$ glands in this model mirrors what has been seen clinically observed in humans, as higher stage tumors with >50% myometrial invasion are frequently associated with *Lkb1* loss [22]. Importantly, this opens the door for clinical testing of therapeutic agents that can target active pathways associated with *Lkb1* loss with potential clinical relevance in humans.

As mentioned, LKB1 phosphorylates an entire family of AMPK-like kinases that can control different cellular functions [17]. Among these, LKB1

regulation of polarity was explored using the *Sprr2f-cre* model because 1) high grade, poorly differentiated tumors show loss of LKB1 expression in endometrial cancer [22], 2) loss of polarity is associated with enhanced metastatic and invasive behavior of tumors [30, 130], the latter especially seen in the *Sprr2f-cre* model, and 3) incomplete recombination at an early age in this model allows visual, side by side comparisons of polarity features in $Lkb1^{+/+}$ and $Lkb1^{-/-}$ cells with a validated LKB1 antibody [134] co-stained with other polarity markers.

The use of lentiviral shRNA to knock down LKB1 in Ishikawa cells, a cancer cell line akin to the mouse model by its well-differentiated appearance [135], was used to examine polarity effects in vitro. In parallel, these two systems would test the hypothesis that LKB1-driven EMCAs occur due to polarity loss. Cell line studies would then facilitate the discovery of novel LKB1 effectors that regulate polarity, and subsequently, provide potential therapeutic targets that could be tested in the mouse model to prevent invasion $Lkb1^{-/-}$ glands.

LKB1 loss in vitro does not affect cytoskeletal organization or cell size

Fifty-percent *Cre*-mediated recombination at 6 weeks of age in *Sprr2f* animals results in a heterogeneous population of $Lkb1^{+/+}$ and $Lkb1^{-/-}$ cells in the endometrium, a feature visually detectable by IHC [134]. Interestingly, cells staining positive for LKB1 consistently appeared longer and more columnar-like (**Fig. 4.1A, rectangular line**) compared to LKB1 null cells (**Fig. 4.1A, square line**), suggesting that LKB1 can regulate cell size in the endometrium. This effect

was not unexpected, as LKB1 has been shown to regulate actin assembly [136] and cell size [137].

Thus, I further explored the possibility that LKB1 loss in vitro would result in the disruption of actin filaments, cell size, and overall cytoskeletal structures. To test this, Ishikawa cells were stably transfected with lentiviruses encoding either non-targeted shRNA or one of two LKB1 shRNAs. Efficient LKB1 knockdown was confirmed via western blot (**Fig. 4.S1A**). To outline the shape of the cells, as well as distinguish the formation of cytoskeletal structures, each cell line was grown at 50% confluency on glass coverslips and then stained with phalloidin, a probe for actin filaments. Confocal microscopy on mounted slides confirmed the presence of actin-assembled structures such as fillopodia (**Fig. 4.1B, middle panel, arrows**) and lamellipodia (**Fig. 4.1B, third panel, arrows**) in cell lines.

Importantly, both fillopodia and lamellipodia are extremely common in invasive, metastatic cancer cells [138]. To see whether or not LKB1 loss resulted in abundance of these structures, I evaluated and scored 100 total samples per cell line based on the presence of fillopodia (scored 1), lamellipodia (scored 2), or complete absence of structures (scored 0) (**Fig. 4.1B, first-third panels**). The average score from 100 cells was taken, which showed no difference between LKB1 positive and LKB1 null cells. Notably, an invasive fibrosarcoma cell line (HT1080 [139]) scored substantially higher than the other cell lines while also showing high metastatic activity (**Fig. 4.1D**), thus confirming the validity of this assay.

Lkb1 loss at 6 weeks of age appeared to reduce cell size in endometrial epithelium. To see if this was the case in vitro, I used image quantification analysis to measure the area of 100 samples per cell line but found no difference between cell lines (**Fig. 4.1C**). Consistent with the lack of actin structure formation or abnormal change in cell size, LKB1 cells exhibited no metastatic behavior in a conventional wound healing assay (**Fig. 4.1D**).

Lkb1 loss in vivo does not affect epithelial integrity

Though modeling *Lkb1*-driven polarity loss in vitro was not accomplished, the epithelial integrity of invasive glands in early (12 week) and late (20 week) disease of *Sprrf2-Cre; Lkb1*$^{f/f}$ mice was still examined by immunofluorescent costaining of the cell-to-cell adhesion marker E-cadherin along with GM130, a marker for the golgi apparatus. Consistent with prior electron microscopy data [22], tissue architecture of invasive glands appeared stable at early disease. As glands continued invasion from myometrium to uterine serosa, cell structure and polarity was remarkably unaltered throughout disease progression. In both early and late stage disease, E-cadherin was widely expressed in epithelium at cell to cell junctures and GM130 localized to the apical (luminal) side of epithelium (**Fig. 4.2A**).

To see if *Lkb1* loss affected the actual development of glandular structures, I had taken advantage of a recently published protocol [114] that allowed for the formation of endometrial glands in three-dimensional cultures

with matrigel. Primary cells from tumor and normal uterine tissue were harvested for this assay. Regardless of LKB1 status, primary cells from normal and tumor uteri formed symmetrical spheroid structures in culture (**Fig. 4.2B**), suggesting that development of glandular epithelium is not affected by LKB1 status.

Discussion

Loss of polarity is one of the hallmarks of cancer [140], as disruption of tissue cytoskeletal components and tissue architecture facilitate a mesenchymal, migratory phenotype in cells that can provoke invasion and migration [108]. LKB1 has been shown to regulate polarity via phosphorylation of various members of the AMPK family such as MARK [130], SIK [104], and NUAK [104], as well as physical interactions with the SRC kinase family members [113]. Loss of *Lkb1* cooperates with oncogenic *Kras* to produce invasive, metastatic tumors of the lung [30] and skin [112, 130]. Concurrent loss of *Lkb1* and *Pten* via adeno-*Cre* deletion in the endometrium leads to poorly differentiated, metastatic growths in the lung [25], suggesting a role for mTOR activation in the development of these tumors.

My early studies were based on utilizing the *Sprrf2-Cre* mouse model to see whether or not genetic ablation of *Lkb1* affected polarity in the endometrium. This was in light of the development of highly invasive adenocarcinomas in this model, which migrated from endometrial stroma to myometrium to serosa in late stage disease. Importantly, like the *Lkb1/Pten* model which produced metastatic

tumors, *Lkb1* tumors displayed hyper-mTOR activation [23]. Therefore, it was plausible that polarity loss could be examined in this model and further elucidated with LKB1 knockdown in well-differentiated human cancer cell lines such as Ishikawa.

In these cells, close to 100% efficient knockdown of LKB1 produced no changes in actin organization and cytoskeletal structures such as fillopodia and lamellipodia, nor alterations in cell size. Changes in cell size were investigated because in six week old $Lkb1^{-/-}$ animals that have not undergone complete loss of *Lkb1*, adjacent $Lkb1^{+/+}$ cells in luminal and glandular epithelium appeared larger in appearance than $Lkb1^{-/-}$ cells with LKB1 antibody staining. However, further H&E staining of serial sections used for IHC revealed undetectable differences in cell size, owing to perhaps the staining signal observed by the antibody used.

Although $Lkb1^{-/-}$ glands in the endometrium are highly invasive, the epithelial integrity of these cells is remarkably maintained throughout all stages of disease. E-cadherin is highly expressed between the lateral compartments of cells, suggesting that 1) these cells have not undergone epithelial to mesenchymal transition and 2) $Lkb1^{-/-}$ glands are highly polarized. In support of this, staining of the golgi marker GM130 is apical in $Lkb1^{-/-}$ tumors, resembling the physiological organization of glandular cells that secrete proteins into the lumenal cavity. Visually, establishment of $Lkb1^{-/-}$ glands in three-dimensional cultures did not differ in appearance from $Lkb1^{+/+}$ glands, with both types assembling into spheroid structures.

Taken together, these results suggest that LKB1 status alone does not influence polarity in *Lkb1*$^{-/-}$ mouse models of endometrial cancer, and that additional oncogenic hits are necessary to study these effects. This should not rule out LKB1 as a polarity regulator in human tissues, however. Poorly differentiated, high grade tumors in humans show substantial loss of LKB1 expression (see chapter 6). Such tumor subtypes would thus serve as an excellent resource for the discovery of aberrant gene expression in endometrial cancers via deep sequencing, and the generation of mice harboring these defective alleles in cooperation with *Lkb1* loss to see if polarity effects could be modeled in vivo.

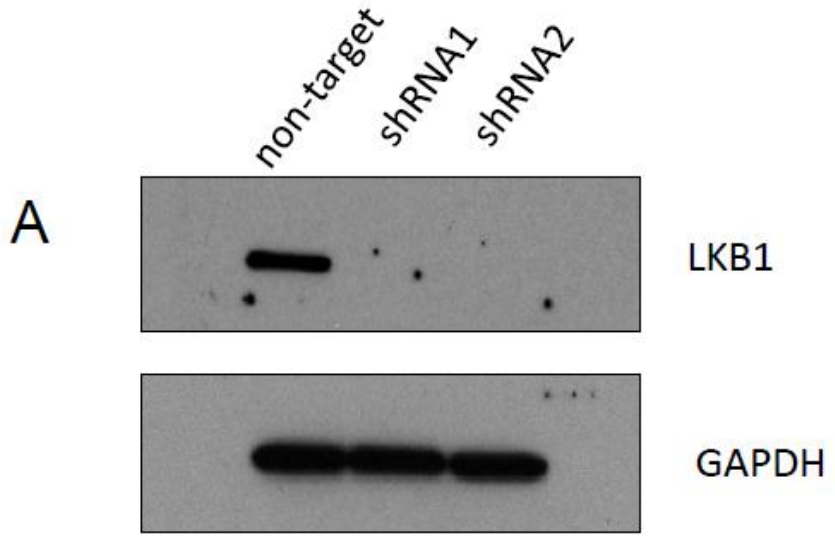

Supplementary Figure 4.1 Validation of LKB1 loss in Ishikawa cells. A) Western blot of Ishikawa cells stably transduced with lentivirus encoding either non-target shRNA, or one of two different LKB1 shRNAs (shRNA1, shRNA2) that resulted in efficient LKB1 knockdown.

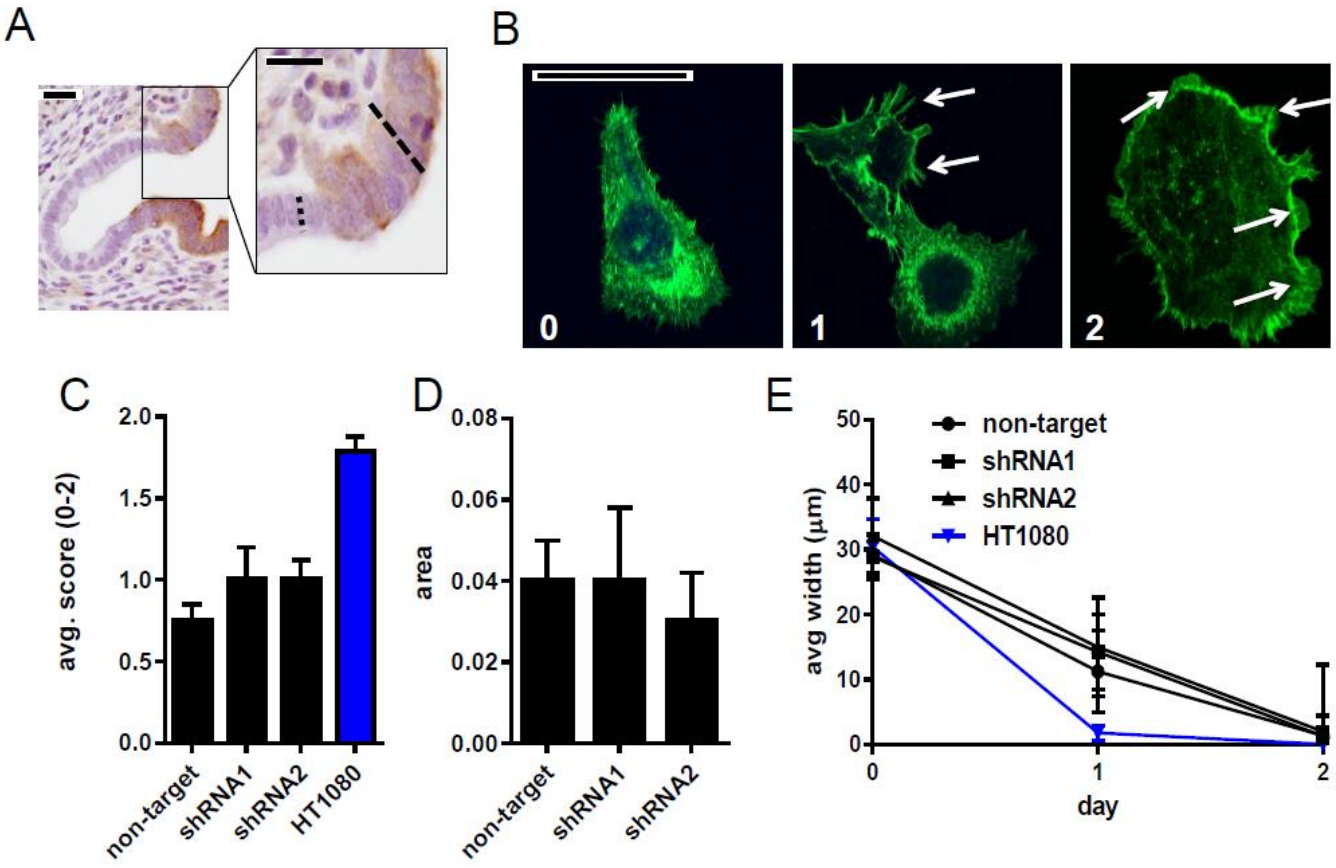

Figure 4.1 Cell size and cytoskeletal structures based on LKB1 status. A) LKB1 immunohistochemistry of uterine tissue sections from 6 week old mosaic *Lkb1*$^{-/-}$ mice showing variable cell size in positive stained tissue (rectangular dashed line) versus unstained tissue (square dashed line). B) Phalloidin staining of Ishikawa cells showing fillopodia (second panel, arrows) and lamellipodia (third panel, arrows). Absence of structures in cells was scored "0" while "1" and "2" were the designated scores of fillopodia and lamellipodia, respectively. C) Average scores taken from each cell line after counting 100 different cells. HT1080 cells are highly motile and invasive, and were thus used as a positive control reference. D) Average cell size of 100 counts per cell line. E) Wound healing assay showing width of wound (µm) over time. Error bars=S.E.M. Size bars=50µm.

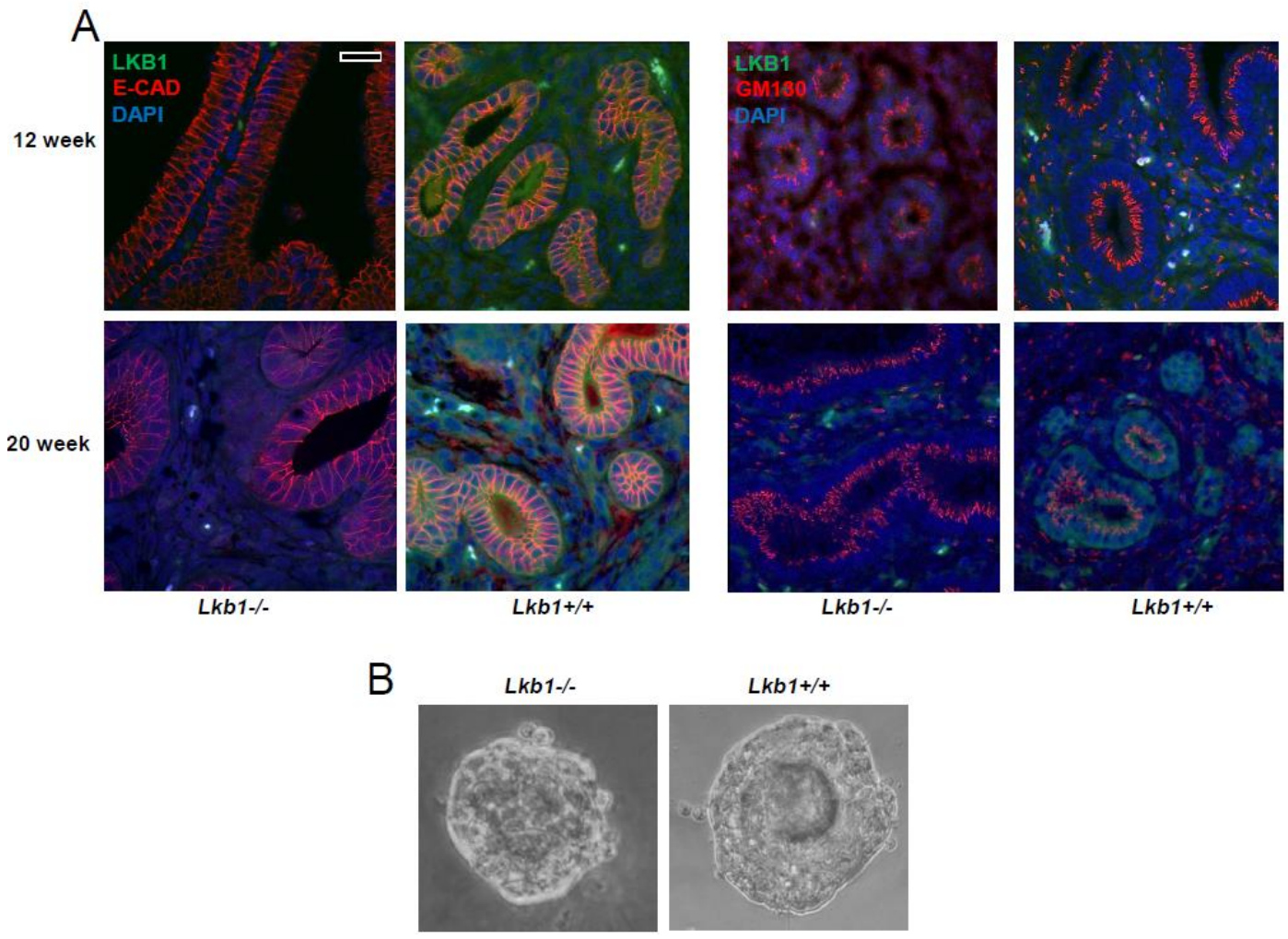

Figure 4.2 Regulation of epithelial integrity in vivo by *Lkb1* loss. A) Immunofluorescent staining of polarity markers in early (12 week) and late (20 week) stage disease of $Lkb1^{-/-}$ mice and $Lkb1^{+/+}$ age-matched controls. B) Bright-field imaging of three dimensional cultures established from primary cells in $Lkb1^{+/+}$ and $Lkb1^{-/-}$ mice. Size bars=50µm.

CHAPTER FIVE

METHODOLOGY

Creation of stable, LKB1 knockdown cell lines by lentiviral shRNA

Nonoverlapping LKB1 shRNA sequences (shRNA1, 5'-CCGGGCCAACGTGAAGAAGGAAATTCTCGAGAATTTCCTTCTTCACGTTGGCTTTTT-3', or shRNA2, 5'-CCGGGATCCTCAAGAAGAAGAAGTTCTCGAGAACTTCTTCTTCTTGAGGATCTTTTT-3') were cloned into AgeI-EcoRI sites of the pLKO.1 vector (Sigma, cat#SHC002). FuGENE HD transfection reagent (Promega, cat# E2311) was used to cotransfect each shRNA vector or a non-target control vector (Sigma, cat#SCH001) with lentiviral packaging plasmid (psPAX2, Addgene cat#12260) and VSV-G envelope expressing plasmid (pMD2.G, Addgene cat#12259) into HEC293T cells for 15 hours. Transfection medium was replaced and incubated in fresh media at 37°C for 24 hours to produce lentivirus particles.

An immortalized, endometrial epithelial cell line (EM cells) [159] was grown in DMEM/F-12, HEPES buffer (Life Technologies, cat#11330) supplemented with 10% fetal bovine serum. EM cells (150,000 cells) were individually infected with lentivirus (non-target, shRNA1, or shRNA2) for 24 hours with polybrene (4µg/ml) (Sigma-Aldrich cat#H9268) followed by replacement of the culture medium with fresh medium. Stably transfected cells were selected by adding 1 µg/mL puromycin (Clontech, cat#631305) over a span

of 1.5 weeks. Three biological replicates of EM cells per lentivirus were created to produce a total of 9 cell lines.

RNA preparation and qRT-PCR

Total mRNA was isolated from EM cells using the RNeasy Mini Kit (Qiagen, cat#74104) per the manufacturer's protocol. cDNA (0.5 µg) was synthesized using mRNA via Superscript VILO (Life Technologies, cat#11754) and diluted in TaqMan Universal PCR Master Mix (Life technologies, cat#4304437) with appropriate TaqMan probes (Life technologies, cat# 4453320). Probes included MXRA5 (Hs01019147_m1), LKB1 (Hs00176092_m1), CRIP2 (Hs00373842_g1), GCNT2 (Hs00377334_m1), FABP4 (Hs01086177_m1), CXCL6 (Hs00605742_g1), FST (Hs00246256_m1), and CCL2 (Hs00234140_m1). qRT-PCR was performed on master mixes in triplicate using Applied Biosystems StepOnePlus real time PCR machine. Cycle threshold (CT) values per gene were averaged together before computing fold change by the ΔΔCT method using GAPDH as a reference gene and EM non-target shRNA cells as reference samples.

Microarray and gene ontology analysis

Microarray hybridization was performed per the manufacturer's specifications with 500 ng of labeled total RNA. Preparation of samples and

loading of RNA onto the HumanHT-12 v4 Expression BeadChip was performed by the University of Texas Southwestern (UTSW) DNA Microarray Core Facility. Three biological replicates of RNA from non-target, shRNA1, and shRNA2 cells were loaded onto the chip.

Array analysis was performed using Illumina GenomeStudio 2011 Software v2011.1. A confidence interval of $p<0.05$ was used to filter out non-specific binding of probes to RNA. Probe intensities of shRNA1 or shRNA2 were normalized to non-target probe intensities and resultant values <3x were excluded. Intensity values that differed in directionality between shRNA1 and shRNA2 were additionally filtered out, leaving 59 probe sets unique to shRNA1, 142 probe sets unique to shRNA2, and 43 probe sets in common. Gene ontology analysis was performed on tabulated genes from the filtered probe sets using a Web-based Gene Set Analysis Toolkit (WebGestalt) [191].

Lysate preparation for immunoblotting and ELISA

Cells in culture were washed in PBS following media aspiration. Cells were mechanically detached from culture dishes in RIPA Buffer (Pierce, cat#89900) supplemented with protease (Roche, cat#11836170001) and phosphatase inhibitors (Sigma, cat#P5726) on ice. Normal and cancerous uteri from mice were rinsed in PBS before homogenization in RIPA buffer. Protein from cells and tissue lysate was quantified using the Pierce BCA Protein Assay Kit (cat#23227). Equal amounts of protein for loaded for western blots and

ELISA. ELISA for murine tumor lysate and serum CCL2 was performed using Mouse/Rat CCL2/JE/MCP-1 Quantikine ELISA Kit per manufacturer's instructions (R&D Systems, cat#MJE00).

In vitro cell culture studies

EM cells (non-target, shRNA1, shRNA2) were plated at a density of 75,000 cells/plate in 6 well plates (Corning, cat#CLS3516). Cells were allowed to grow for 24 hours, rinsed in PBS, and replaced with fresh medium containing either PBS (vehicle), 0.5 mM AICAR (Sigma, cat# A9978) or 5mM metformin (Sigma, cat#PHR1084). Lysates and conditioned media were harvested from cells 24 hours after drug treatment. Western blotting on lysates (including non-drug studies) was done using 1:1000 dilutions of the following antibodies (all from Cell Signaling Technologies) in 5% milk in Tris Buffered Saline: LKB1 (cat#D60C5) pAMPK (Thr172) (cat#2535), AMPK (cat#2603), pS6 (cat#4857), S6 (cat#2217), p4EBP1 (cat#9455), 4EBP1 (cat#9452), and GAPDH (cat#2118). ELISA on conditioned media (including non-drug studies) for CCL2 was performed using Human CCL2/MCP-1 Quantikine ELISA Kit according to manufacturer's instructions (R&D Systems, cat#DCP00).

Growth and migration assays were done as described [112]. CCL2 cDNA subcloned into a pDream2.1 plasmid was purchased through Genescript, cat#SD0222). Transfection into Ishikawa cells was performed with Lipofectamine reagent (Life Technologies, cat#11668) per manufacturer's instructions. Agarose

plugs for testing of IHC protocols were prepared as described [134]. Briefly, cells were grown to 75% confluency, harvested with a cell scraper, and spun down. After rinsing in PBS, cells were pelleted and resuspended in 10% formalin for one hour. Cells were washed again in PBS, pelleted, and resuspended in 2% agarose that was loaded into 96 well casts. After allowing agarose to dry for 30 minutes, solid agarose was pulled from the cast, rinsed in PBS, then processed and embedded in paraffin.

Mouse husbandry and procedures involving tissues or live animals

Mice were housed in a pathogen-free animal facility in microisolator cages and fed ad libitum on standard chow under standard lighting conditions. Control animals (Lkb1L/L) and *Sprr2f-Cre; Lkb1*$^{L/L}$ endometrial *Lkb1*-knockout mice were bred and generated as previously described [23]. *Ccl2*$^{-/-}$ mice (B6.129S4-Ccl2$^{tm1Rol/J}$) were obtained from Jackson Laboratories. Mouse blood was obtained by retro-orbital bleeding and collected in EDTA-tubes for CBC counts (IDEXX ProCyte Dx Hematology Analyzer) or eppendorf tubes and allowed to coagulate before serum collection. ELISA for murine tumor lysate and serum CCL2 was performed using Mouse/Rat CCL2/JE/MCP-1 Quantikine ELISA Kit per manufacturer's instructions (R&D Systems, cat#MJE00).

For clodronate treatment, nine-week old *Lkb1*$^{-/-}$ females were treated with intraperitoneal injections of liposomal clodronate or liposomal PBS (0.4 mL of

suspension per 25 g animal weight four times a week) for 9 weeks. Liposomal clodronate and control liposomes were purchased from clodronateliposomes.com.

Tissue processing, immunohistochemistry (IHC), immunofluorescence (IF)

Fixation, sectioning, antigen retrieval, blocking, and secondary detection for the following antibody dilutions in 2% BSA was performed as previously described [134]: LKB1 (1:10,000 human tissue, 1:5000 mouse tissue, Cell Signaling Technologies cat#D60C5F10), CD68 (1:250, Dako cat#M0876), CCL2 (1:250, Sigma cat#HPA019163), and pAMPK (Thr172) (1:75, Cell Signaling Technologies, cat#2535). Prior to addition of primary antibodies, slides were washed in a graded ethanol series and boiled in sodium citrate for 15 minutes for antigen retrieval. Endogenous peroxidase activity was quenched by rinsing slides for 30 minutes in hydrogen peroxide. Blocking was done with 1% BSA in PBS. Secondary detection was done using proper DAKO secondary antibodies. DAB chromagen solution was used to visualize secondary detection.

Antigen retrieval for F4/80 immunostaining (1:100, Abd Serotec, cat#MCA497) on formalin fixed paraffin embedded tissue was performed using 0.005% Pepsin in 0.01 M HCl at 37˚ for 15 minutes, followed by water and PBS rinses. Blocking and secondary detection for F4/80 was performed as described [134].

Immunofluorescence was performed by embedding frozen tissues in OCT solution, crysectioning, 5 minute fixation in cold acetone, and blocking in 3%

BSA for the following antibody dilutions in 3% BSA: rat anti-mouse F4/80 (1:100, Abd serotec), goat anti-mouse CD163 (1:50, Santa Cruz, cat#sc33560), rabbit anti-mouse Arg1 (1:100, Santa Cruz, cat#sc18351), and rat anti-mouse CCL2 (1:50, Clone ECE2, Novus Biologicals cat#NBP1-42312). Alexafluor-conjugated secondary antibodies (Life technologies) included: 488 donkey anti-rat (cat#A21208), 488 donkey anti-goat (cat#A11055), and 555 goat anti-rabbit (cat#A21429).

Flow cytometry

Cell suspensions were obtained from mice by enzymatic digestion and washed in FACS Buffer (1% BSA, 0.01% NaN3 in PBS). Cells were blocked for 5 minutes with Fc blocking reagent (BD Pharmingen, cat#553142) prior to labeling with fluorescent conjugated antibodies diluted in FACS buffer: F4/80-PerCy5.5 (1:200, Tonbo Biosciences, cat#65-4801), and CCR2-APC (1:50, R&D Systems, cat#FAB5538A). Flow cytometry was performed using a FACSCalibur and analyzed with FlowJo software.

Histological scoring scheme for TMA

The generation of the TMA was previously described [22]. A four category classification scheme was employed to score protein expression for LKB1 and CCL2 based on the staining intensity within epithelium. For CD68,

scoring reflected macrophage numbers in each tissue core (including both the stroma and epithelium). The four categories for CD68 were: “0”≤100 macrophages; “1”=101-200; “2”=201-300, and “3“>300 total macrophages per intact core.

Statistical Analysis

Data is presented as means +/- S.E.M. unless otherwise indicated. To determine P values, Student’s t-test was performed (unless otherwise indicated). A P value <0.05 was assumed as statistically significant. For survival curves, Kaplan–Meier analysis was used, with statistical comparison among curves performed with the log rank test. Overlap among the two shRNA gene sets was calculated by the hypergeometric test. Kendall's tau correlation coefficients were calculated using Wessa Statistics Software. Routine statistical analyses were performed with either GraphPad Prism (Version 6.05) or Microsoft Excel. P values are listed within the figures and figure legends. No statistical method was used to predetermine sample size. The experiments were not randomized and the investigators were not blinded to allocation during experiments and outcome assessment.

CHAPTER SIX

Results

LKB1 LOSS PROMOTES ENDOMETRIAL CANCER PROGRESSION VIA THE CCL2-DEPENDENT RECRUITMENT OF MACROPHAGES

Introduction

LKB1 (*STK11*) was initially identified as the tumor suppressor gene mutated in Peutz-Jeghers Syndrome (PJS), a hereditary, autosomal dominant condition characterized by a dramatically elevated (15-20x) incidence of cancer [15, 19]. Interestingly, individuals with PJS, who harbor monoallelic germline *LKB1* mutations, have a propensity to develop epithelial malignancies (i.e. carcinomas)—particularly of the lung and uterus—but not sarcomas or lymphomas [112, 141, 142]. Subsequent studies found that somatic *LKB1* inactivating mutations are common in melanomas and carcinomas of diverse anatomic sites [28, 30, 143]. In human tumors [28, 144] and diverse conditional mouse models [22, 23, 28, 30, 112, 145], LKB1 loss is associated with rapid disease progression and spread, leading to unfavorable clinical outcomes across tumor types. LKB1 protein stability and activity are regulated by diverse post-translational mechanisms [46, 146] and decreased LKB1 protein expression in primary tumors in various anatomic locations correlates with poor prognosis [22, 147-150], suggesting that diverse mechanisms in addition to direct mutational

inactivation can lead to loss of LKB1 activity in cancer. The *LKB1* locus (19p13.3) undergoes frequent loss-of-heterozygosity in cancers; for example, 19p13.3 is the most frequently deleted chromosomal region in endometrial cancer [9], and is also recurrently deleted in lung cancer [151]. Monoallelic *LKB1* inactivation can lead to loss-of-function phenotypes, as LKB1 can function as a haploinsufficient tumor suppressor [29].

LKB1 is a highly conserved serine/threonine kinase and the master upstream kinase activating the AMPK-related family of kinases (AMPK-RKs), comprising the AMPK, BRSK, MARK, NUAK, and SIK subfamilies [142, 152]. LKB1 phosphorylates the AMPK-RKs at conserved consensus sequences. The principal LKB1 phosphorylation site in AMPKα is threonine 172 (Thr172), a residue which lies in the activation loop of the AMPKα catalytic domain. Thr172 and its analogous residues in the other AMPK-RKs can also be phosphorylated by other kinases, such as CaMKKβ [153]. LKB1 function is closely tied to AMPK, a regulator of cellular metabolism under conditions of energy deprivation, and some of LKB1's actions as a tumor suppressor are clearly mediated by its control of cellular metabolism and growth via AMPK and mTOR. However, LKB1 also controls diverse biological pathways relevant to cancer via other members of the AMPK-RK family. For example, LKB1, regulates epithelial cell polarity via the MARK kinases, and axon branching via the NUAK kinases [154]. LKB1 also controls distinct forms of cell motility—notably cell migration along extracellular matrix (haptotaxis)—via the MARK kinases [130]. Thus, LKB1 functions as a tumor suppressor through a combination of AMPK-dependent and independent

pathways. Loss of either LKB1 or AMPK function elicits a number of cancer-associated metabolic phenotypes, including enhanced aerobic glycolysis and macromolecular biosynthesis [76].

We previously developed a mouse model of uterine cancer based on conditional inactivation of LKB1 in endometrial epithelium. One of the remarkable properties of this model is that inactivation of a single tumor suppressor—LKB1—is sufficient to give rise to endometrial adenocarcinomas with complete penetrance and short latency. These LKB1-deficient uterine tumors progress swiftly, leading to death in all animals [23]. In contrast, most cancers require multiple cooperating mutations, and in virtually all mouse cancer models described to date, concurrent genetic "hits" are needed to give rise to invasive cancers [145]. For example, homozygous inactivation of *LKB1* alone does not lead to lung cancer or even precancers, whereas *LKB1* inactivation combined with *KRAS* activation or *PTEN* inactivation provokes lung cancers with 100% incidence [30, 128]. In our *LKB1*-based endometrial cancer model, pharmacologic inhibition of mTOR slowed tumor progression, implicating AMPK as an important effector of LKB1 in endometrial cancer [23]. However, the aggressive nature of these LKB1-driven uterine tumors is not readily explained by misregulation of the AMPK-mTOR axis alone, particularly as the tumors were unusually well-differentiated, and no overt defects in cellular polarity were observed [23]. These paradoxical findings and the particularly aggressive tumor progression phenotype strongly suggested the existence of novel biological activities and unknown tumor suppressing functions under the control of LKB1.

Furthermore, several attributes of this mouse model, including its monogenic constitution, make it particularly attractive for investigations into the diverse biological manifestations of LKB1's functions as a tumor suppressor.

Unexpectedly, our human cell line studies combined with detailed analyses of this model implicated LKB1 in the control of the tumor microenvironment. We found that LKB1 loss led to abnormal patterns of gene expression in endometrial epithelium characterized by misregulation of secreted factors, suggesting a novel LKB1 function in regulating the tumor microenvironment (TME). Specifically, loss of LKB1 in endometrial epithelium led to the abnormal production of the pro-inflammatory cytokine CCL2 (chemokine C-C motif ligand 2). CCL2 exerted systemic effects, leading to the recruitment of pro-tumorigenic macrophages. Finally, investigations conducted on a large number of human endometrial specimens lent further support to a model where LKB1 regulates the tumor microenvironment via CCL2-dependent recruitment of macrophages.

Systematic identification of aberrantly-expressed transcripts in endometrial epithelial cells following LKB1 loss

In addition to its previously mentioned functions, LKB1 has potent effects in shaping the cellular transcriptome through multiple mechanisms including direct phosphorylation of CREB-regulated transcription activators [88, 91], phosphorylation by AMPK of diverse transcriptional activators such as the

FOXOs [155], and suppression of Snail1 [156], MYC [157], and Wnt signaling [158]. We thus sought to identify transcripts whose aberrant expression following LKB1 loss contributed to LKB1-dependent endometrial carcinogenesis. We stably transduced immortalized, non-transformed endometrial epithelial cells (EM cells) [159] with lentiviruses encoding either non-targeted shRNA or one of two non-overlapping LKB1 shRNAs. Western blotting confirmed efficient LKB1 knockdown in each LKB1 shRNA cell line (shRNA1 and shRNA2) compared to the non-target shRNA cell line (**Fig. 6.1A**). As expected, LKB1 knockdown resulted in hypophosphorylation of its canonical target AMPK (at the Thr172 activation loop site), with more modest effects on the phosphorylation status of downstream components of the AMPK/mTOR pathway (S6 and 4EBP1). Interestingly, LKB1 knockdown did not by itself result in obvious phenotypic changes in EM cells such as alterations in growth rate or motility (**Fig. 6.S1**), consistent with the idea that additional genetic changes are needed to transform EM cells, but also in agreement with studies in diverse cell types showing that LKB1 has a relatively modest impact on cell proliferation and instead acts as a tumor suppressor principally through its control of other biological processes [30, 160].

Total RNA was prepared from the three cell lines and subjected to transcriptional profiling with Illumina BeadChip Human HT-12 v4 arrays (n=3 biological replicates per cell line, a total of 9 arrays). Signals were normalized to the non-target controls, and transcripts exhibiting changes in abundance of >3x were tabulated. With these criteria, shRNA2 consistently yielded more than twice

as many targets as shRNA1 (121 vs. 53), which may reflect additional "off-target" effects with shRNA2. However, more than half of the genes identified with shRNA1 (36/53, or 68%) were also identified with shRNA2, clearly demonstrating that most of the tabulated genes were deregulated as a consequence of LKB1 knockdown (**Table 6.S1**). These observations thus validated the overall gene discovery strategy including the use of two non-overlapping shRNAs to filter out off-targets (**Fig. 6.1B, P<0.0001**). Notably, changes in transcript abundance for all 36 genes occurred with the same directionality (i.e., either up or down) with both shRNAs, further validating our data sets. Finally, *LKB1* itself was among the common shRNA1/2 tabulated gene set, serving as an additional internal control (**Table 6.S1**).

To determine if LKB1 regulation of the transcriptome might relate to distinct biological processes, gene ontology analysis was performed on these tabulated genes. Gene ontology terms for which significant enrichment was observed in the identified gene set included "receptor binding" ($P=7x10^{-4}$) and "structural composition of the extracellular region of cells" (i.e. secreted factors) ($P=7x10^{-6}$) (**Table 6.S2**). The regulation of some extracellular factors such as MMP12 by LKB1 in endometrial cells was not completely unanticipated, as prior studies have implicated LKB1 in the transcriptional regulation of secreted proteins, including tissue metalloproteases [161]. Nonetheless, a significant role of LKB1 in regulating secreted chemokines such as CCL2 has not been previously documented. We also note that several genes in the common set encode factors that modulate Wnt or Hedgehog signaling (e.g. WNT2,

SMOOTHENED, SFRP1) consistent with prior studies implicating LKB1 in the regulation of these pathways [158, 162]; however related gene ontology terms did not achieve statistical significance. In light of these findings, our results suggest a broader biological function for LKB1 in terms of regulating the extracellular environment by diverse, secreted factors than previously anticipated.

Validation of targets deregulated following LKB1 loss and identification of the chemokine CCL2 as biologically-relevant candidate

To confirm alteration of transcript levels, we employed quantitative real time PCR. Eight genes were selected for this analysis, including *LKB1,* and *CCL2,* which showed the greatest fold-alteration in expression levels among all genes in the Illumina analysis, and six other genes selected at random. These analyses were conducted on cells and RNA samples prepared independently from those used for the initial profiling. All 8 genes showed changes in magnitude (i.e. up or down) consistent with those observed in the Illumina BeadChip analyses (**Fig. 6.1C**). These analyses also confirmed the downregulation of *LKB1* transcripts and the upregulation of *CCL2* transcripts following *LKB1* knockdown (**Fig. 6.1C**).

CCL2 was a particularly intriguing candidate as a mediator of LKB1-driven endometrial tumor progression. First, the changes in CCL2 transcript levels were dramatic, more than a ten-fold increase (**Table 6.S1, Fig. 6.1C**). Second, CCL2 (a.k.a. MCP-1, monocyte chemoattractant protein-1) is a major

inflammatory chemokine with important if incompletely understood roles in tumor progression, particularly in breast and prostate cancer, where it is largely protumorigenic [163, 164]. Among other functions, CCL2 is a major macrophage chemoattractant and recruits macrophages in the context of diverse forms of tissue damage [165]. This finding suggested that LKB1 may have an unexpected role in modulating the TME through the control of intratumoral CCL2 levels. Furthermore, the significant upregulation of a potentially protumorigenic secreted factor such as CCL2 appeared plausible as a novel mechanism underlying the incompletely understood tumor-promoting actions of LKB1 inactivation.

As a first step to further explore this possibility, CCL2 enzyme-linked immunosorbent assays (ELISA) were performed on tissue culture media conditioned for 24 hours. LKB1 knockdown with shRNA1 and 2 resulted in 14x and 7.0x increased concentrations of CCL2 in the media relative to the control non-target shRNA (**Fig. 6.2A**). Furthermore, addition to the media of 5-aminoimidazole-4-carboxamide ribonucleotide (AICAR) or metformin, two drugs that promote the activation of AMPK [166, 167], significantly suppressed the effect of LKB1 knockdown on CCL2 levels, suggesting that LKB1 regulates CCL2 via AMPK (**Fig. 6.2B**). Concordantly, AICAR and metformin also significantly suppressed CCL2 production in the non-target controls, further emphasizing that AMPK normally suppresses CCL2 production even when functional LKB1 is present. The restoration of pAMPK (Thr172) levels was only partial in shRNA1 and 2 knockdown cells, consistent with the fact that LKB1 is the major (but not sole) Thr172 kinase in most cells [168] and also with the

observation that AICAR and metformin only partially restored CCL2 levels (**Fig. 6.2B,C**). Thus, taken together, these results demonstrate that the LKB1/AMPK axis regulates CCL2 production within EM cells.

Misregulation of CCL2 in an Lkb1-based genetically-engineered murine endometrial cancer model

To further investigate these findings in vivo, we took advantage of a well-described mouse model of endometrial cancer based on *Lkb1* ablation. In this model, homozygous deletion of *Lkb1* in endometrial epithelium with the *Sprr2f-Cre* driver results in well-differentiated but highly aggressive cancers with early invasion beginning at 12 weeks of age, with all females eventually succumbing to the relentlessly progressing cancers [22, 23, 72]. As previously described [23], *Sprr2f-Cre*; $Lkb1^{f/f}$ females (abbreviated hereafter as $Lkb1^{-/-}$) developed invasive endometrial adenocarcinomas beginning at 12 weeks of age, whereas sibling control $Lkb1^{f/f}$ females not harboring *Sprr2f-Cre* (abbreviated hereafter as $Lkb1^{+/+}$) never developed cancers. To study early tumor progression, mice were euthanized at 12 weeks of age, the timepoint coinciding with the earliest appearance of invasive cancer but prior to the formation of advanced, bulky tumors. Per ELISA, $Lkb1^{-/-}$ uterine lysates contained significantly more CCL2 than $Lkb1^{+/+}$ sibling controls (**Fig. 6.3A**). Interestingly, CCL2 levels were also increased in the peripheral blood (serum) of $Lkb1^{-/-}$ females, consistent with the idea that CCL2 produced by the tumorous uteri enters the circulation, and thus

could 1) exert systemic effects and 2) serve as a useful cancer biomarker of disease progression (**Fig. 6.3A**). CCL2 concentrations showed a significant correlation with uterine tumor mass at 12 weeks of age (P=0.001, r^2=0.39) (**Fig. 6.3B**).

To further define the cellular source of CCL2 within uteri, tissue sections were immunostained with a validated CCL2 antibody [169]. In control animals, CCL2 signals were weak, being limited to sporadic (and likely nonspecific) signals in the endometrial stromal cells and occasional faint signals in the apical cytoplasm (**Fig. 6.3D**). In contrast, there was increased CCL2 immunoreactivity in *Lkb1*$^{-/-}$ uterine epithelium, predominantly in the apical cytoplasm, consistent with a secreted protein, although occasional cells exhibited some basal CCL2 localization (**Fig. 6.3D, asterisks**). In mutant *Ccl2* animals (described below), the CCL2-associated signals were abolished, confirming the specificity of immunodetection in the epithelium. Image analyses (n=3 animals per genotype) confirmed these observations (**Fig. 6.3C**). Lastly, we documented AMPK hypophosphorylation (Thr172) in the LKB1-deficient epithelium (**Fig. 6.3E**), confirming that AMPK is a bona fide physiologic target of LKB1 in vivo, as previously reported [58, 68] and indicating that the observed changes in CCL2 are likely AMPK-dependent, as was the case in vitro (**Fig. 6.2B,C**).

Increased macrophage recruitment in Lkb1-driven endometrial cancers and their pro-tumorigenic role

This increased production of CCL2 and its known function as a proinflammatory chemokine led us to investigate the potential contribution of tumor-associated macrophages (TAMs) in the growth and progression of *Lkb1*-driven endometrial cancers. We employed the murine macrophage marker F4/80 to quantitate macrophage density in uterine tissue sections at twelve weeks of age. There was a significant increase (per unit area) in the number of endometrial $F4/80^{+}$ macrophages in $Lkb1^{-/-}$ mice relative to controls (**Fig. 6.4A, B**). Since the density of inflammatory cells varies throughout the murine estrus cycle [170], these studies were performed on mice at proestrus (as determined by routine exfoliated vaginal cell cytology). TAMs can have anti- or pro-tumor effects depending on the tumor type, age and size of tumor, and other variables [171]. It is believed that alternatively activated macrophages, known as M2 macrophages, promote tumor growth and invasion through diverse mechanisms including immune suppression and responding to altered local metabolic effects [172, 173]. M2 macrophages can be distinguished by various markers including expression of the CD163 receptor and the anti-inflammatory molecule arginase I (ARG1) [174]. Most macrophages in $Lkb1^{-/-}$ tumors expressed CD163 and ARG1, suggesting that TAMs in *Lkb1* endometrial tumors are generally tumor-promoting and express markers previously associated with tumor-promoting macrophage subtypes (**Fig. 6.4C**).

To assess the contribution of macrophages to tumor progression, we treated $Lkb1^{-/-}$ mice with liposome encapsulated clodronate, which is phagocytized by macrophages, resulting in their apoptosis and depletion [175].

Free clodronate (i.e. released from the dying macrophages) has an extremely short half-life and does not have long-term systemic effects [176]. Nine-week old females were treated with intraperitoneal injections of liposomal clodronate or liposomal PBS (control) for 9 weeks and then necropsied. The treatment was well-tolerated by all animals with no apparent side effects, deaths, or overall weight loss at any point in the treatment regimen. Among diverse control organs, only the spleen showed a significant reduction in size/weight, consistent with efficient systemic macrophage depletion, as red pulp macrophages constitute a large cell population in the spleen (**Fig. 6.5A**). F4/80 immunostaining showed a significantly fewer macrophages within the endometrium, confirming the effectiveness of the clodronate regimen in depleting uterine macrophages (**Fig. 6.5B**).

Remarkably, macrophage depletion significantly inhibited tumor progression. Whereas invasive tumor glands were abundant and diffuse in the myometria of untreated animals at the end of the regimen (i.e. at 18 weeks of age), such invasive glands were greatly diminished following clodronate treatment (**Fig. 6.5C**). Concordantly, uterine tumor burden was dramatically decreased following clodronate treatment (**Fig. 6.5D**) with a 10x reduction in overall uterine tumor weights (P=0.001), a difference readily apparent by gross examination of the tumorous uteri (**Fig. 6.5E**). These experiments thus demonstrate that the TAMs recruited to *Lkb1*-driven endometrial cancers have a predominantly tumor-promoting effect.

Dependence of Lkb1-driven endometrial tumor progression on CCL2

These experiments were provocative in showing that the TAMs recruited in the context of LKB1 loss and ensuing CCL2 overproduction promote tumor progression. However, these studies did not formally establish a role of CCL2 in this process. To rigorously explore this question, an additional cohort of mice was generated by breeding *Sprr2f-Cre* and the *Lkb1* floxed allele into a *Ccl2*-deficient background. *Ccl2*-null mice, described in prior studies, are externally normal and exhibit good overall health, including normal fertility [177]. Absence of circulating CCL2 in animals homozygous for the *Ccl2* null mutation was confirmed by ELISA (**Fig. 6.S2A**). *Sprr2f-Cre; Lkb1$^{f/f}$; Ccl2$^{-/-}$* mice (hereafter abbreviated as *Lkb1$^{-/-}$*; *Ccl2$^{-/-}$*) were born at expected Mendelian ratios. A cohort of *Lkb1$^{-/-}$*; *Ccl2$^{-/-}$* females, together with sibling *Lkb1$^{-/-}$* and *Lkb1$^{+/+}$* cohorts, were allowed to age for survival analysis. No tumors were observed in the *Lkb1$^{+/+}$* controls. However, loss of CCL2 increased the maximal lifespan of the *Lkb1* conditional knockout mice from 301 to 406 days and resulted in a statistically-significant extension of overall survival (P=0.004, log-rank test) (**Fig. 6.6A**). To further study tumor progression, a set of animals separate from the survival cohorts was euthanized at 26 weeks of age. Uterine tumor burden was significantly decreased (>2x) in *Lkb1$^{-/-}$*; *Ccl2$^{-/-}$* vs. *Lkb1$^{-/-}$* females (P=0.04; n=6 *Lkb1$^{-/-}$* and n=3 *Lkb1$^{-/-}$; Ccl2$^{-/-}$*) (**Fig. 6.6B, C**). Thus, although genetic ablation of CCL2 did not entirely suppress the formation and progression of *Lkb1*-driven endometrial cancers, it did significantly slow the progression of these tumors,

confirming that CCL2 is a critical mediator of LKB1 loss in the context of endometrial cancer growth and progression in vivo.

Uterine macrophages were further analyzed and quantitated by flow cytometry for F4/80 and CCR2, another general macrophage marker and the receptor for CCL2 [178]. These analyses demonstrated that at 26 weeks, both $F4/80^+$ and $F4/80^+/CCR2^+$ double-positive uterine macrophages were significantly decreased in *Lkb1*$^{-/-}$; *Ccl2*$^{-/-}$ vs. *Lkb1*$^{-/-}$ females (**Fig. 6.S3A**), which was further confirmed by visual inspection of F4/80-immunostained uterine sections (**Fig. 6.S3B**). These analyses confirmed the existence of a uterine macrophage population capable of responding to CCL2, and together with our prior observations, are consistent with the idea that $CCR2^+$ macrophages play a role in the *Lkb1* model. Interestingly, while *Lkb1*-null mice harbored increased circulating monocytes and decreased lymphocytes, these effects were reversed by loss of CCL2 (n=6 *Lkb1*$^{-/-}$, n=3 *Lkb1*$^{-/-;}$ *Ccl2*$^{-/-}$) (**Fig. 6.S3C**). Overall, these results suggest that CCL2 plays an important part in *Lkb1*-driven tumorigenesis by stimulating 1) increased peripheral monocyte numbers and 2) monocyte recruitment to the endometrial tumors.

The LKB1/CCL2/TAM axis plays an important role in the progression of primary human endometrial cancers

To study the LKB1/CCL2/TAM axis in human tumors, an endometrial cancer tissue microarray (TMA) was constructed with duplicate cores for nearly

200 independent primary tumors, predominantly of the endometrioid subtype, which is the most common (**Table 6.S3**). TMA slides were stained for CCL2, CD68 (a human macrophage marker), and LKB1. Since many antibodies do not reliably detect their corresponding antigen in paraffin-embedded formalin-fixed tissues (PEFFT), and few immunohistochemical (IHC) studies have been conducted on CCL2 in human PEFFT, we first validated our CCL2 IHC protocol on Ishikawa endometrial cancer cell line overexpressing CCL2. After fixation in 10% buffered formalin followed by paraffin-embedding (to simulate processing of human tissues in the clinical pathology laboratory), the CCL2-overexpressing cells gave a much higher signal than control Ishikawa cells (**Fig. 6.S4**). For detection of LKB1, we employed an IHC assay that has been previously validated and proven robust for the detection of endogenous LKB1 protein in PEFFT [134]. Sufficient tumor was present to permit scoring of all three markers for n=175 independent cases of endometrial cancer. Based on the observed patterns and intensity of staining, a semi-quantitative 0-3 scoring scale was established for all three markers (**illustrated in Fig. 6.S5; see also methods for detailed description of scoring criteria**). Note that, while CCL2 and LKB1 IHC was used to assess protein levels in a semi-quantitative manner, CD68 immunostains were used to assess macrophage density. In some primary tumors, CCL2 was expressed primarily on the apical epithelial cytoplasm, while in other tumors, CCL2 was located diffusely throughout the apical and basal cytoplasm (**Fig. 6.S5B**).

After all of the scoring was completed, heat maps were generated to explore associations among the markers. There was a strong negative association

between CCL2 and LKB1, both for Grade 1 and Grade 1-4 endometrial cancers (P=0.00019; τ_κ=-0.45 and P=0.000278; τ_κ=-0.19 respectively). There was also a strong negative association between CD68 scores (i.e. macrophage density) and LKB1, again in both Grade 1 and Grade 1-4 cancers (P=0.000373; τ_κ=-0.43 and P=2.72×10^{-8}; τ_κ=-0.36, respectively) (**Fig. 6.7A**).

We then categorized expression of each protein by clinical stage in addition to grade. FIGO (International Federation of Gynecology and Obstetrics, 1988) Stage 1A tumors are defined by the absence of myometrial invasion, whereas 1B tumors invade through less than half of the myometrium and 1C tumors invade through greater than half of the myometrial thickness [179]. There was a trend toward higher numbers of cases with low LKB1 (protein score=0) expression among Stage 1C cases, although this did not achieve statistical significance. However, there was a statistically significant increase in cases with low LKB1 expression in Grade 3 vs. Grade 1. For CCL2 and CD68, there was again a trend towards increased expression in Stage 1C vs. 1A that did not achieve significance, while there was a statistically significant increase in cases expressing high levels of these cancers in Grade 1 vs. Grade 3 tumors (**$p<0.005$**, **Fig. 6.7B**). These studies, conducted in a large set of human primary endometrial cancers, provide strong support for a model where LKB1 loss promotes tumor progression through increased CCL2 secretion by the primary tumor, leading to increased macrophage recruitment to the tumor. This data is also consistent with a number of studies that have consistently demonstrated a strong association

between TAM density in primary endometrial tumors and grade, stage, and clinical outcome [180-183].

Discussion

At the initiation of these studies, the paradoxically aggressive phenotypes we had previously described for LKB1-deficient uterine cancers [23, 28] strongly suggested that LKB1 acted as uterine tumor suppressor via unknown biological mechanisms. This study, which began with expression profiling of isogenic cell lines to pinpoint such novel biological pathways, demonstrated that LKB1 regulates the transcription of multiple secreted factors of potential relevance to LKB1's actions as a tumor suppressor. Additional investigations, which included analyses of a genetically-engineered mouse model as well as primary human tumors, led to the unexpected discovery that that one of these factors—the chemokine CCL2—is a physiologically important effector of Lkb1-driven endometrial cancers. Our studies revealed an unanticipated but essential role for LKB1 in the control of the tumor microenvironment (TME) in addition to the well-known effects of LKB1 on cell-autonomous metabolism and signaling. Specifically, we showed that LKB1 loss in endometrial epithelial cells leads to increased expression and secretion of CCL2 in a cell-autonomous manner, and that increased intratumoral CCL2 derived from epithelial cells in turn leads to accelerated tumor growth via the recruitment of pro-tumorigenic macrophages. Our study thus forges new links between endometrial carcinogenesis, the LKB1

tumor suppressor, CCL2/CCR2, and TAMs, and provides new insights into the particularly aggressive tumor phenotypes associated with LKB1 loss.

Our data are in line with growing evidence implicating inflammatory chemokines in general, and CCL2 in particular, with tumor progression. Chronic inflammation is a hallmark of cancer, and extensive epidemiologic data has linked chronic inflammation with the initiation of carcinomas at a variety of anatomic sites. In carcinomas of the breast, prostate, colon, liver, and bladder, production of CCL2 by tumor cells is associated with increased infiltration of TAMs and early clinical relapse [163, 184]. For example, in uterine cervical cancer, absence of *CCL2* mRNA expression correlated with decreased TAM density and significantly improved overall survival [185]. Our study is thus consistent with prior data that CCL2 expression is a significant prognostic factor in cancer [163].

A variety of cell surface receptors expressed on monocytes/macrophages together with their corresponding ligands, including CCR2/CCL2, VEGFR1/VEGF-A, and CX3CR1/CX3CL1, regulate monocyte recruitment into tumors. In general, the expression of one or more of these ligands positively correlates with TAM numbers. CCL2 is a potent chemoattractant of monocytes/macrophages, and appears to be the main determinant of monocyte/macrophage recruitment within primary tumors. CCL2 production in distant metastatic deposits can also lead to the recruitment of monocytes and thereby promote growth of these deposits [186]. Normal, uninjured tissues produce low levels of CCL2, whereas tumors often express and produce higher CCL2 levels. Some monocyte chemoattractants (e.g. VEGF-A) are generally

produced within carcinomas by non-epithelial cells (such as fibroblasts). In contrast, CCL2 is largely produced by the malignant epithelial cells, although other cells in the primary TME can also serve as sources of CCL2.

In our model, CCL2 produced by the primary endometrial cancer was detectable in the circulation. Furthermore, increased circulating monocytes were observed in these *Lkb1*$^{-/-}$ female mice, consistent with the well-established role of the CCL2/CCR2 axis in the mobilization of monocytes from the bone marrow to the blood [187], and further signifying that the CCL2 produced by tumors can exert systemic, as well as local effects. Consistent with this idea, serum CCL2 (sCCL2) represents a potential circulating biomarker to monitor tumor progression or predict progression risk. In patients with gastric and hepatocellular carcinomas, preoperative levels of sCCL2 were significantly higher than in control patients, and correlated with stage [188]. However, studies of sCCL2 are in their early stages, and data on sCCL2 circulating levels in women with endometrial cancer are not yet available.

CCL2 produced by malignant epithelial cells within a tumor serves to recruit monocytes and promote their differentiation (paracrine effects) but can also directly impact the malignant cells themselves (autocrine effects). High-grade urothelial (bladder) carcinomas expressing high levels of CCL2 stimulate their own growth, migration, and invasive capacity in a cell-autonomous, CCR2-dependent manner [163]. CCL2 also promotes prostate cancer chemotaxis, invasion and metastasis via CCR2 and its downstream effectors, which include PI3K/AKT, Rac, and RhoA [184]. Although we did not directly evaluate the

contributions of such CCL2-dependent autocrine mechanisms on endometrial cancer progression in our models, we have documented expression of the CCR2 receptor protein in all uterine cancer cell lines we have analyzed, including both endometrial and cervical cancer cell lines (see chapter 7). Thus, we believe that such autocrine effects are not only plausible but likely, and deserve further investigation. Another intriguing possibility is that CCL2/CCR2 interactions could have cell autonomous effects on intracellular metabolism, which might in turn further synergize with the LKB1-AMPK-mTOR axis.

Multiple studies have found that increased TAM density in human endometrial cancer is associated with a significantly worse clinical prognosis. Macrophages are the most abundant leukocyte population in the mouse and human endometrium, where they serve diverse physiologic functions during endometrial cycling and pregnancy. In a large recent study of n=163 primary endometrial cancers, increased TAM density correlated strongly with advanced tumor stage and grade, lymphovascular space involvement, and decreased recurrence-free and overall survival. Interestingly, intratumoral density of other immune cellular subsets, such as regulatory T cells (T_{regs}) did not correlate with these clinical parameters [183]. Both our mouse and human studies confirm that TAMs in primary endometrial tumors have protumorigenic roles, and implicate the LKB1/AMPK axis as an important regulator of TAM density in tumors via CCL2.

Although most chemokines bind and act through multiple receptors, CCL2 exerts its biological roles exclusively via CCR2, which is highly expressed in

classical monocytes. Conversely, CCR2 is not known to be activated by any chemokines other than CCL2. This exclusive relationship suggests that, for those tumors characterized by high levels of CCL2, inhibition of CCR2 through neutralizing antibodies or through small molecule drugs in clinical development might prove a useful therapeutic approach [189]. New therapeutic strategies for endometrial cancer are urgently needed, as there are as yet no curative treatments for advanced disease, although recently objective responses have been documented for temsirolimus, an mTOR inhibitor [190]. Our study and prior data demonstrating that TAM density is an important driver of human endometrial tumor progression lend further support to the notion that the LKB1/CCL2/TAM axis is a particularly attractive target for new therapeutic strategies. Our demonstration that genetic inactivation of *Ccl2* suppresses *Lkb1*-driven tumors in vivo also lends strong support of this idea. Further validation for anti-CCL2/CCR2 therapeutic strategies and additional biological insights are likely to be gained by additional investigations of the $Lkb1^{-/-}$ mouse model, particularly since the complete penetrance of endometrial adenocarcinomas and stereotypical tumor progression make this a highly tractable model. Taken together, our data indicate that $Lkb1^{-/-}$ mice should serve as an optimal preclinical platform for testing diverse agents currently in various stages of clinical development, including CCL2- or CCR2-neutralizing antibodies or small molecule inhibitors that target CCR2. It will also be interesting to test the efficacy of such agents either alone or in combinations with agents (such as temsirolimus) likely to

synergize with LKB1 loss and the ensuing hyperactivation of AMPK/mTOR pathways [23].

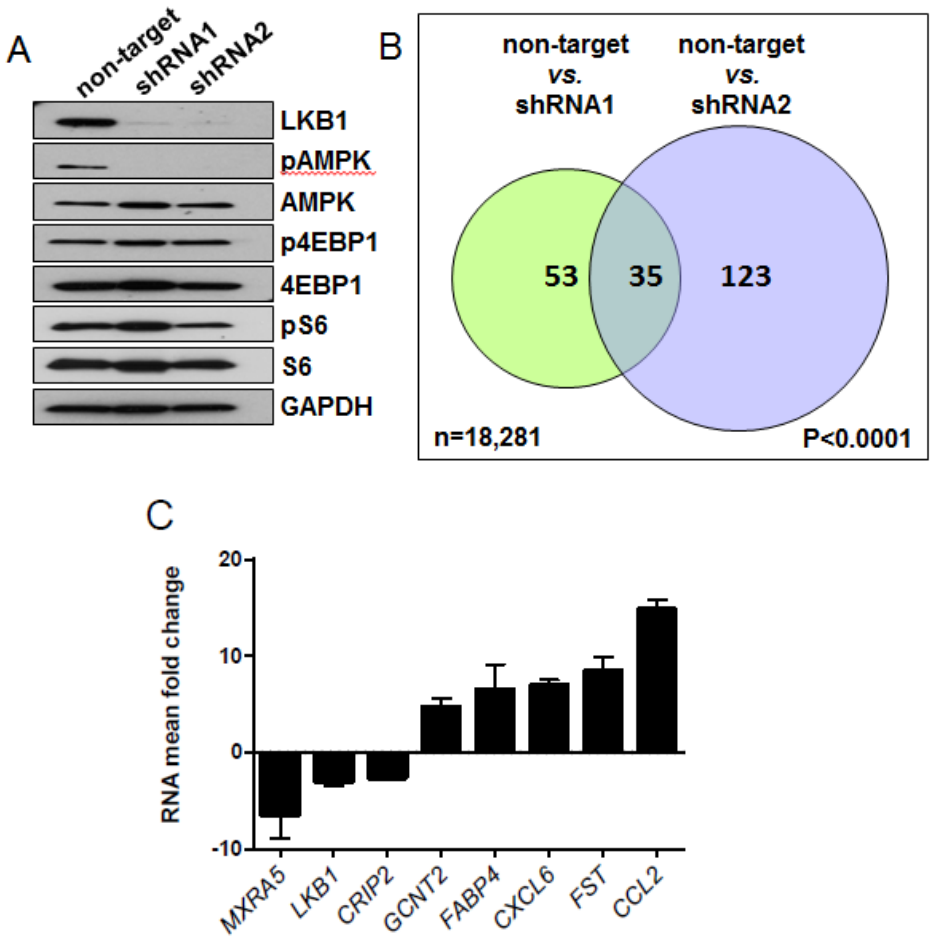

Figure 6.1 Discovery and validation of transcripts regulated by LKB1 in endometrial epithelium by gene expression profiling. A) Western blot of immortalized, non-transformed endometrial cells (EM) stably transduced with lentivirus encoding either non-target shRNA, or one of two different LKB1 shRNAs (shRNA1, shRNA2) that resulted in efficient LKB1 knockdown. LKB1 knockdown led to lower pAMPK levels as expected and modest effects on the levels of the phosphorylated forms of downstream mTOR signaling components pS6 or p4EBP1. B) Venn diagram of stably transduced cell lines showing the number of genes differentially expressed following LKB1 knockdown with the

two shRNAs at a threshold of $\geq$3x and a confidence interval of $p<0.05$ (Illumina Microarray Human HT-12 v4 BeadChip, n=3 biological replicates per shRNA). There was significant overlap (n=35; $P<0.0001$ per hypergeometric test) among differentially-expressed genes following shRNA1 and shRNA2 knockdown (n=53 and 121 respectively, among n=18,281 genes represented in microarray) demonstrating that our experimental strategy was capable of identifying bona fide LKB1 targets. C) Validation of gene expression alterations by quantitative RT-PCR, $\Delta\Delta$CT method, depicting the mean fold change of shRNA1 and shRNA2 per gene analyzed (n=3 independent samples distinct from those used for microarray expression profiling). Note that all gene expression changes were consistent with the microarray data and also that *LKB1*, which is downregulated as expected, serves as internal control. *CCL2* showed the greatest alteration in expression levels per both microarray and RT-PCR among the subset of genes selected for validation. Error bars represent standard error of the mean (S.E.M).

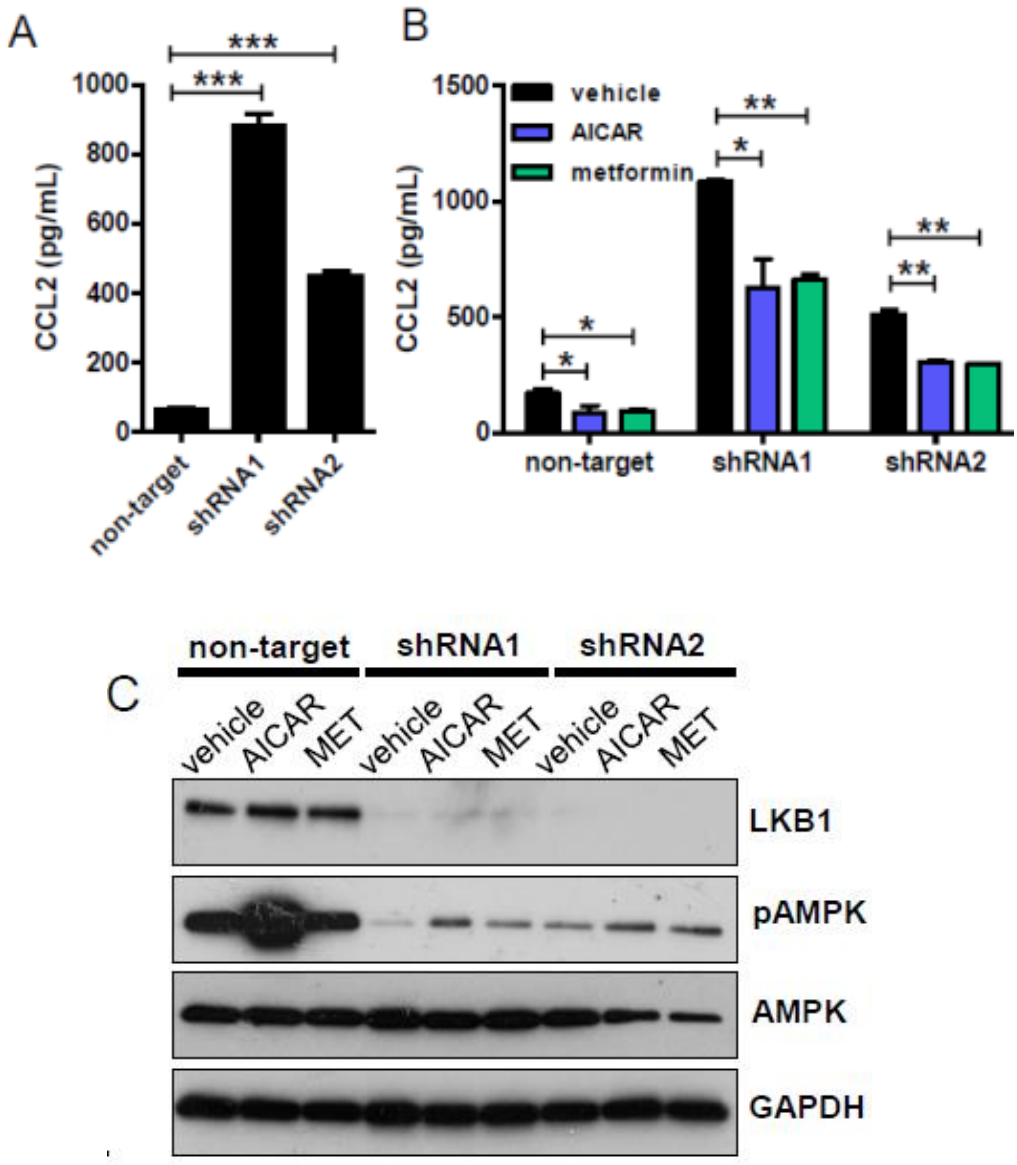

Figure 6.2 LKB1 suppresses CCL2 production in human endometrial epithelial cells via an AMPK-dependent mechanism. A) Human CCL2 ELISA of conditioned media harvested 24 hours after plating of EM cells previously transduced with lentivirus. LKB1 knockdown lead to a significant increase of CCL2 in the media (n=3 biological replicates per experiment). B) Human CCL2 ELISA on conditioned media containing AICAR [0.5 mM], metformin [5mM], or

vehicle (PBS) only. AICAR or metformin significantly reduced CCL2 secretion 24 hours after addition of drug (n=3 biological replicates). C) Representative western blot of lysates from cells shown in panel B revealing partial restoration of pAMPK levels. ***P<0.0001, **P<0.001, *P<0.05 for all panels per student's t test. Error bars=S.E.M.

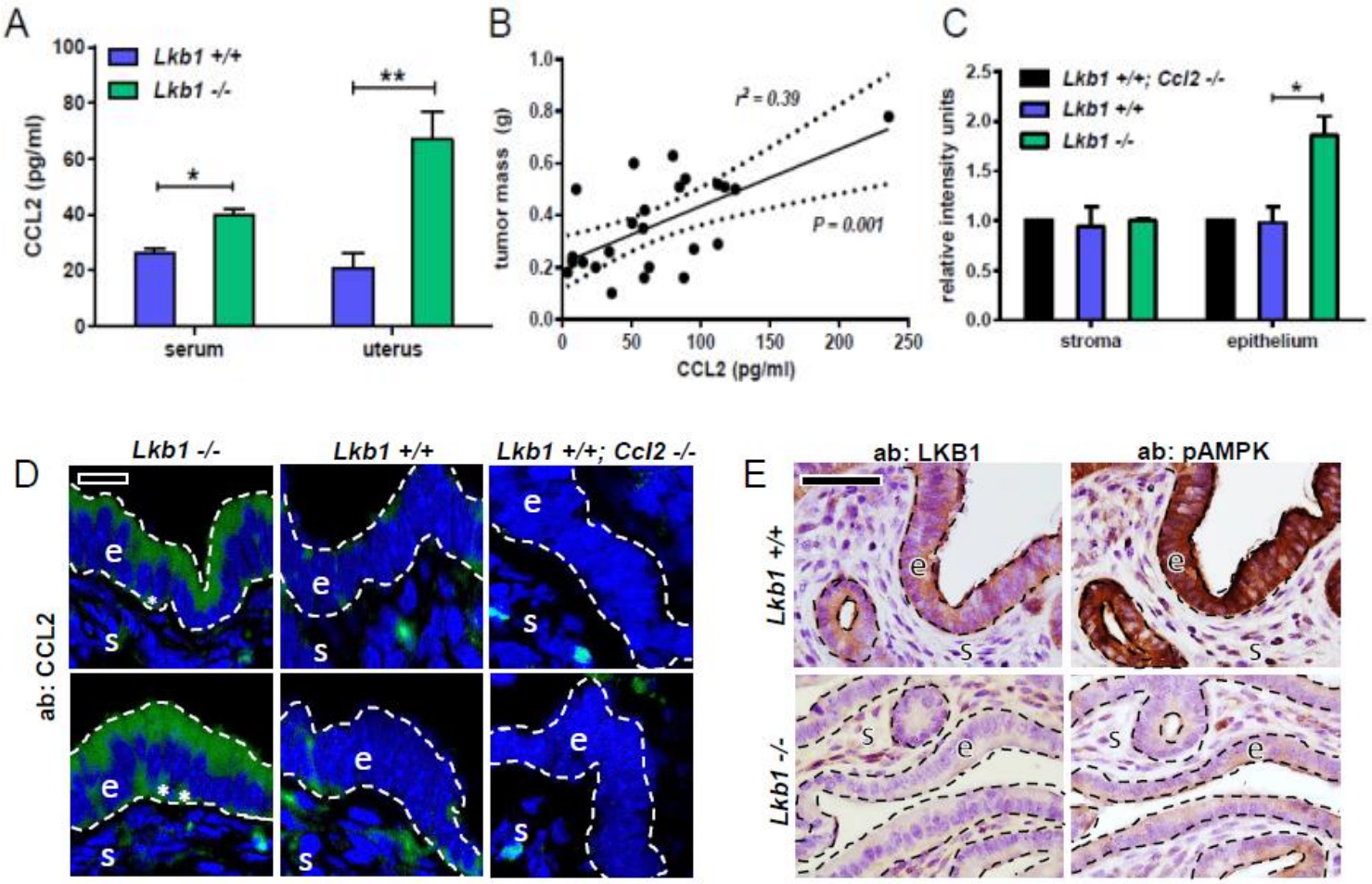

Figure 6.3 Conditional *Lkb1* knockout in murine endometrial epithelium results in endometrial cancers characterized by high CCL2 production. All experiments were conducted in conditional knockout *Sprr2-Cre*; $Lkb1^{f/f}$ (abbreviated *Lkb1 -/-*) and sibling control $Lkb1^{L/L}$ (abbreviated *Lkb1 +/+*) female mice not harboring the *Sprr2f-Cre* driver at 12 weeks of age, the time point when myometrial invasion first occurs in this well-characterized model. Tissues were harvested at proestrus. A) ELISA of serum or uterine protein lysates showing a significant increase of CCL2 levels following *LKB1* deletion (n=14 $Lkb1^{+/+}$, n=24 $Lkb1^{-/-}$). B) CCL2 levels in tumor lysates (per ELISA) plotted against tumor mass

from *Lkb1*$^{-/-}$ animals, showing a direct correlation between tumor mass and CCL2 levels (n=24 mice, Pearson coefficient r^2=0.39 with P=0.001 per two tailed t test). C) CCL2 expression in endometrial epithelium by image analysis (regions analyzed correspond to those enclosed by dashed lines in the next panel). Tissue sections were stained with a validated CCL2 antibody and green CCL2 signal quantitation was performed using ImageJ (n=3 animals per experiment). Expression was normalized to the background signal present in *Ccl2*$^{-/-}$; *Lkb1*$^{+/+}$ uterine epithelium. D) CCL2 immunofluorescence of uterine tissue sections; s=stroma, e=epithelium. Asterisks denote basal CCL2 expression. Two different regions are shown for each genotype. E) LKB1 and pAMPK (Thr172) immunohistochemistry of uterine tissue sections from *Lkb1*$^{+/+}$ and *Lkb1*$^{-/-}$ mice. As expected, *Lkb1* deletion in endometrial epithelium resulted in undetectable LKB1 protein as well as reduced pAMPK compared to control siblings. Statistical significance in panels A and C was determined by student's t test. **P<0.001, *P<0.005 for all panels. Bars=50 μm in all panels. Error bars=S.E.M.

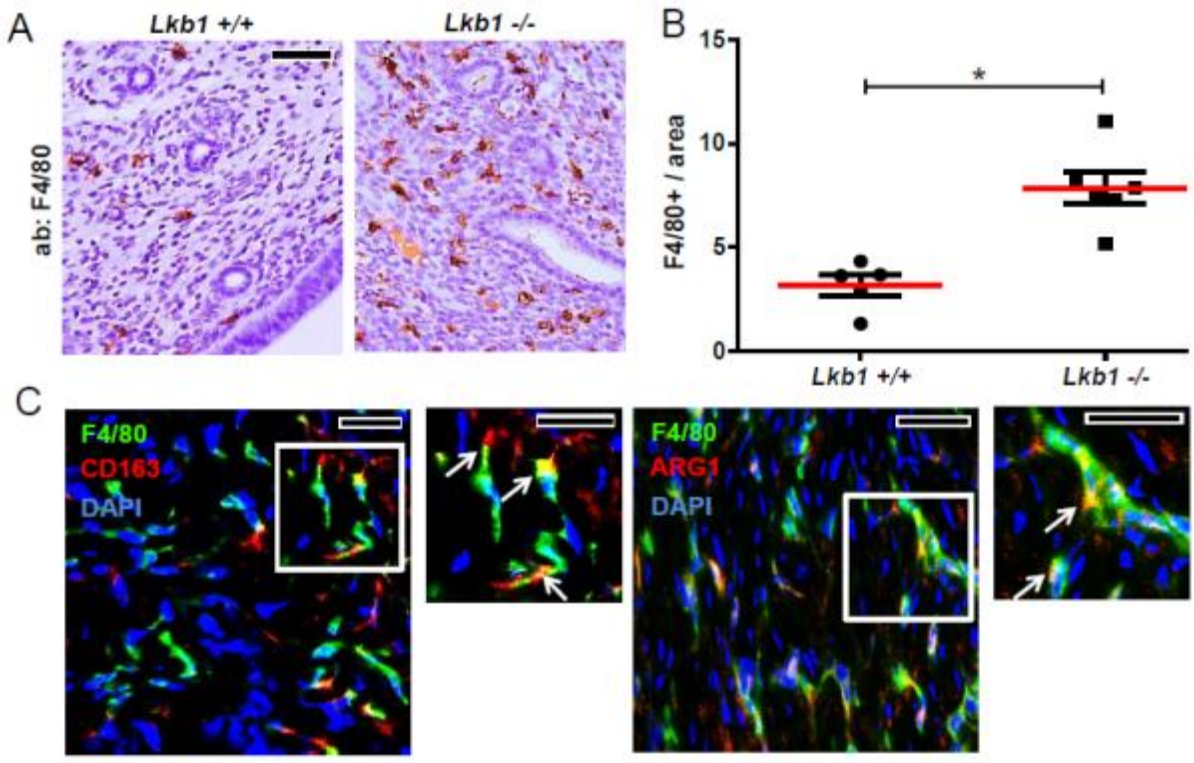

Figure 6.4 LKB1 loss in endometrium promotes recruitment of macrophages that express markers associated with alternative macrophage activation. Experiments were conducted in 12 week old animals at proestrus. A) Macrophage density by F4/80 immunohistochemistry. B) Quantitation of macrophages in uterine tissue sections immunostained for F4/80. Positive cells were counted in 5 separate fields and normalized by total area for every mouse analyzed (n=5 for *Lkb1*$^{+/+}$, n=6 for *Lkb1*$^{-/-}$ mice). There were significantly increased macrophage numbers in *Lkb1*$^{-/-}$ endometrium (*P<0.005) per student's t test. C) Presence of alternatively activated macrophages characterized by ARG1 and CD163 expression. Uterine tumor sections were stained with F4/80 and CD163 or ARG1. Arrows in the inset highlight F4/80 cells that are also positive for the other markers. Bars=50 μm in all panels. Error bars=S.E.M.

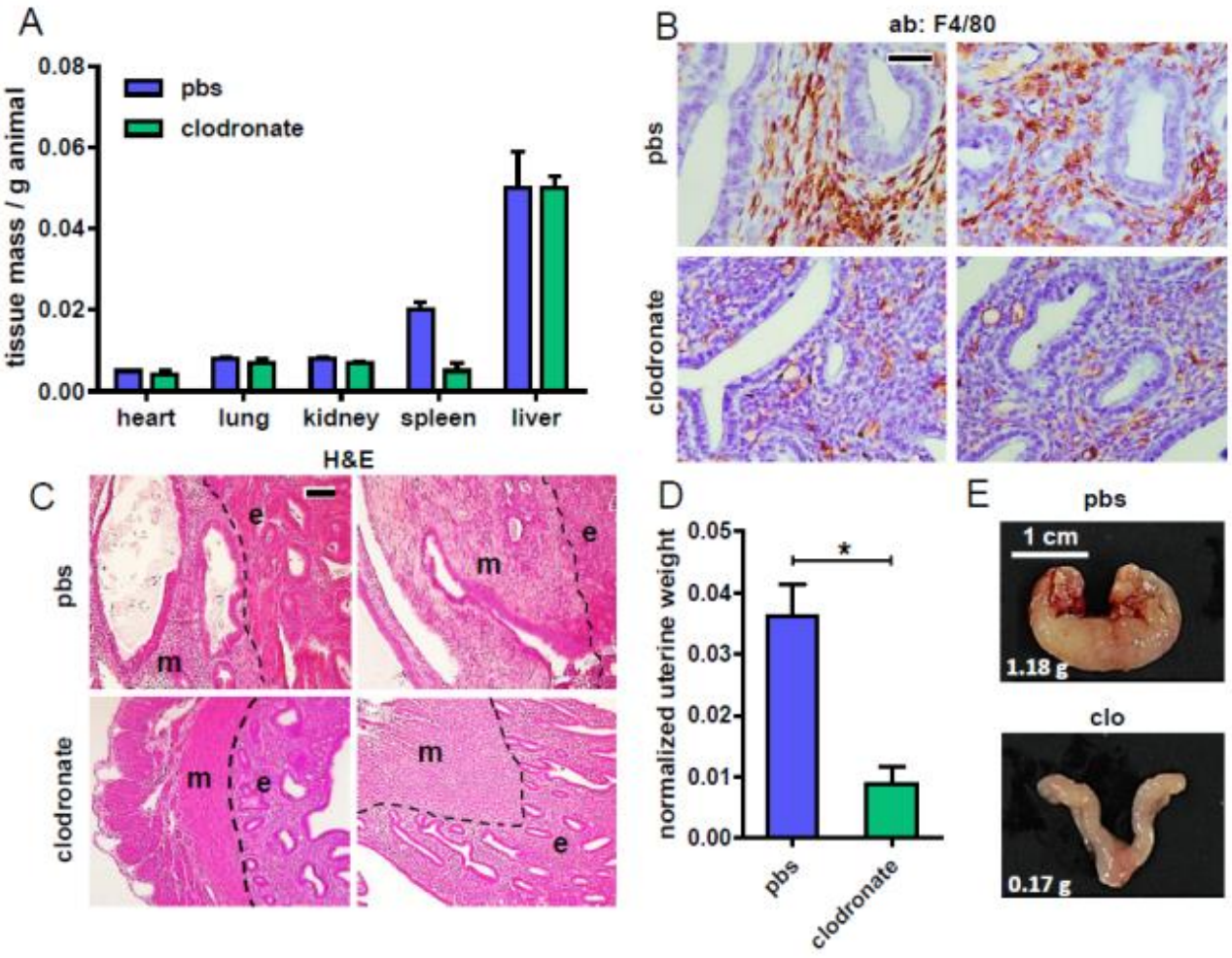

Figure 6.5 Tumor-associated macrophages in *Lkb1*-driven endometrial cancers promote invasion and accelerate tumor progression. Tumor bearing *Lkb1*$^{-/-}$ animals were treated with liposomal PBS (n=4) or liposomal clodronate (n=4) for 9 weeks. A) Confirmation of systemic macrophage depletion. Among diverse organs only spleen showed decrease in mass following the clodronate regimen, as expected (macrophages make up a significant percentage of cells in the spleen). B) F4/80 immunohistochemistry of uterine tissue section confirming macrophage depletion following treatment with clodronate. C) H&E staining

showing greatly decreased myometrial invasion in clodronate-treated *Lkb1*$^{-/-}$ mice; e=endometrium; m=myometrium; dashed line=endometrial/myometrial interface. D) Tumor burden, as determined by uterine weight at conclusion of treatment. There was a significant reduction in tumor mass in clodronate treated animals; p value per student's t test (*P<0.01). E) Gross photographs of uteri at conclusion of treatment. Weights for uteri in grams shown in lower left-hand corner. Bars=50 μm in all panels. Error bars=S.E.M.

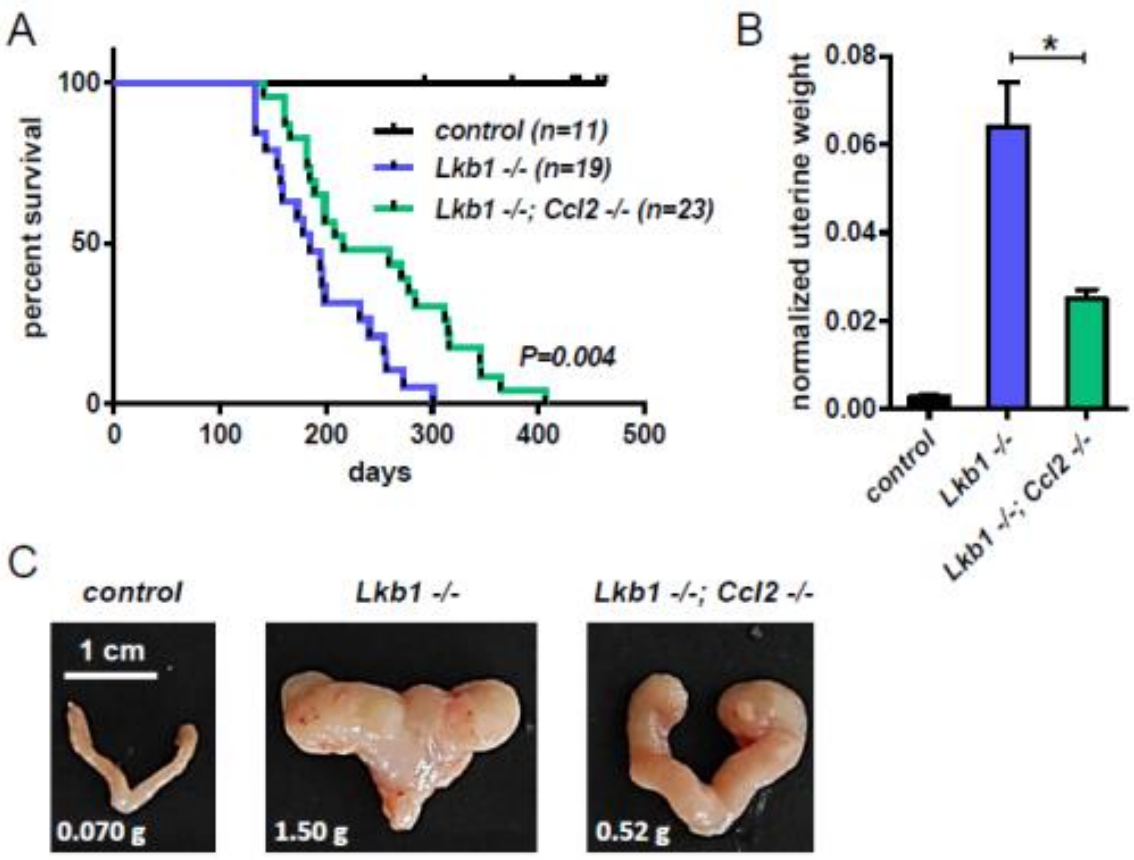

Figure 6.6 Endometrial cancers driven by LKB1 loss are CCL2-dependent in vivo. A) Survival curves for two experimental genotypes and control *Lkb1*$^{f/f}$ mice not harboring *Sprr2f-Cre*; statistical significance calculated by log-rank test. B) Tumor burden at 180 days (n=6 *Lkb1*$^{-/-}$, n=3 *Lkb1*$^{-/-}$; *Ccl2*$^{-/-}$) as determined by uterine weight; p value per student's t test (*P<0.05). C) Gross photographs of uteri at 180 days of age. Weights for uteri in grams shown in lower left-hand corner. Left uterus image was cropped, rotated 180˚ to align uterine horns with those of the right uterus image, and the image placed on a black background. Error bars=S.E.M.

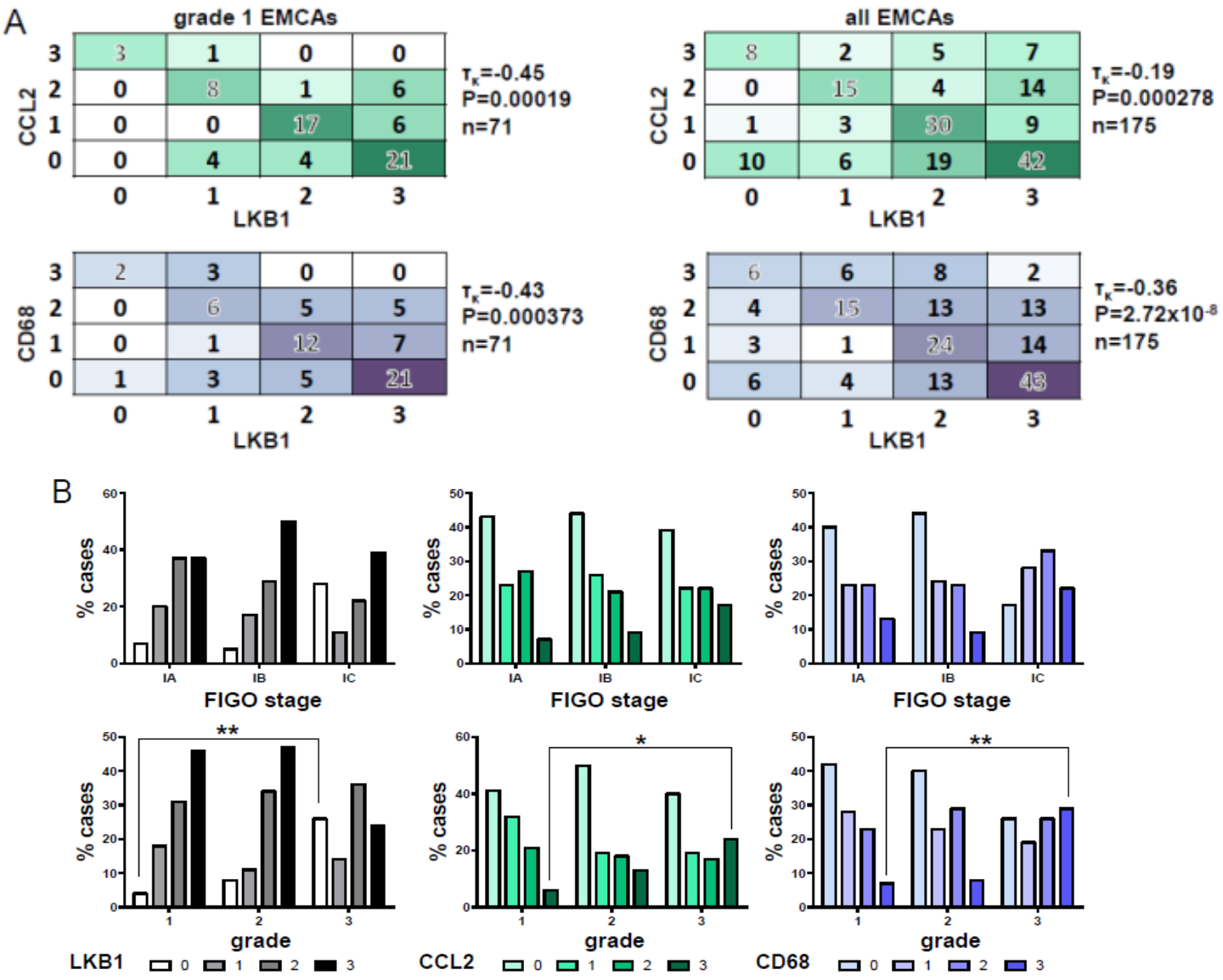

Figure 6.7 Low LKB1 protein levels in primary human endometrial cancers are strongly correlated with high CCL2 expression and increased macrophage density. A human endometrial cancer TMA was stained and scored for each marker per the schema illustrated in Figure S5. A total of 175 separate cases of primary endometrial cancer were scored. Pair-wise correlations were evaluated by with Kendall's tau coefficient, with P values determined by two

tailed t tests. A) Heat maps showing significant negative correlations among grade 1 and grade 1-4 endometrial adenocarcinomas. B) *Top panels*: Number of cases with specific staining scores (0-3) among tumors of different clinical stages (FIGO 1A, 1B, 1C). In cases with >50% myometrial invasion (defined as stage 1C), the percentage of cases with low LKB1 expression or high CCL2/CD68 expression was significantly increased. *Bottom panels*: Number of cases with specific staining scores (0-3) among tumors of different histopathological grades (1, 2, 3). There was a significantly greater percentage of cases expressing low levels of LKB1 protein among high grade tumors (n=113). Additionally, there was a significantly greater percentage of cases expressing high levels of CCL2 (n=113) and CD68 cases (n=113) among high grade tumors. **P<0.001, *P<0.005 per Fisher's exact t test.

shRNA 1 (n=59 probes)		shRNA 2 (n=142 probes)		Common (43 probes)		
Probe ID	*Gene Notation*	*Probe ID*	*Gene Notation*	*Probe ID*	*Gene Notation*	*Common Fold Change*
ILMN_1747627	ABCA1	ILMN_1713124	AKR1C3	ILMN_3237488	AKR1C2	+4.03
ILMN_1740938	APOE	ILMN_2215824	ANKRD20A1	ILMN_1696048	C13orf33	-3.76
ILMN_1734611	BDKRB1	ILMN_1776936	ANKRD38	ILMN_1761941	C4orf18	+4.78
ILMN_1754076	CACNA2D3	ILMN_1689431	APCDD1L	ILMN_1672124	C4orf18	+4.78
ILMN_1733669	CDH18	ILMN_2232478	APOBEC3G	ILMN_1720048	CCL2	+13.92
ILMN_1720482	CEND1	ILMN_1690241	BATF2	ILMN_1732799	CD34	+3.06
ILMN_1784294	CPA4	ILMN_1813043	BHMT2	ILMN_1694432	CRIP2	-3.47
ILMN_1693338	CYP1B1	ILMN_1723480	BST2	ILMN_2161577	CXCL6	+4.87
ILMN_1784420	DDX12	ILMN_1764109	C1R	ILMN_1779234	CXCL6	+4.87
ILMN_2072178	ECHDC3	ILMN_1677198	C1R	ILMN_1752478	DHRS3	+3.42
ILMN_1698673	EFCAB7	ILMN_1677603	C1S	ILMN_2269256	DNAJC12	+5.61
ILMN_2350634	EFEMP1	ILMN_1793572	C21orf81	ILMN_1802653	EBI3	+7.47
ILMN_1751375	ENAM	ILMN_1754920	C6orf58	ILMN_1773006	FABP4	+6.74
ILMN_1672022	EPHA4	ILMN_1656369	C8orf4	ILMN_1805665	FLRT3	+3.71
ILMN_1669617	GRB10	ILMN_1748840	CALB2	ILMN_1700081	FST	+4.56
ILMN_2119123	GRPR	ILMN_2105573	CCL3L3	ILMN_1712896	FST	+4.56
ILMN_1813851	GRPR	ILMN_1773352	CCL5	ILMN_1680390	GCNT2	+3.07
ILMN_2372124	HNF4A	ILMN_2098126	CCL5	ILMN_1791280	HSPB8	+3.53
ILMN_2160428	IL1RAPL1	ILMN_2067656	CCND2	ILMN_2139396	IGDCC4	-5.04
ILMN_1813704	KIAA1199	ILMN_1784602	CDKN1A	ILMN_1704353	IGSF3	-3.24
ILMN_2209260	KRTAP1-3	ILMN_1774287	CFB	ILMN_2212999	KIF5C	+6.75
ILMN_1707652	KRTAP1-5	ILMN_1725338	CLDN23	ILMN_1746517	KYNU	+5.16
ILMN_1668194	LMTK3	ILMN_1783621	CMPK2	ILMN_1737514	KYNU	+5.16
ILMN_3244876	LOC100133171	ILMN_1711514	COCH	ILMN_3199798	LOC389342	+3.19
ILMN_3288032	LOC646576	ILMN_1791759	CXCL10	ILMN_3241303	LOC728255	+4.39
ILMN_1677925	LOC646617	ILMN_1728478	CXCL16	ILMN_1669119	LOC728946	+5.29
ILMN_1667631	LOC648718	ILMN_1682636	CXCL2	ILMN_3251711	LOC728951	+4.92
ILMN_1696731	LOC652683	ILMN_1752562	CXCL5	ILMN_3251718	LOC728956	+4.46
ILMN_3247132	LOC730743	ILMN_1812297	CYP26B1	ILMN_2331544	MBP	+5.19
ILMN_2172497	LPPR4	ILMN_1797001	DDX58	ILMN_2073758	MMP12	+12.03
ILMN_2139125	LRFN5	ILMN_1795181	DDX60	ILMN_1768035	MMP12	+12.03
ILMN_1773650	LRRN3	ILMN_1725726	DHRS2	ILMN_1718766	MT1F	+5.34
ILMN_1785402	LTBP1	ILMN_2384857	DHRS2	ILMN_1803213	MXRA5	-4.87
ILMN_1696162	MME	ILMN_1678422	DHX58	ILMN_1809364	NTF3	+7.30
ILMN_1659086	NEFL	ILMN_1791679	DNER	ILMN_2363141	PAGE5	+6.20
ILMN_2215989	NEFM	ILMN_2370296	ENAH	ILMN_1744656	PAGE5	+6.20
ILMN_2357086	NETO1	ILMN_1775931	EPHA3	ILMN_1790761	POSTN	+3.91
ILMN_1690993	NEUROG2	ILMN_1652280	FBXO32	ILMN_2196328	POSTN	+3.91

ILMN_1763750	NPTX1
ILMN_1703572	PCDH20
ILMN_1680339	PDGFRL
ILMN_2413158	PODXL
ILMN_1711311	PODXL
ILMN_1795166	PTH1R
ILMN_1785699	PTHLH
ILMN_1813561	SCIN
ILMN_3240314	SCXA
ILMN_2150851	SERPINB2
ILMN_2150856	SERPINB2
ILMN_2395139	SERPINB7
ILMN_1767685	SERPINB7
ILMN_1670305	SERPING1
ILMN_1700448	SIM2
ILMN_1676449	SLIT2
ILMN_3242729	SPANXD
ILMN_1732781	SPANXE
ILMN_2132100	SPANXE
ILMN_1713125	SPANXE
ILMN_1688295	ZNF219

ILMN_1703955	FBXO32
ILMN_1698725	FRMD3
ILMN_1772910	GAS1
ILMN_1729487	GMPR
ILMN_1655348	GPR1
ILMN_1803945	HCP5
ILMN_1729749	HERC5
ILMN_1654639	HERC6
ILMN_1752502	HKDC1
ILMN_1762861	HLA-F
ILMN_3239965	IDO1
ILMN_2058782	IFI27
ILMN_1745374	IFI35
ILMN_1760062	IFI44
ILMN_1723912	IFI44L
ILMN_1687384	IFI6
ILMN_1781373	IFIH1
ILMN_1707695	IFIT1
ILMN_1699331	IFIT1
ILMN_1739428	IFIT2
ILMN_2239754	IFIT3
ILMN_1664543	IFIT3
ILMN_1701789	IFIT3
ILMN_1801246	IFITM1
ILMN_1750324	IGFBP5
ILMN_1699651	IL6
ILMN_2349061	IRF7
ILMN_1798181	IRF7
ILMN_2054019	ISG15
ILMN_1659913	ISG20
ILMN_2359287	ITGA6
ILMN_1750373	KAL1
ILMN_1784630	KBTBD11
ILMN_1662038	LARGE
ILMN_1662932	LCP1
ILMN_2412214	LGALS9
ILMN_1807016	LHX2
ILMN_2235851	LINCR
ILMN_3253787	LOC100128274
ILMN_3259146	LOC100129681
ILMN_3235379	LOC100134265
ILMN_1893633	LOC439949

ILMN_1740842	SALL2	+3.62
ILMN_2149164	SFRP1	+4.16
ILMN_2408080	SNAP25	+3.35
ILMN_1751871	STK11	-3.64
ILMN_2068104	TFPI2	+6.44

ILMN_1672000	LOC642460
ILMN_1808122	LOC652377
ILMN_1713182	LOC653879
ILMN_1766184	LOC654346
ILMN_2088876	MAGEC2
ILMN_1766914	MFAP4
ILMN_1784459	MMP3
ILMN_1662358	MX1
ILMN_2231928	MX2
ILMN_1692058	NDN
ILMN_2410826	OAS1
ILMN_1658247	OAS1
ILMN_1675640	OAS1
ILMN_1736729	OAS2
ILMN_1709333	OAS2
ILMN_1674063	OAS2
ILMN_1745397	OAS3
ILMN_1681721	OASL
ILMN_1674811	OASL
ILMN_1778623	PAGE1
ILMN_1731224	PARP9
ILMN_2329625	PCDH11X
ILMN_2391400	PITX2
ILMN_2110422	PKD1L1
ILMN_1745242	PLSCR1
ILMN_1753312	PLXDC2
ILMN_1785646	PMP22
ILMN_1713846	PPM1H
ILMN_1685312	PSG3
ILMN_2103709	PSG5
ILMN_1801776	PSG9
ILMN_2339835	PTGS1
ILMN_1665100	PTGS1
ILMN_2054297	PTGS2
ILMN_1658576	PTPRN
ILMN_1791840	RALBP1
ILMN_1701613	RARRES3
ILMN_1657871	RSAD2
ILMN_2173975	RTP4
ILMN_1814305	SAMD9
ILMN_1721026	SAMHD1
ILMN_1782098	SMO
ILMN_2406501	SOD2

ILMN_1731418	SP110
ILMN_1813455	SP110
ILMN_1672661	SP110
ILMN_2415144	SP110
ILMN_2329914	SPRY1
ILMN_1691860	SPRY1
ILMN_1691364	STAT1
ILMN_1777325	STAT1
ILMN_1669709	TMEM108
ILMN_1738116	TMEM119
ILMN_1736863	TMEM140
ILMN_1758418	TNFSF13B
ILMN_1703273	UACA
ILMN_1794612	UBA7
ILMN_3240420	USP18
ILMN_1690365	USP41
ILMN_2153495	WNT7B
ILMN_1742618	XAF1
ILMN_2370573	XAF1

Supplementary Table 6.1 List of differentially-expressed transcripts following LKB1 knockdown (>3x). Illumina probe ID and gene notation are shown. “Common” transcripts are those deregulated in the same direction with both shRNA1 and shRNA2; + indicates upregulation, - downregulation.

Receptor binding (n=29 genes) P=7x10^{-4}		
Probe ID	***Gene notation***	***Gene name***
ILMN_1720048	CCL2*	chemokine (C-C motif) ligand 2
ILMN_2161577	CXCL6*	chemokine (C-X-C motif) ligand 6 (granulocyte chemotactic protein 2)
ILMN_2212999	KIF5C*	kinesin family member 5C
ILMN_1809364	NTF3*	neurotrophin 3
ILMN_1802653	EBI3*	Epstein-Barr virus induced 3
ILMN_1699651	IL6	interleukin 6 (interferon, beta 2)
ILMN_1782098	SMO	smoothened, frizzled family receptor
ILMN_1740938	APOE	apolipoprotein E
ILMN_2149164	SFRP1*	secreted frizzled-related protein 1
ILMN_1682636	CXCL2	chemokine (C-X-C motif) ligand 2
ILMN_1681721	OASL	2'-5'-oligoadenylate synthetase-like
ILMN_1773352	CCL5	chemokine (C-C motif) ligand 5
ILMN_1791679	DNER	delta/notch-like EGF repeat containing
ILMN_1752562	CXCL5	chemokine (C-X-C motif) ligand 5
ILMN_2350634	EFEMP1	EGF containing fibulin-like extracellular matrix protein 1
ILMN_1728478	CXCL16	chemokine (C-X-C motif) ligand 16
ILMN_1791759	CXCL10	chemokine (C-X-C motif) ligand 10
ILMN_1766914	MFAP4	microfibrillar-associated protein 4
ILMN_1691364	STAT1	signal transducer and activator of transcription 1, 91kDa
ILMN_2105573	CCL3L3	chemokine (C-C motif) ligand 3-like 3
ILMN_1669617	GRB10	growth factor receptor-bound protein 10
ILMN_2160428	IL1RAPL1	interleukin 1 receptor accessory protein-like 1
ILMN_2372124	HNF4A	hepatocyte nuclear factor 4, alpha
ILMN_1745242	PLSCR1	phospholipid scramblase 1
ILMN_1785699	PTHLH	parathyroid hormone-like hormone
ILMN_1758418	TNFSF13B	tumor necrosis factor (ligand) superfamily, member 13b
ILMN_1672022	EPHA4	EPH receptor A4
ILMN_2160428	IL1RAPL1	interleukin 1 receptor accessory protein-like 1
ILMN_1676449	SLIT2	slit homolog 2 (Drosophila)

Extracellular region part (n=31 genes) P=7x10^{-6}		
Probe ID	***Gene notation***	***Gene name***
ILMN_2073758	MMP12*	matrix metallopeptidase 12 (macrophage elastase)
ILMN_2068104	TFPI2*	tissue factor pathway inhibitor 2
ILMN_1720048	CCL2*	chemokine (C-C motif) ligand 2
ILMN_1802653	EBI3*	Epstein-Barr virus induced 3
ILMN_2196328	POSTN*	periostin, osteoblast specific factor
ILMN_1805665	FLRT3*	fibronectin leucine rich transmembrane protein 3
ILMN_1699651	IL6	interleukin 6 (interferon, beta 2)
ILMN_2132982	IGFBP5	insulin-like growth factor binding protein 5
ILMN_1740938	APOE	apolipoprotein E
ILMN_2149164	SFRP1*	secreted frizzled-related protein 1
ILMN_2341229	CD34*	CD34 molecule
ILMN_1676449	SLIT2	slit homolog 2 (Drosophila)
ILMN_1751375	ENAM	enamelin
ILMN_1711514	COCH	coagulation factor C homolog, cochlin (Limulus polyphemus)
ILMN_2153495	WNT7B	wingless-type MMTV integration site family, member 7B
ILMN_2054019	ISG15	ISG15 ubiquitin-like modifier
ILMN_1752562	CXCL5	chemokine (C-X-C motif) ligand 5
ILMN_1791759	CXCL10	chemokine (C-X-C motif) ligand 10
ILMN_1784459	MMP3	matrix metallopeptidase 3 (stromelysin 1, progelatinase)
ILMN_1766914	MFAP4	microfibrillar-associated protein 4
ILMN_1750373	KAL1	Kallmann syndrome 1 sequence
ILMN_2105573	CCL3L3	chemokine (C-C motif) ligand 3-like 3
ILMN_1785402	LTBP1	latent transforming growth factor beta binding protein 1
ILMN_1785699	PTHLH	parathyroid hormone-like hormone
ILMN_1758418	TNFSF13B	tumor necrosis factor (ligand) superfamily, member 13b
ILMN_1682636	CXCL2	chemokine (C-X-C motif) ligand 2
ILMN_1773352	CCL5	chemokine (C-C motif) ligand 5
ILMN_2350634	EFEMP1	EGF containing fibulin-like extracellular matrix protein 1
ILMN_1728478	CXCL16	chemokine (C-X-C motif) ligand 16
ILMN_1670305	SERPING1	serpin peptidase inhibitor, clade G (C1 inhibitor), member 1

ILMN_1805665	FLRT3	fibronectin leucine rich transmembrane protein 3

Supplementary Table 6.2. Gene ontology analysis of common LKB1 regulated transcripts. Illumina probe ID, gene notation, and gene names are shown for two highly significant gene ontology categories (Receptor binding, n=29 genes, $P=7x10^{-4}$; Extracellular region part, n=31 genes, $P=7x10^{-6}$) per hypergeometric test. Asterisks indicate gene sets shared by shRNA1 and shRNA2.

Age	**(yr)**
Median	59
Mean	58
Range	24-89
Stage	**(%)**
I (n=114)	65%
II (n=17)	10%
III (n=16)	9%
IV (n=20)	11%
unstaged (n=8)	5%
Grade	**(%)**
I (n=71)	41%
II (n=62)	35%
III (n=42)	24%
Histology	**(%)**
Endometrioid (n=161)	92%
other (n=14)	8%

Supplementary Table 6.3 Characteristics of 175 patients in the study population. Clinical data for patients and endometrial tumors represented in TMA. "Other" histotypes include serous and clear cell carcinoma.

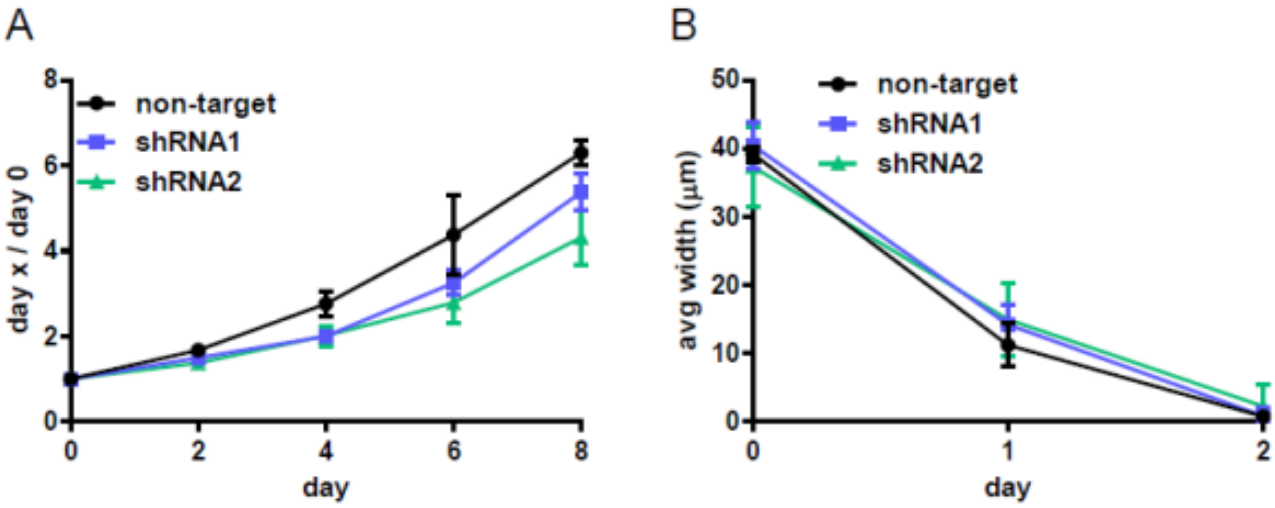

Supplementary Figure 6.1 LKB1 knockdown does not affect growth rate or migration of EM cells. A) Growth curve of isogenic EM cells over an 8 day period. Values were obtained by calculating mean intensity of crystal violet staining per day normalized to day 0. B) Wound healing assay showing width of wound (µm) over time. Error bars=S.E.M.

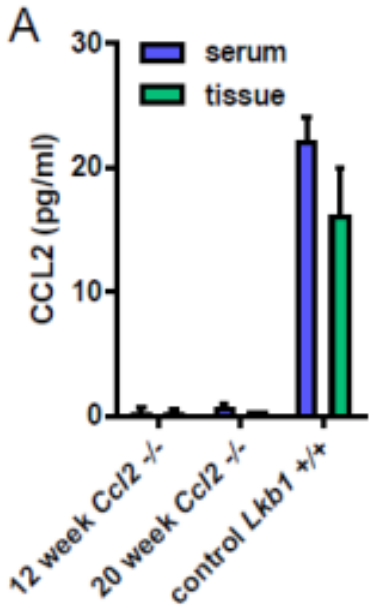

Supplementary Figure 6.2 Validation of *Ccl2*$^{-/-}$ transgenic mouse line. A) ELISA on serum and uterine tissue showing undetectable amounts of CCL2 in younger (12 week) and older (20 week) *Ccl2*$^{-/-}$ mice. *Lkb1*$^{+/+}$ mice, which are *Ccl2*$^{+/+}$, served as a positive control for CCL2 detection.

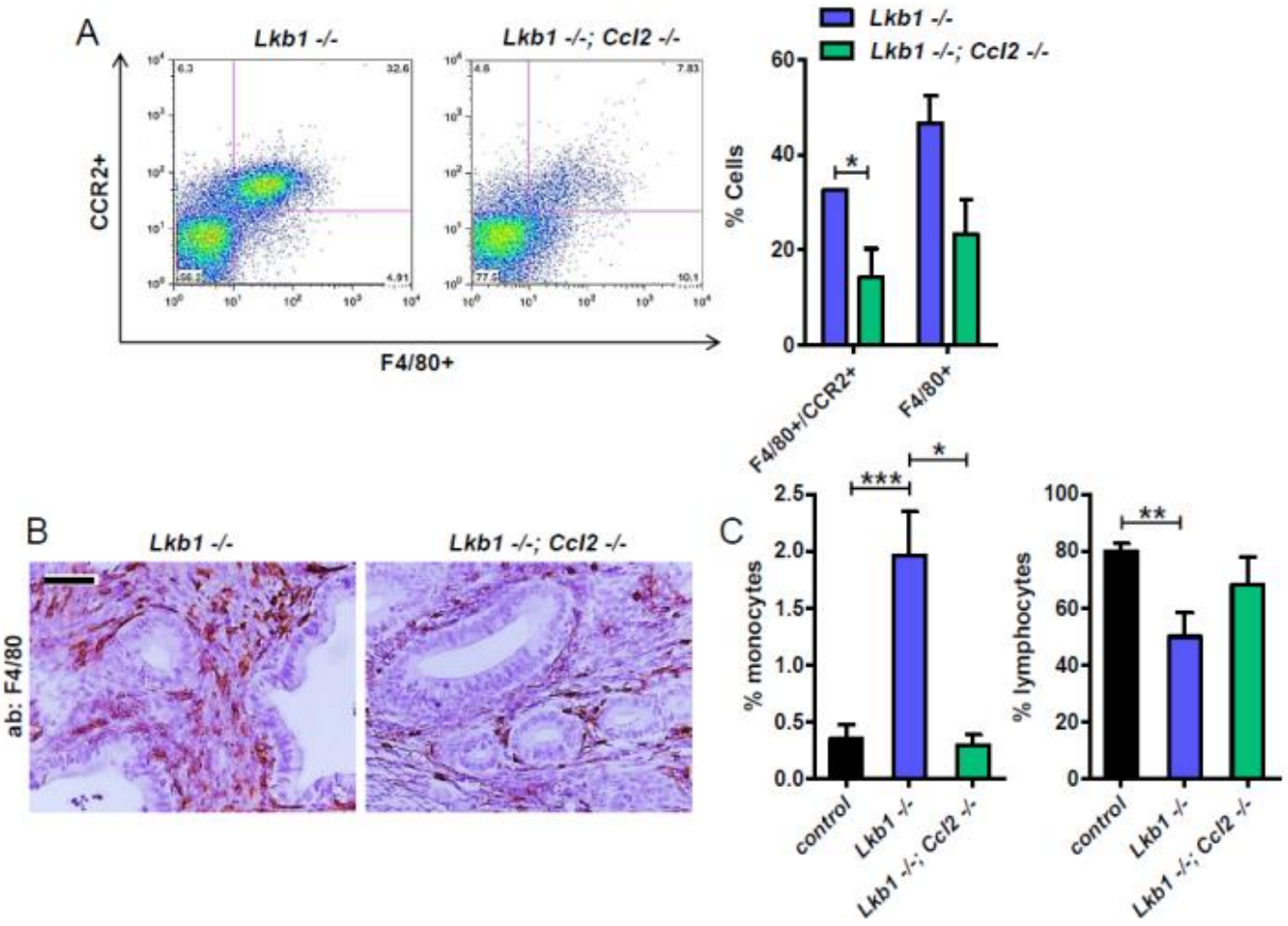

Supplementary Figure 6.3 LKB1 tumor-associated phenotypes including recruitment of macrophages and systemic effects are CCL2-dependent. A) Flow cytometry to quantitate F4/80^{+}/CCR2^{+} macrophages in tumors driven by *Sprr2f-Cre* at 180 days. *Lkb1*$^{-/-}$ tumorous uteri, which overexpress CCL2, contained a significantly greater percentage of F4/80^{+}/CCR2^{+} and total F4/80^{+} cells than *Lkb1*$^{-/-}$*; Ccl2*$^{-/-}$ tumors. This data demonstrates that LKB1 loss leads to increased macrophage recruitment to the tumor microenvironment in a CCL2-dependent manner. B) Macrophage density by F4/80 staining confirmed the presence of fewer macrophages in *Lkb1*$^{-/-}$*; Ccl2*$^{-/-}$ endometrial tumors. C)

Complete blood counts showing CCL2-dependent effects in circulating monocyte and lymphocyte numbers. Statistical significance in panels A and C was determined by student's t test. ***P<0.0005, **P<0.001, *P<0.05 for all panels. Bars=50 μm in all panels. Error bars=S.E.M.

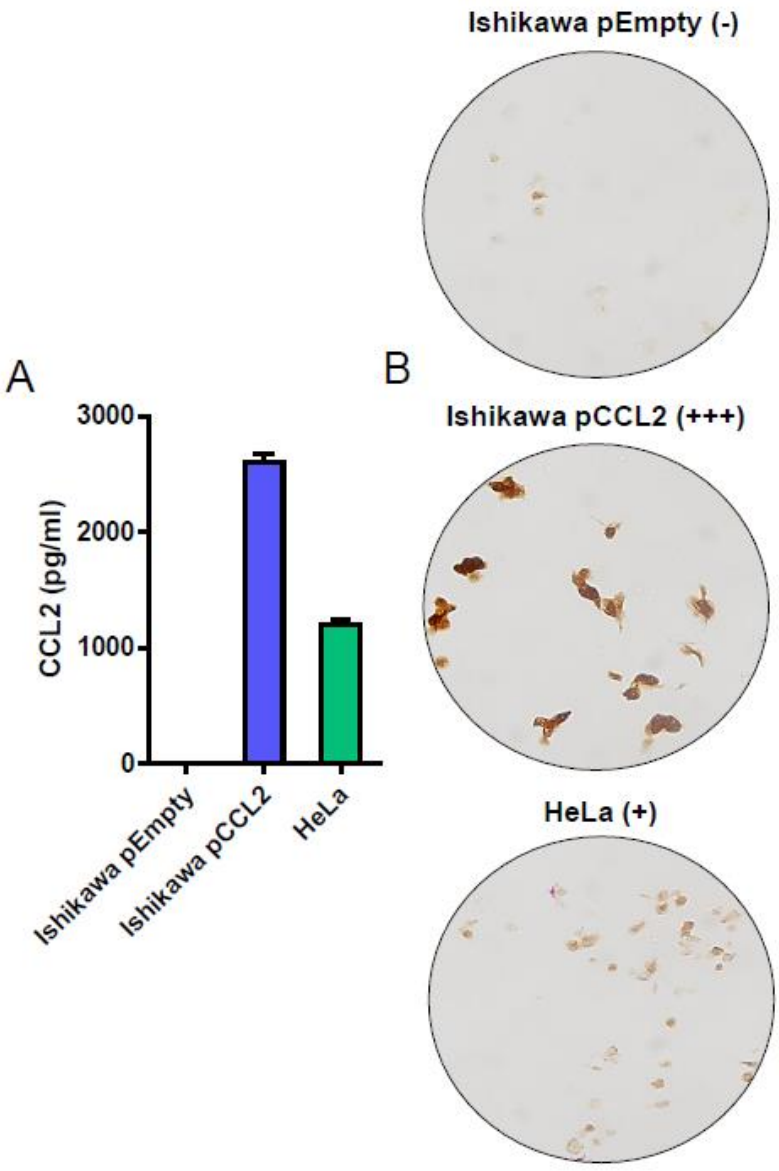

Supplementary Figure 6.4 Validation of human CCL2 antibody for TMA studies. A) ELISA on media conditioned for 48h from Ishikawa endometrial cell line transfected with either empty vector or *CCL2* cDNA. HeLa cells, which were non-transfected, are also shown. As expected, cDNA transfection resulted in significantly higher levels of CCL2 in the media compared to empty vector. HeLa

cells endogenously produced an intermediate level of CCL2. B) CCL2 immunostaining of cell lines following fixation in 10% buffered formalin and paraffin-embedding to simulate clinical pathology laboratory conditions.

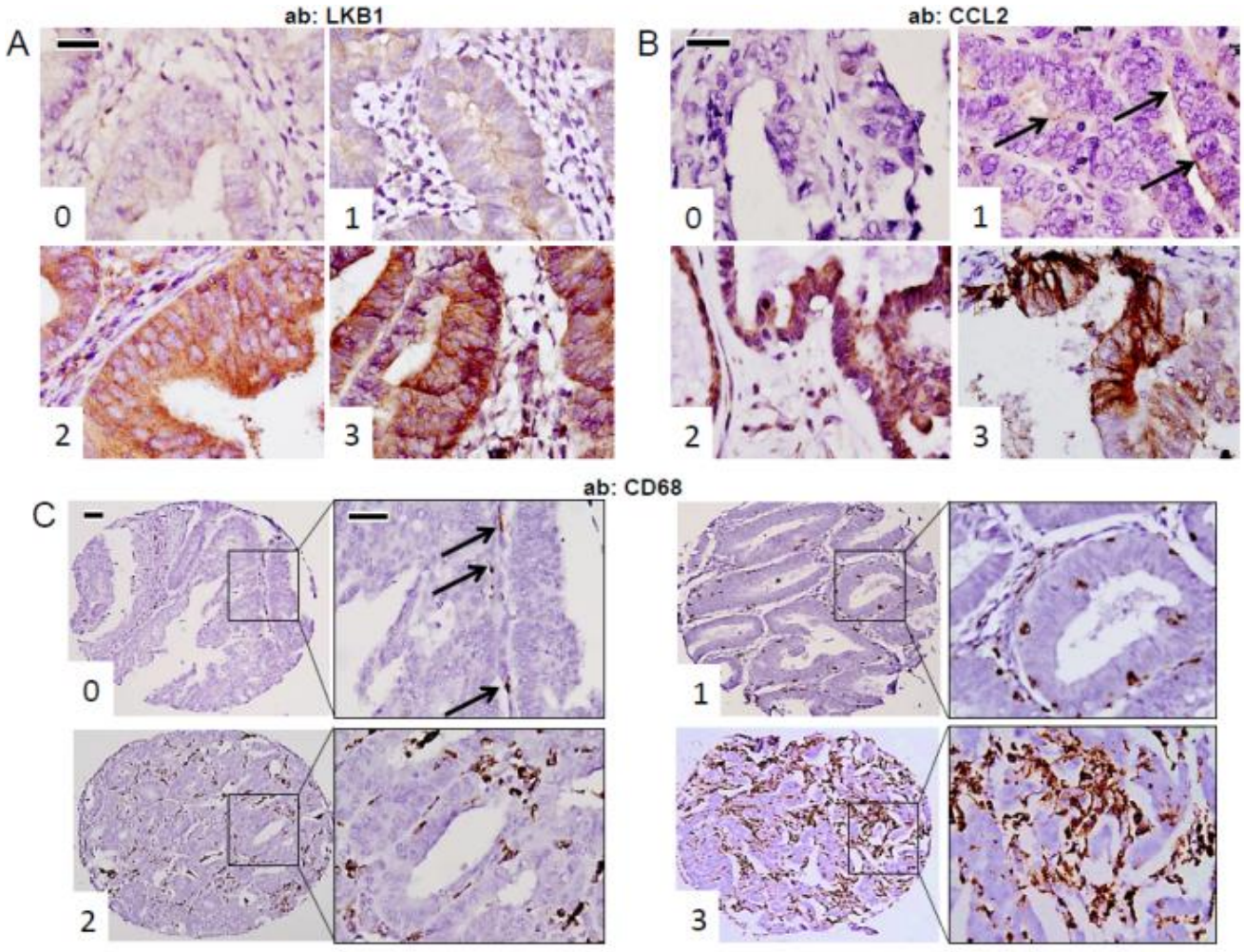

Supplementary Figure 6.5 Histological scoring schema for LKB1, CCL2, and CD68 expression by immunohistochemical analysis of human endometrial adenocarcinomas. Immunohistochemical staining of A) LKB1 B) CCL2 or C) CD68 in representative cases illustrating 0-3 scoring system employed to analyze the TMA. For LKB1 and CCL2, only staining in epithelium was scored. For CD68, which was used for macrophage quantitation, staining was evaluated in the epithelial and stromal compartments combined (insets show higher magnification). Arrows in panels B and C highlight positive staining. See

methods section for detailed explanation of scoring schema for each marker.

Bars=50 μm in all panels.

CHAPTER SEVEN

Conclusions and Recommendations

Introduction

The discovery of the LKB1/CCL2/TAM axis is novel in that it is the first to identify CCL2 as an important mediator of *Lkb1*-driven EMCAs in mice and humans. CCL2 is responsible for the recruitment of a population of macrophages expressing CCR2, which is necessary for tumor growth and progression (**Fig. 7.1A,B**). Therefore, the LKB1/CCL2/TAM axis plays a role in endometrial cancer progression, and in particular, the invasion of LKB1 deficient glands observed in high stage human tumors as well as during late disease in mouse models. Given these newly established relationships, there are still important questions that need to be addressed.

Identifying the mechanism for Lkb1 regulation of CCL2 and other factors in EM cells

As described, LKB1 knockdown with shRNA resulted in the aberrant expression of nearly 40 mRNA transcripts, including *CCL2*, common among two different shRNA constructs. However, LKB1's role in transcriptional regulation of *CCL2* is still unclear (**Fig. 7.1A,B**). LKB1-AMPK modulation with AICAR

and metformin affected basal levels of CCL2 secretion, suggesting that activated AMPK regulates CCL2 and many of the other transcripts identified in this study. In support of this, prior investigations have shown that pAMPK can regulate CREB transcriptional co-activator (CRTC) family members, which in turn influence gene activation [88-91]. Mechanistically, AMPK phosphorylates CRTCs, which prevents their localization into the nucleus where they bind to and activate CREB.

Therefore, it is plausible that loss of LKB1 results in reduced phosphorylation of AMPK and activation of the CRTCs and CREB targets. I tested this hypothesis by first examining the level of mRNA of CRTC family members in cell lines (non-target, shRNA1, and shRNA2) from our microarray study. Probe intensity analysis of all cell lines revealed high expression of CRTC2 and CRTC3, with no differences caused by LKB1 knockdown (**Fig. 7.2A**). I continuously passaged cell lines and used ELISA to test for enhanced CCL2 secretion as a readout for LKB1 knockdown, prior to harvesting tissue for western blot analysis (**Fig. 7.2B**). As expected, CCL2 levels were still higher in EM cells upon LKB1 knockdown. I then isolated cytoplasmic and nuclear protein fractions from cell lines and probed for CRTC2/3, the highest expressed family members in these cells. CRTC2/3, however, did not greatly accumulate in nuclear fractions with LKB1 loss (**Fig. 7.2C**), suggesting that the CRTC family members are not solely regulated by LKB1 in these cells.

Besides CRTC/CREB, it would be important to examine the FOXO family of transcription factors in these cell lines, which have also been shown to be

regulated by pAMPK [155]. Further, WNT/Beta-catenin signaling should be explored given its role in endometrial cancer [9] and the appearance of several WNT factors in our shRNA screen.

Of the 211 total transcripts identified in this study, a significant portion is enriched for proteins that form the extra-cellular matrix or bind to receptors. Given the role of many of these proteins in tumorigenesis across tissue types, it should be examined whether or not LKB1 status influences their aberrant transcription in other types of cancer. This is especially important for CCL2 because it has been shown to play an important role in the recruitment of macrophages that shape the tumor microenvironment, and it can also act in an autocrine fashion to stimulate mitogenic pathways. The byproduct of either scenario is enhanced invasion and metastasis across many tumor types [163], a phenotype highly common in mouse models with genetic *Lkb1* ablation [30, 112]. Testing if deregulated factors like CCL2 contribute to these phenotypes would prove helpful in uncovering different modes of LKB1 driven cancers.

The cell-autonomous role of CCL2 in endometrial cancer

Many cancer cell lines aberrantly express CCR2, the cognate receptor for CCL2. Adding recombinant human CCL2 (rhCCL2) to these cell lines has resulted in increased cell proliferation, cell motility, and enhanced invasion [163]. Thus, I wanted to see if 1) endometrial cell lines expressed CCR2 and 2) whether or not rhCCL2 could induce these effects. The cell line used in my study (EM

cells) did not express CCR2, and both Ishikawa and RL95 EMCA cell lines showed faint expression regardless of LKB1 status (**Fig. 7.3A**). I then looked at cervical cancer cell lines HeLa and SW756. These cell lines innately harbor LKB1 deletions, which we have restored through the use of a stably transfected tetracycline inducible *LKB1* promoter. Consistent with endometrial cell lines, CCR2 expression was not influenced by LKB1 status. However, CCR2 expression in cervical cancer cell lines was higher than endometrial cell lines (**Fig. 7.3A**).

Ishikawa and SW756 cells were then tested for invasive capacity by Boyden Chamber assay. To see if CCL2 served as a chemoattractant that could induce motility and invasion in cancer cells, rhCCL2 was placed in the bottom of the chamber with either Ishikawa or SW756 placed in the top chamber. Cells that invaded after twenty four hours were counted by crystal violet staining. In this scenario, neither cell line responded chemotactically to rhCCl2 compared to vehicle control (**Fig. 7.3B**). To see if rhCCL2 was needed to transform cells prior to invasion, Ishikawa and SW756 cells were incubated with rhCCL2 24 hours prior to their placement in the top chamber. The next day, cells were counted in the same manner but showed no change regardless of treatment (**Fig. 7.3C**).

These in vitro experiments show that human endometrial and cervical cell lines do not become invasive in response to CCL2. However, other types of CCL2 cell autonomous effects such as cell growth [191] and resistance to apoptosis [192] have yet to be explored in these cell lines. Additionally, a role for cell-autonomous CCL2 effects has yet to be explored in the *Sprr2f-Cre* model.

This was largely due to difficulty finding a specific antibody that could accurately stain CCR2 expression in endometrial epithelium. Producing such an antibody would prove helpful in addressing this question, given that *Lkb1*$^{-/-}$*; Ccl2*$^{-/-}$ animals had significantly slower disease progression. Though these animals had less macrophages in tumors, it does not rule out that CCL2-mediated cell autonomous effects were also attenuated.

LKB1 and TAMS

Tumor associated macrophages and the chemokine CCL2 play an important role in the progression of endometrial cancers characterized by LKB1 loss. However, the behavior of these macrophages in the uterus has yet to be elucidated (**Fig. 7.1A,B**). In this study, we showed that TAMS in *Lkb1*$^{-/-}$ tumors expressed markers of alternative activation, or "M2-like" markers. To further characterize these macrophages in the uterus, we are currently employing RNA-seq on isolated F4/80+ cells from tumors. This is important, as M2 macrophages specialize in anti-inflammatory responses that result in cell proliferation, tissue repair, and enhanced angiogenesis [193]. In contrast, "M1-like" TAMS are primarily responsible for inflammation, tissue damage, and cell death [193]. Thus, identifying transcripts of the F4/80+ macrophage population will help uncover tumorigenic effectors and solidify the claim that these macrophages are important for tumor progression.

Polarization into M1 or M2-like TAMS is highly dependent on a variety of secreted factors in the tumor microenvironment [194], as well as structures located on cancer cells and tumor vasculature [195-197] that are recognized by surrounding immune cells. Given this, it has yet to be seen if a role for *Lkb1*$^{-/-}$ cells exists for inducing M2 polarization in the uterus via secreted factors or other mechanisms. Thus, establishing a co-culturing system with Lkb1 epithelia, macrophages, and even stromal cells would go far in addressing this question.

EM cells as a tool for exploring LKB1 endometrial biology

Immortalized endometrial cells are transformed by the addition of E6, E7, and telomerase; the combination of which allows cells to freely enter the cell cycle and proliferate without becoming senescent [159]. Importantly, these cells were non-tumorigenic when assayed by growth in soft agar or xenotransplantation in mice. Thus, they were the closest cell line that resembled the "clean" genetic background of the *Sprr2f-Cre* mouse model, where it took deletion of only one gene (*Lkb1*) to malignantly transform the uterus. Even though LKB1 knockdown didn't produce tumorigenic phenotypes in vitro, the lack of other mutations and the chromosomal instability previously described in this cell line provided enough resolution to see a direct interaction between *LKB1* and *CCL2* at the transcriptional and translational level, which could then be applied to the mouse model. This is by no means implying that EM cells completely reflect *Lkb1* biology in the mouse; rather, they serve as an excellent platform for high

throughput discovery than can be tested in *Sprr2fcre; Lkb1*$^{f/f}$ mice. In light of this, future studies should utilize these two powerful tools in parallel for uncovering novel LKB1-directed pathways that can contribute to tumorigenesis.

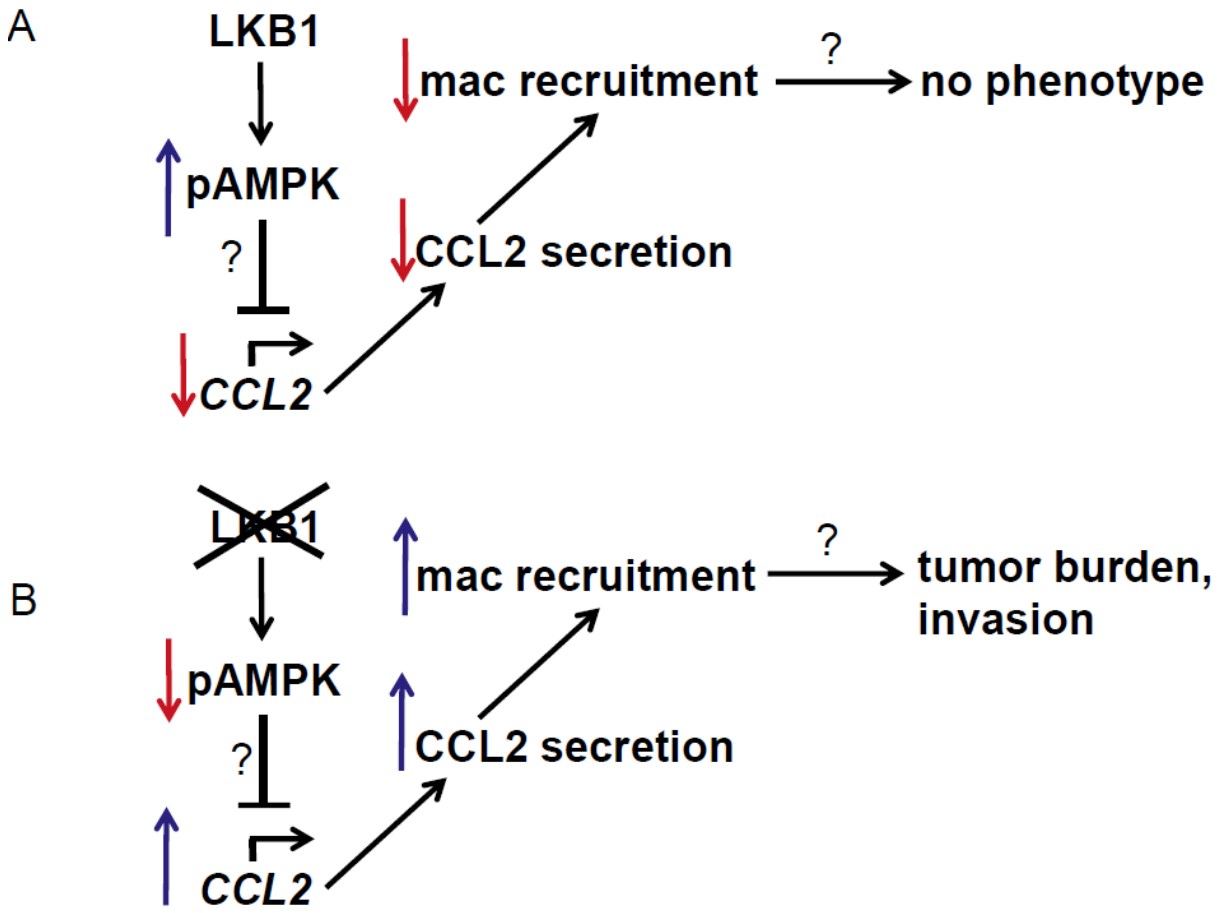

Figure 7.1 The LKB1/CCL2/TAM axis. Proposed mechanism for CCL2 and macrophage regulation via LKB1 in (A) normal and (B) diseased states. Question marks denote mechanisms in need of further investigation.

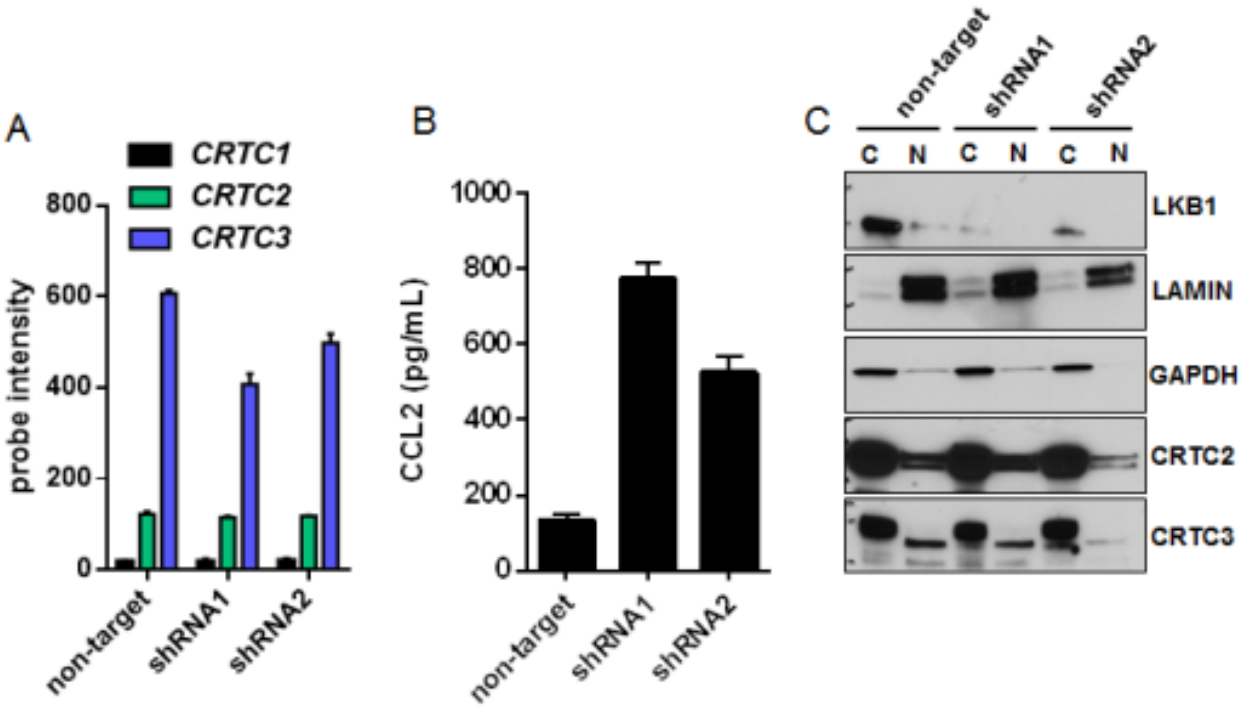

Figure 7.2 Analysis of CRTC family members in EM cells. A) Digital northern comparing RNA expression of CRTC family members across cell lines. B) Confirmation of enhanced CCL2 secretion in passaged cell lines over time via ELISA. C) Western blot depicting cytoplasmic and nuclear localization of CRTC family members.

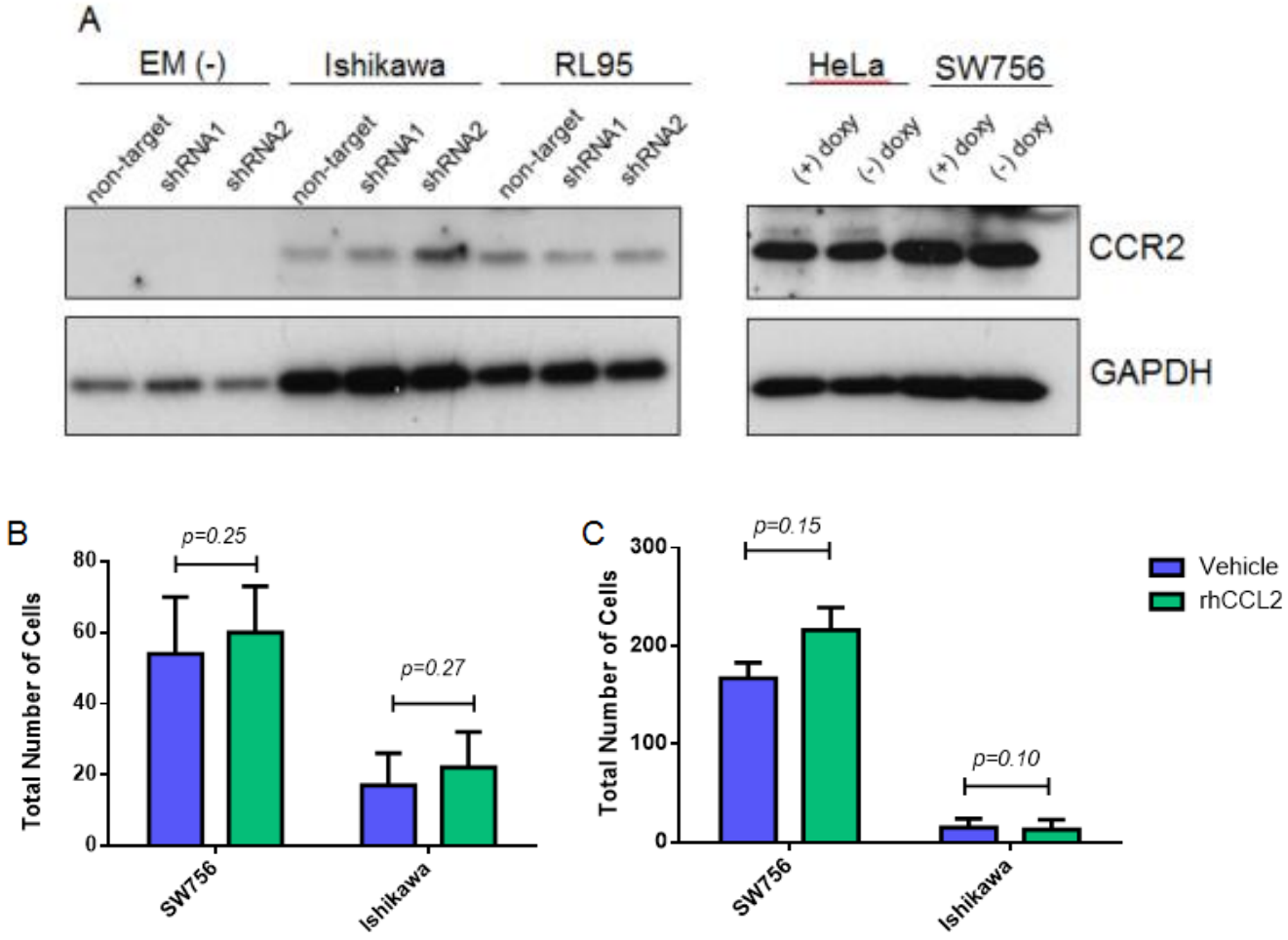

Figure 7.3 Assaying for cell autonomous effects of CCL2. A) Western blot depicting CCR2 expression across cell lines. B) Boyden Chamber assay showing the number of cells migrating through matrigel in response to rhCCL2 or C) when stimulated with rhCCL2 24 hours before beginning of assay.

REFERENCES

1. Filant, J. and T.E. Spencer, *Uterine glands: biological roles in conceptus implantation, uterine receptivity and decidualization.* Int J Dev Biol, 2014. **58**(2-4): p. 107-16.
2. Donjacour, A.A. and G.R. Cunha, *Stromal regulation of epithelial function.* Cancer Treat Res, 1991. **53**: p. 335-64.
3. Riemer, R.K. and M.A. Heymann, *Regulation of uterine smooth muscle function during gestation.* Pediatr Res, 1998. **44**(5): p. 615-27.
4. D'Angelo, E. and J. Prat, *Uterine sarcomas: a review.* Gynecol Oncol, 2010. **116**(1): p. 131-9.
5. Deligdisch, L., *Hormonal pathology of the endometrium.* Mod Pathol, 2000. **13**(3): p. 285-94.
6. Jemal, A., et al., *Cancer statistics, 2009.* CA Cancer J Clin, 2009. **59**(4): p. 225-49.
7. Di Cristofano, A. and L.H. Ellenson, *Endometrial carcinoma.* Annu Rev Pathol, 2007. **2**: p. 57-85.
8. Lax, S.F. and R.J. Kurman, *A dualistic model for endometrial carcinogenesis based on immunohistochemical and molecular genetic analyses.* Verh Dtsch Ges Pathol, 1997. **81**: p. 228-32.
9. Cancer Genome Atlas Research, N., et al., *Integrated genomic characterization of endometrial carcinoma.* Nature, 2013. **497**(7447): p. 67-73.
10. Lax, S.F., *Molecular genetic pathways in various types of endometrial carcinoma: from a phenotypical to a molecular-based classification.* Virchows Arch, 2004. **444**(3): p. 213-23.
11. Wang, Y., et al., *Genomic characterization of gene copy-number aberrations in endometrial carcinoma cell lines derived from endometrioid-type endometrial adenocarcinoma.* Technol Cancer Res Treat, 2010. **9**(2): p. 179-89.
12. Grundker, C., A.R. Gunthert, and G. Emons, *Hormonal heterogeneity of endometrial cancer.* Adv Exp Med Biol, 2008. **630**: p. 166-88.
13. Hemminki, A., et al., *Localization of a susceptibility locus for Peutz-Jeghers syndrome to 19p using comparative genomic hybridization and targeted linkage analysis.* Nat Genet, 1997. **15**(1): p. 87-90.
14. Sanchez-Cespedes, M., *A role for LKB1 gene in human cancer beyond the Peutz-Jeghers syndrome.* Oncogene, 2007. **26**(57): p. 7825-32.
15. Hemminki, A., et al., *A serine/threonine kinase gene defective in Peutz-Jeghers syndrome.* Nature, 1998. **391**(6663): p. 184-7.
16. Mehenni, H., et al., *Loss of LKB1 kinase activity in Peutz-Jeghers syndrome, and evidence for allelic and locus heterogeneity.* Am J Hum Genet, 1998. **63**(6): p. 1641-50.

17. Hezel, A.F. and N. Bardeesy, *LKB1; linking cell structure and tumor suppression.* Oncogene, 2008. **27**(55): p. 6908-19.
18. Beggs, A.D., et al., *Peutz-Jeghers syndrome: a systematic review and recommendations for management.* Gut, 2010. **59**(7): p. 975-86.
19. Hearle, N., et al., *Frequency and spectrum of cancers in the Peutz-Jeghers syndrome.* Clin Cancer Res, 2006. **12**(10): p. 3209-15.
20. Giardiello, F.M., et al., *Very high risk of cancer in familial Peutz-Jeghers syndrome.* Gastroenterology, 2000. **119**(6): p. 1447-53.
21. Lu, K.H., et al., *Loss of tuberous sclerosis complex-2 function and activation of mammalian target of rapamycin signaling in endometrial carcinoma.* Clin Cancer Res, 2008. **14**(9): p. 2543-50.
22. Contreras, C.M., et al., *Loss of Lkb1 provokes highly invasive endometrial adenocarcinomas.* Cancer Res, 2008. **68**(3): p. 759-66.
23. Contreras, C.M., et al., *Lkb1 inactivation is sufficient to drive endometrial cancers that are aggressive yet highly responsive to mTOR inhibitor monotherapy.* Dis Model Mech, 2010. **3**(3-4): p. 181-93.
24. Tanwar, P.S., et al., *Stromal liver kinase B1 [STK11] signaling loss induces oviductal adenomas and endometrial cancer by activating mammalian Target of Rapamycin Complex 1.* PLoS Genet, 2012. **8**(8): p. e1002906.
25. Cheng, H., et al., *A genetic mouse model of invasive endometrial cancer driven by concurrent loss of Pten and Lkb1 Is highly responsive to mTOR inhibition.* Cancer Res, 2014. **74**(1): p. 15-23.
26. Sapkota, G.P., et al., *Identification and characterization of four novel phosphorylation sites (Ser31, Ser325, Thr336 and Thr366) on LKB1/STK11, the protein kinase mutated in Peutz-Jeghers cancer syndrome.* Biochem J, 2002. **362**(Pt 2): p. 481-90.
27. Rowan, A., et al., *In situ analysis of LKB1/STK11 mRNA expression in human normal tissues and tumours.* J Pathol, 2000. **192**(2): p. 203-6.
28. Wingo, S.N., et al., *Somatic LKB1 mutations promote cervical cancer progression.* PLoS One, 2009. **4**(4): p. e5137.
29. Morton, J.P., et al., *LKB1 haploinsufficiency cooperates with Kras to promote pancreatic cancer through suppression of p21-dependent growth arrest.* Gastroenterology, 2010. **139**(2): p. 586-97, 597 e1-6.
30. Ji, H., et al., *LKB1 modulates lung cancer differentiation and metastasis.* Nature, 2007. **448**(7155): p. 807-10.
31. Wei, C., et al., *Mutation of Lkb1 and p53 genes exert a cooperative effect on tumorigenesis.* Cancer Res, 2005. **65**(24): p. 11297-303.
32. Brown, K.A., et al., *LKB1 expression is inhibited by estradiol-17beta in MCF-7 cells.* J Steroid Biochem Mol Biol, 2011. **127**(3-5): p. 439-43.
33. Linher-Melville, K. and G. Singh, *The transcriptional responsiveness of LKB1 to STAT-mediated signaling is differentially modulated by prolactin in human breast cancer cells.* BMC Cancer, 2014. **14**: p. 415.
34. Co, N.N., et al., *Loss of LKB1 in high-grade endometrial carcinoma: LKB1 is a novel transcriptional target of p53.* Cancer, 2014. **120**(22): p. 3457-68.

35. Linher-Melville, K., S. Zantinge, and G. Singh, *Liver kinase B1 expression (LKB1) is repressed by estrogen receptor alpha (ERalpha) in MCF-7 human breast cancer cells.* Biochem Biophys Res Commun, 2012. **417**(3): p. 1063-8.
36. Bokhman, J.V., *Two pathogenetic types of endometrial carcinoma.* Gynecol Oncol, 1983. **15**(1): p. 10-7.
37. Tashiro, H., et al., *p53 gene mutations are common in uterine serous carcinoma and occur early in their pathogenesis.* Am J Pathol, 1997. **150**(1): p. 177-85.
38. Trojan, J., et al., *5'-CpG island methylation of the LKB1/STK11 promoter and allelic loss at chromosome 19p13.3 in sporadic colorectal cancer.* Gut, 2000. **47**(2): p. 272-6.
39. Esteller, M., et al., *Epigenetic inactivation of LKB1 in primary tumors associated with the Peutz-Jeghers syndrome.* Oncogene, 2000. **19**(1): p. 164-8.
40. Qanungo, S., S. Haldar, and A. Basu, *Restoration of silenced Peutz-Jeghers syndrome gene, LKB1, induces apoptosis in pancreatic carcinoma cells.* Neoplasia, 2003. **5**(4): p. 367-74.
41. Sapkota, G.P., et al., *Ionizing radiation induces ataxia telangiectasia mutated kinase (ATM)-mediated phosphorylation of LKB1/STK11 at Thr-366.* Biochem J, 2002. **368**(Pt 2): p. 507-16.
42. Song, P., et al., *Reactive nitrogen species induced by hyperglycemia suppresses Akt signaling and triggers apoptosis by upregulating phosphatase PTEN (phosphatase and tensin homologue deleted on chromosome 10) in an LKB1-dependent manner.* Circulation, 2007. **116**(14): p. 1585-95.
43. Sapkota, G.P., et al., *Phosphorylation of the protein kinase mutated in Peutz-Jeghers cancer syndrome, LKB1/STK11, at Ser431 by p90(RSK) and cAMP-dependent protein kinase, but not its farnesylation at Cys(433), is essential for LKB1 to suppress cell vrowth.* J Biol Chem, 2001. **276**(22): p. 19469-82.
44. Collins, S.P., et al., *LKB1, a novel serine/threonine protein kinase and potential tumour suppressor, is phosphorylated by cAMP-dependent protein kinase (PKA) and prenylated in vivo.* Biochem J, 2000. **345 Pt 3**: p. 673-80.
45. Nony, P., et al., *Stability of the Peutz-Jeghers syndrome kinase LKB1 requires its binding to the molecular chaperones Hsp90/Cdc37.* Oncogene, 2003. **22**(57): p. 9165-75.
46. Gaude, H., et al., *Molecular chaperone complexes with antagonizing activities regulate stability and activity of the tumor suppressor LKB1.* Oncogene, 2012. **31**(12): p. 1582-91.
47. Zeqiraj, E., et al., *Structure of the LKB1-STRAD-MO25 complex reveals an allosteric mechanism of kinase activation.* Science, 2009. **326**(5960): p. 1707-11.

48. Milburn, C.C., et al., *Crystal structure of MO25 alpha in complex with the C terminus of the pseudo kinase STE20-related adaptor.* Nat Struct Mol Biol, 2004. **11**(2): p. 193-200.
49. Baas, A.F., et al., *Activation of the tumour suppressor kinase LKB1 by the STE20-like pseudokinase STRAD.* EMBO J, 2003. **22**(12): p. 3062-72.
50. Boudeau, J., et al., *MO25alpha/beta interact with STRADalpha/beta enhancing their ability to bind, activate and localize LKB1 in the cytoplasm.* EMBO J, 2003. **22**(19): p. 5102-14.
51. de Leng, W.W., et al., *STRAD in Peutz-Jeghers syndrome and sporadic cancers.* J Clin Pathol, 2005. **58**(10): p. 1091-5.
52. Alhopuro, P., et al., *Mutation analysis of three genes encoding novel LKB1-interacting proteins, BRG1, STRADalpha, and MO25alpha, in Peutz-Jeghers syndrome.* Br J Cancer, 2005. **92**(6): p. 1126-9.
53. Nath, N., R.R. McCartney, and M.C. Schmidt, *Yeast Pak1 kinase associates with and activates Snf1.* Mol Cell Biol, 2003. **23**(11): p. 3909-17.
54. Sutherland, C.M., et al., *Elm1p is one of three upstream kinases for the Saccharomyces cerevisiae SNF1 complex.* Curr Biol, 2003. **13**(15): p. 1299-305.
55. Hong, S.P., et al., *Activation of yeast Snf1 and mammalian AMP-activated protein kinase by upstream kinases.* Proc Natl Acad Sci U S A, 2003. **100**(15): p. 8839-43.
56. Hawley, S.A., et al., *Complexes between the LKB1 tumor suppressor, STRAD alpha/beta and MO25 alpha/beta are upstream kinases in the AMP-activated protein kinase cascade.* J Biol, 2003. **2**(4): p. 28.
57. Woods, A., et al., *LKB1 is the upstream kinase in the AMP-activated protein kinase cascade.* Curr Biol, 2003. **13**(22): p. 2004-8.
58. Lizcano, J.M., et al., *LKB1 is a master kinase that activates 13 kinases of the AMPK subfamily, including MARK/PAR-1.* EMBO J, 2004. **23**(4): p. 833-43.
59. Woods, A., et al., *Characterization of AMP-activated protein kinase beta and gamma subunits. Assembly of the heterotrimeric complex in vitro.* J Biol Chem, 1996. **271**(17): p. 10282-90.
60. Scott, J.W., et al., *CBS domains form energy-sensing modules whose binding of adenosine ligands is disrupted by disease mutations.* J Clin Invest, 2004. **113**(2): p. 274-84.
61. Hardie, D.G., et al., *Management of cellular energy by the AMP-activated protein kinase system.* FEBS Lett, 2003. **546**(1): p. 113-20.
62. Carling, D., V.A. Zammit, and D.G. Hardie, *A common bicyclic protein kinase cascade inactivates the regulatory enzymes of fatty acid and cholesterol biosynthesis.* FEBS Lett, 1987. **223**(2): p. 217-22.
63. Hardie, D.G., *AMP-activated/SNF1 protein kinases: conserved guardians of cellular energy.* Nat Rev Mol Cell Biol, 2007. **8**(10): p. 774-85.
64. Inoki, K., T. Zhu, and K.L. Guan, *TSC2 mediates cellular energy response to control cell growth and survival.* Cell, 2003. **115**(5): p. 577-90.

65. Gwinn, D.M., et al., *AMPK phosphorylation of raptor mediates a metabolic checkpoint.* Mol Cell, 2008. **30**(2): p. 214-26.
66. Shamji, A.F., P. Nghiem, and S.L. Schreiber, *Integration of growth factor and nutrient signaling: implications for cancer biology.* Mol Cell, 2003. **12**(2): p. 271-80.
67. Goncharova, E.A., et al., *Tuberin regulates p70 S6 kinase activation and ribosomal protein S6 phosphorylation. A role for the TSC2 tumor suppressor gene in pulmonary lymphangioleiomyomatosis (LAM).* J Biol Chem, 2002. **277**(34): p. 30958-67.
68. Shaw, R.J., et al., *The LKB1 tumor suppressor negatively regulates mTOR signaling.* Cancer Cell, 2004. **6**(1): p. 91-9.
69. Shaw, R.J., et al., *The kinase LKB1 mediates glucose homeostasis in liver and therapeutic effects of metformin.* Science, 2005. **310**(5754): p. 1642-6.
70. Andrade-Vieira, R., et al., *Loss of LKB1 expression reduces the latency of ErbB2-mediated mammary gland tumorigenesis, promoting changes in metabolic pathways.* PLoS One, 2013. **8**(2): p. e56567.
71. Shaw, R.J., et al., *The tumor suppressor LKB1 kinase directly activates AMP-activated kinase and regulates apoptosis in response to energy stress.* Proc Natl Acad Sci U S A, 2004. **101**(10): p. 3329-35.
72. Bardeesy, N., et al., *Loss of the Lkb1 tumour suppressor provokes intestinal polyposis but resistance to transformation.* Nature, 2002. **419**(6903): p. 162-7.
73. Kato, K., et al., *Critical roles of AMP-activated protein kinase in constitutive tolerance of cancer cells to nutrient deprivation and tumor formation.* Oncogene, 2002. **21**(39): p. 6082-90.
74. Liang, J., et al., *The energy sensing LKB1-AMPK pathway regulates p27(kip1) phosphorylation mediating the decision to enter autophagy or apoptosis.* Nat Cell Biol, 2007. **9**(2): p. 218-24.
75. Faubert, B., et al., *Loss of the tumor suppressor LKB1 promotes metabolic reprogramming of cancer cells via HIF-1alpha.* Proc Natl Acad Sci U S A, 2014. **111**(7): p. 2554-9.
76. Faubert, B., et al., *AMPK is a negative regulator of the Warburg effect and suppresses tumor growth in vivo.* Cell Metab, 2013. **17**(1): p. 113-24.
77. Gao, Y., et al., *LKB1 inhibits lung cancer progression through lysyl oxidase and extracellular matrix remodeling.* Proc Natl Acad Sci U S A, 2010. **107**(44): p. 18892-7.
78. Gera, J.F., et al., *AKT activity determines sensitivity to mammalian target of rapamycin (mTOR) inhibitors by regulating cyclin D1 and c-myc expression.* J Biol Chem, 2004. **279**(4): p. 2737-46.
79. Porstmann, T., et al., *SREBP activity is regulated by mTORC1 and contributes to Akt-dependent cell growth.* Cell Metab, 2008. **8**(3): p. 224-36.
80. Conkright, M.D., et al., *TORCs: transducers of regulated CREB activity.* Mol Cell, 2003. **12**(2): p. 413-23.

81. Iourgenko, V., et al., *Identification of a family of cAMP response element-binding protein coactivators by genome-scale functional analysis in mammalian cells.* Proc Natl Acad Sci U S A, 2003. **100**(21): p. 12147-52.
82. Altarejos, J.Y. and M. Montminy, *CREB and the CRTC co-activators: sensors for hormonal and metabolic signals.* Nat Rev Mol Cell Biol, 2011. **12**(3): p. 141-51.
83. Koo, S.H., et al., *The CREB coactivator TORC2 is a key regulator of fasting glucose metabolism.* Nature, 2005. **437**(7062): p. 1109-11.
84. Katoh, Y., et al., *Silencing the constitutive active transcription factor CREB by the LKB1-SIK signaling cascade.* FEBS J, 2006. **273**(12): p. 2730-48.
85. Clark, K., et al., *Phosphorylation of CRTC3 by the salt-inducible kinases controls the interconversion of classically activated and regulatory macrophages.* Proc Natl Acad Sci U S A, 2012. **109**(42): p. 16986-91.
86. Tonon, G., et al., *t(11;19)(q21;p13) translocation in mucoepidermoid carcinoma creates a novel fusion product that disrupts a Notch signaling pathway.* Nat Genet, 2003. **33**(2): p. 208-13.
87. Coxon, A., et al., *Mect1-Maml2 fusion oncogene linked to the aberrant activation of cyclic AMP/CREB regulated genes.* Cancer Res, 2005. **65**(16): p. 7137-44.
88. Komiya, T., et al., *Enhanced activity of the CREB co-activator Crtc1 in LKB1 null lung cancer.* Oncogene, 2010. **29**(11): p. 1672-80.
89. Feng, Y., et al., *The CRTC1-NEDD9 signaling axis mediates lung cancer progression caused by LKB1 loss.* Cancer Res, 2012. **72**(24): p. 6502-11.
90. Gu, Y., et al., *Altered LKB1/CREB-regulated transcription co-activator (CRTC) signaling axis promotes esophageal cancer cell migration and invasion.* Oncogene, 2012. **31**(4): p. 469-79.
91. Cao, C., et al., *Role of LKB1-CRTC1 on glycosylated COX-2 and response to COX-2 inhibition in lung cancer.* J Natl Cancer Inst, 2015. **107**(1): p. 358.
92. Casaburi, I., et al., *Chenodeoxycholic acid through a TGR5-dependent CREB signaling activation enhances cyclin D1 expression and promotes human endometrial cancer cell proliferation.* Cell Cycle, 2012. **11**(14): p. 2699-710.
93. Catalano, S., et al., *Evidence that leptin through STAT and CREB signaling enhances cyclin D1 expression and promotes human endometrial cancer proliferation.* J Cell Physiol, 2009. **218**(3): p. 490-500.
94. Corsini, M., et al., *Cyclic adenosine monophosphate-response element-binding protein mediates the proangiogenic or proinflammatory activity of gremlin.* Arterioscler Thromb Vasc Biol, 2014. **34**(1): p. 136-45.
95. Dje N'Guessan, P., et al., *Statins control oxidized LDL-mediated histone modifications and gene expression in cultured human endothelial cells.* Arterioscler Thromb Vasc Biol, 2009. **29**(3): p. 380-6.
96. Armaiz-Pena, G.N., et al., *Adrenergic regulation of monocyte chemotactic protein 1 leads to enhanced macrophage recruitment and ovarian carcinoma growth.* Oncotarget, 2014.

97. Watts, J.L., et al., *The C. elegans par-4 gene encodes a putative serine-threonine kinase required for establishing embryonic asymmetry.* Development, 2000. **127**(7): p. 1467-75.
98. Martin, S.G. and D. St Johnston, *A role for Drosophila LKB1 in anterior-posterior axis formation and epithelial polarity.* Nature, 2003. **421**(6921): p. 379-84.
99. Szczepanska, K. and M. Maleszewski, *LKB1/PAR4 protein is asymmetrically localized in mouse oocytes and associates with meiotic spindle.* Gene Expr Patterns, 2005. **6**(1): p. 86-93.
100. Zheng, B. and L.C. Cantley, *Regulation of epithelial tight junction assembly and disassembly by AMP-activated protein kinase.* Proc Natl Acad Sci U S A, 2007. **104**(3): p. 819-22.
101. Zhang, L., et al., *AMP-activated protein kinase regulates the assembly of epithelial tight junctions.* Proc Natl Acad Sci U S A, 2006. **103**(46): p. 17272-7.
102. Tanwar, P.S., et al., *Altered LKB1/AMPK/TSC1/TSC2/mTOR signaling causes disruption of Sertoli cell polarity and spermatogenesis.* Hum Mol Genet, 2012. **21**(20): p. 4394-405.
103. Barnes, A.P., et al., *LKB1 and SAD kinases define a pathway required for the polarization of cortical neurons.* Cell, 2007. **129**(3): p. 549-63.
104. Amin, N., et al., *LKB1 regulates polarity remodeling and adherens junction formation in the Drosophila eye.* Proc Natl Acad Sci U S A, 2009. **106**(22): p. 8941-6.
105. Pease, J.C. and J.S. Tirnauer, *Mitotic spindle misorientation in cancer--out of alignment and into the fire.* J Cell Sci, 2011. **124**(Pt 7): p. 1007-16.
106. Partanen, J.I., et al., *Tumor suppressor function of Liver kinase B1 (Lkb1) is linked to regulation of epithelial integrity.* Proc Natl Acad Sci U S A, 2012. **109**(7): p. E388-97.
107. Royer, C. and X. Lu, *Epithelial cell polarity: a major gatekeeper against cancer?* Cell Death Differ, 2011. **18**(9): p. 1470-7.
108. Muschler, J. and C.H. Streuli, *Cell-matrix interactions in mammary gland development and breast cancer.* Cold Spring Harb Perspect Biol, 2010. **2**(10): p. a003202.
109. Baas, A.F., et al., *Complete polarization of single intestinal epithelial cells upon activation of LKB1 by STRAD.* Cell, 2004. **116**(3): p. 457-66.
110. Eggers, C.M., et al., *STE20-related kinase adaptor protein alpha (STRADalpha) regulates cell polarity and invasion through PAK1 signaling in LKB1-null cells.* J Biol Chem, 2012. **287**(22): p. 18758-68.
111. Nakada, D., T.L. Saunders, and S.J. Morrison, *Lkb1 regulates cell cycle and energy metabolism in haematopoietic stem cells.* Nature, 2010. **468**(7324): p. 653-8.
112. Liu, W., et al., *LKB1/STK11 inactivation leads to expansion of a prometastatic tumor subpopulation in melanoma.* Cancer Cell, 2012. **21**(6): p. 751-64.
113. Sen, B. and F.M. Johnson, *Regulation of SRC family kinases in human cancers.* J Signal Transduct, 2011. **2011**: p. 865819.

114. Eritja, N., et al., *A novel three-dimensional culture system of polarized epithelial cells to study endometrial carcinogenesis.* Am J Pathol, 2010. **176**(6): p. 2722-31.
115. Clement, P.B. and R.H. Young, *Endometrioid carcinoma of the uterine corpus: a review of its pathology with emphasis on recent advances and problematic aspects.* Adv Anat Pathol, 2002. **9**(3): p. 145-84.
116. Karuman, P., et al., *The Peutz-Jegher gene product LKB1 is a mediator of p53-dependent cell death.* Mol Cell, 2001. **7**(6): p. 1307-19.
117. Chen, Z., et al., *A murine lung cancer co-clinical trial identifies genetic modifiers of therapeutic response.* Nature, 2012. **483**(7391): p. 613-7.
118. Tiainen, M., et al., *Growth arrest by the LKB1 tumor suppressor: induction of p21(WAF1/CIP1).* Hum Mol Genet, 2002. **11**(13): p. 1497-504.
119. Zeng, P.Y. and S.L. Berger, *LKB1 is recruited to the p21/WAF1 promoter by p53 to mediate transcriptional activation.* Cancer Res, 2006. **66**(22): p. 10701-8.
120. Tiainen, M., A. Ylikorkala, and T.P. Makela, *Growth suppression by Lkb1 is mediated by a G(1) cell cycle arrest.* Proc Natl Acad Sci U S A, 1999. **96**(16): p. 9248-51.
121. Hou, X., et al., *A new role of NUAK1: directly phosphorylating p53 and regulating cell proliferation.* Oncogene, 2011. **30**(26): p. 2933-42.
122. Akbay, E.A., et al., *Cooperation between p53 and the telomere-protecting shelterin component Pot1a in endometrial carcinogenesis.* Oncogene, 2013. **32**(17): p. 2211-9.
123. Akbay, E.A., et al., *Differential roles of telomere attrition in type I and II endometrial carcinogenesis.* Am J Pathol, 2008. **173**(2): p. 536-44.
124. Chalhoub, N. and S.J. Baker, *PTEN and the PI3-kinase pathway in cancer.* Annu Rev Pathol, 2009. **4**: p. 127-50.
125. Mehenni, H., et al., *LKB1 interacts with and phosphorylates PTEN: a functional link between two proteins involved in cancer predisposing syndromes.* Hum Mol Genet, 2005. **14**(15): p. 2209-19.
126. Tanwar, P.S., et al., *Loss of LKB1 and PTEN tumor suppressor genes in the ovarian surface epithelium induces papillary serous ovarian cancer.* Carcinogenesis, 2014. **35**(3): p. 546-53.
127. Shorning, B.Y., D. Griffiths, and A.R. Clarke, *Lkb1 and Pten synergise to suppress mTOR-mediated tumorigenesis and epithelial-mesenchymal transition in the mouse bladder.* PLoS One, 2011. **6**(1): p. e16209.
128. Xu, C., et al., *Loss of Lkb1 and Pten leads to lung squamous cell carcinoma with elevated PD-L1 expression.* Cancer Cell, 2014. **25**(5): p. 590-604.
129. Normanno, N., et al., *Implications for KRAS status and EGFR-targeted therapies in metastatic CRC.* Nat Rev Clin Oncol, 2009. **6**(9): p. 519-27.
130. Chan, K.T., et al., *LKB1 loss in melanoma disrupts directional migration toward extracellular matrix cues.* J Cell Biol, 2014. **207**(2): p. 299-315.

131. Birkeland, E., et al., *KRAS gene amplification and overexpression but not mutation associates with aggressive and metastatic endometrial cancer.* Br J Cancer, 2012. **107**(12): p. 1997-2004.
132. Caligioni, C.S., *Assessing reproductive status/stages in mice.* Curr Protoc Neurosci, 2009. **Appendix 4**: p. Appendix 4I.
133. Bulletti, C., et al., *Basement membrane components in normal hyperplastic and neoplastic endometrium.* Cancer, 1988. **62**(1): p. 142-9.
134. Nakada, Y., et al., *The LKB1 Tumor Suppressor as a Biomarker in Mouse and Human Tissues.* PLoS One, 2013. **8**(9): p. e73449.
135. Nishida, M., et al., *[Establishment of a new human endometrial adenocarcinoma cell line, Ishikawa cells, containing estrogen and progesterone receptors]*. Nihon Sanka Fujinka Gakkai Zasshi, 1985. **37**(7): p. 1103-11.
136. Xu, X., T. Omelchenko, and A. Hall, *LKB1 tumor suppressor protein regulates actin filament assembly through Rho and its exchange factor Dbl independently of kinase activity.* BMC Cell Biol, 2010. **11**: p. 77.
137. Boehlke, C., et al., *Primary cilia regulate mTORC1 activity and cell size through Lkb1.* Nat Cell Biol, 2010. **12**(11): p. 1115-22.
138. Mejillano, M.R., et al., *Lamellipodial versus filopodial mode of the actin nanomachinery: pivotal role of the filament barbed end.* Cell, 2004. **118**(3): p. 363-73.
139. Zuber, C., et al., *Invasion of tumorigenic HT1080 cells is impeded by blocking or downregulating the 37-kDa/67-kDa laminin receptor.* J Mol Biol, 2008. **378**(3): p. 530-9.
140. Lee, M. and V. Vasioukhin, *Cell polarity and cancer--cell and tissue polarity as a non-canonical tumor suppressor.* J Cell Sci, 2008. **121**(Pt 8): p. 1141-50.
141. Guldberg, P., et al., *Somatic mutation of the Peutz-Jeghers syndrome gene, LKB1/STK11, in malignant melanoma.* Oncogene, 1999. **18**(9): p. 1777-80.
142. Alessi, D.R., K. Sakamoto, and J.R. Bayascas, *Lkb1-dependent signaling pathways.* Annu Rev Biochem, 2006. **75**: p. 137-63.
143. Ding, L., et al., *Somatic mutations affect key pathways in lung adenocarcinoma.* Nature, 2008. **455**(7216): p. 1069-75.
144. Zhao, N., et al., *Alterations of LKB1 and KRAS and risk of brain metastasis: Comprehensive characterization by mutation analysis, copy number, and gene expression in non-small-cell lung carcinoma.* Lung Cancer, 2014.
145. Ollila, S. and T.P. Makela, *The tumor suppressor kinase LKB1: lessons from mouse models.* J Mol Cell Biol, 2011. **3**(6): p. 330-40.
146. Boudeau, J., et al., *Heat-shock protein 90 and Cdc37 interact with LKB1 and regulate its stability.* Biochem J, 2003. **370**(Pt 3): p. 849-57.
147. Bouchekioua-Bouzaghou, K., et al., *LKB1 when associated with methylatedERa is a marker of bad prognosis in breast cancer.* Int J Cancer, 2014.

148. Tsai, L.H., et al., *LKB1 loss by alteration of the NKX2-1/p53 pathway promotes tumor malignancy and predicts poor survival and relapse in lung adenocarcinomas.* Oncogene, 2013.
149. Huang, Y.H., et al., *Decreased expression of LKB1 correlates with poor prognosis in hepatocellular carcinoma patients undergoing hepatectomy.* Asian Pac J Cancer Prev, 2013. **14**(3): p. 1985-8.
150. He, T.Y., et al., *LKB1 Loss at Transcriptional Level Promotes Tumor Malignancy and Poor Patient Outcomes in Colorectal Cancer.* Ann Surg Oncol, 2014.
151. Gill, R.K., et al., *Frequent homozygous deletion of the LKB1/STK11 gene in non-small cell lung cancer.* Oncogene, 2011. **30**(35): p. 3784-91.
152. Shackelford, D.B. and R.J. Shaw, *The LKB1-AMPK pathway: metabolism and growth control in tumour suppression.* Nat Rev Cancer, 2009. **9**(8): p. 563-75.
153. Hardie, D.G., F.A. Ross, and S.A. Hawley, *AMPK: a nutrient and energy sensor that maintains energy homeostasis.* Nat Rev Mol Cell Biol, 2012. **13**(4): p. 251-62.
154. Courchet, J., et al., *Terminal axon branching is regulated by the LKB1-NUAK1 kinase pathway via presynaptic mitochondrial capture.* Cell, 2013. **153**(7): p. 1510-25.
155. Greer, E.L., et al., *The energy sensor AMP-activated protein kinase directly regulates the mammalian FOXO3 transcription factor.* J Biol Chem, 2007. **282**(41): p. 30107-19.
156. Goodwin, J.M., et al., *An AMPK-independent signaling pathway downstream of the LKB1 tumor suppressor controls Snail1 and metastatic potential.* Mol Cell, 2014. **55**(3): p. 436-50.
157. Tsai, L.H., et al., *The MZF1/c-MYC axis mediates lung adenocarcinoma progression caused by wild-type lkb1 loss.* Oncogene, 2014.
158. Jacob, L.S., et al., *Genome-wide RNAi screen reveals disease-associated genes that are common to Hedgehog and Wnt signaling.* Sci Signal, 2011. **4**(157): p. ra4.
159. Kyo, S., et al., *Successful immortalization of endometrial glandular cells with normal structural and functional characteristics.* Am J Pathol, 2003. **163**(6): p. 2259-69.
160. Carretero, J., et al., *Integrative genomic and proteomic analyses identify targets for Lkb1-deficient metastatic lung tumors.* Cancer Cell, 2010. **17**(6): p. 547-59.
161. Zhuang, Z.G., et al., *Enhanced expression of LKB1 in breast cancer cells attenuates angiogenesis, invasion, and metastatic potential.* Mol Cancer Res, 2006. **4**(11): p. 843-9.
162. Ossipova, O., et al., *LKB1 (XEEK1) regulates Wnt signalling in vertebrate development.* Nat Cell Biol, 2003. **5**(10): p. 889-94.
163. Borsig, L., et al., *Inflammatory chemokines and metastasis--tracing the accessory.* Oncogene, 2014. **33**(25): p. 3217-24.

164. Tsuyada, A., et al., *CCL2 mediates cross-talk between cancer cells and stromal fibroblasts that regulates breast cancer stem cells.* Cancer Res, 2012. **72**(11): p. 2768-79.
165. Zhang, J., L. Patel, and K.J. Pienta, *Targeting chemokine (C-C motif) ligand 2 (CCL2) as an example of translation of cancer molecular biology to the clinic.* Prog Mol Biol Transl Sci, 2010. **95**: p. 31-53.
166. Zhou, G., et al., *Role of AMP-activated protein kinase in mechanism of metformin action.* J Clin Invest, 2001. **108**(8): p. 1167-74.
167. Sullivan, J.E., et al., *Inhibition of lipolysis and lipogenesis in isolated rat adipocytes with AICAR, a cell-permeable activator of AMP-activated protein kinase.* FEBS Lett, 1994. **353**(1): p. 33-6.
168. Hawley, S.A., et al., *Calmodulin-dependent protein kinase kinase-beta is an alternative upstream kinase for AMP-activated protein kinase.* Cell Metab, 2005. **2**(1): p. 9-19.
169. Zhu, X., et al., *Myeloid cell-specific ABCA1 deletion protects mice from bacterial infection.* Circ Res, 2012. **111**(11): p. 1398-409.
170. Pollard, J.W., E.Y. Lin, and L. Zhu, *Complexity in uterine macrophage responses to cytokines in mice.* Biol Reprod, 1998. **58**(6): p. 1469-75.
171. Comito, G., et al., *Cancer-associated fibroblasts and M2-polarized macrophages synergize during prostate carcinoma progression.* Oncogene, 2014. **33**(19): p. 2423-31.
172. Mantovani, A., et al., *Macrophage polarization: tumor-associated macrophages as a paradigm for polarized M2 mononuclear phagocytes.* Trends Immunol, 2002. **23**(11): p. 549-55.
173. Colegio, O.R., et al., *Functional polarization of tumour-associated macrophages by tumour-derived lactic acid.* Nature, 2014. **513**(7519): p. 559-63.
174. Pesce, J.T., et al., *Arginase-1-expressing macrophages suppress Th2 cytokine-driven inflammation and fibrosis.* PLoS Pathog, 2009. **5**(4): p. e1000371.
175. van Rooijen, N. and E. Hendrikx, *Liposomes for specific depletion of macrophages from organs and tissues.* Methods Mol Biol, 2010. **605**: p. 189-203.
176. Danenberg, H.D., et al., *Macrophage depletion by clodronate-containing liposomes reduces neointimal formation after balloon injury in rats and rabbits.* Circulation, 2002. **106**(5): p. 599-605.
177. Lu, B., et al., *Abnormalities in monocyte recruitment and cytokine expression in monocyte chemoattractant protein 1-deficient mice.* J Exp Med, 1998. **187**(4): p. 601-8.
178. Deshmane, S.L., et al., *Monocyte chemoattractant protein-1 (MCP-1): an overview.* J Interferon Cytokine Res, 2009. **29**(6): p. 313-26.
179. Mikuta, J.J., *International Federation of Gynecology and Obstetrics staging of endometrial cancer 1988.* Cancer, 1993. **71**(4 Suppl): p. 1460-3.
180. Espinosa, I., et al., *Myometrial invasion and lymph node metastasis in endometrioid carcinomas: tumor-associated macrophages, microvessel*

density, and HIF1A have a crucial role. Am J Surg Pathol, 2010. **34**(11): p. 1708-14.
181. Ohno, S., et al., *Correlation of histological localization of tumor-associated macrophages with clinicopathological features in endometrial cancer.* Anticancer Res, 2004. **24**(5C): p. 3335-42.
182. Soeda, S., et al., *Tumor-associated macrophages correlate with vascular space invasion and myometrial invasion in endometrial carcinoma.* Gynecol Oncol, 2008. **109**(1): p. 122-8.
183. Kubler, K., et al., *Prognostic significance of tumor-associated macrophages in endometrial adenocarcinoma.* Gynecol Oncol, 2014. **135**(2): p. 176-83.
184. Zhang, J., Y. Lu, and K.J. Pienta, *Multiple roles of chemokine (C-C motif) ligand 2 in promoting prostate cancer growth.* J Natl Cancer Inst, 2010. **102**(8): p. 522-8.
185. Zijlmans, H.J., et al., *The absence of CCL2 expression in cervical carcinoma is associated with increased survival and loss of heterozygosity at 17q11.2.* J Pathol, 2006. **208**(4): p. 507-17.
186. Qian, B.Z., et al., *CCL2 recruits inflammatory monocytes to facilitate breast-tumour metastasis.* Nature, 2011. **475**(7355): p. 222-5.
187. Shi, C. and E.G. Pamer, *Monocyte recruitment during infection and inflammation.* Nat Rev Immunol, 2011. **11**(11): p. 762-74.
188. Wang, W.W., et al., *Identification of serum monocyte chemoattractant protein-1 and prolactin as potential tumor markers in hepatocellular carcinoma.* PLoS One, 2013. **8**(7): p. e68904.
189. Struthers, M. and A. Pasternak, *CCR2 antagonists.* Curr Top Med Chem, 2010. **10**(13): p. 1278-98.
190. Alvarez, E.A., et al., *Phase II trial of combination bevacizumab and temsirolimus in the treatment of recurrent or persistent endometrial carcinoma: a Gynecologic Oncology Group study.* Gynecol Oncol, 2013. **129**(1): p. 22-7.
191. Loberg, R.D., et al., *CCL2 is a potent regulator of prostate cancer cell migration and proliferation.* Neoplasia, 2006. **8**(7): p. 578-86.
192. Roca, H., Z.S. Varsos, and K.J. Pienta, *CCL2 is a negative regulator of AMP-activated protein kinase to sustain mTOR complex-1 activation, survivin expression, and cell survival in human prostate cancer PC3 cells.* Neoplasia, 2009. **11**(12): p. 1309-17.
193. Mills, C.D., *M1 and M2 Macrophages: Oracles of Health and Disease.* Crit Rev Immunol, 2012. **32**(6): p. 463-88.
194. Martinez, F.O. and S. Gordon, *The M1 and M2 paradigm of macrophage activation: time for reassessment.* F1000Prime Rep, 2014. **6**: p. 13.
195. Utsugi, T., et al., *Elevated expression of phosphatidylserine in the outer membrane leaflet of human tumor cells and recognition by activated human blood monocytes.* Cancer Res, 1991. **51**(11): p. 3062-6.
196. Ran, S., A. Downes, and P.E. Thorpe, *Increased exposure of anionic phospholipids on the surface of tumor blood vessels.* Cancer Res, 2002. **62**(21): p. 6132-40.

197. Ran, S., et al., *Antitumor effects of a monoclonal antibody that binds anionic phospholipids on the surface of tumor blood vessels in mice.* Clin Cancer Res, 2005. **11**(4): p. 1551-62.